UNCERTAINTY IN WELL TEST AND CORE PERMEABILITY ANALYSIS

A THESIS SUBMITTED TO
GRADUATE SCHOOL OF NATURAL AND APPLIED SCIENCES
OF
MIDDLE EAST TECHNICAL UNIVERSITY

BY

CANKAT HAPA

IN PARTIAL FULFILLMENT OF THE REQUIREMENTS
FOR
THE DEGREE OF MASTER OF SCIENCE
IN
PETROLEUM AND NATURAL GAS ENGINEERING

NOVEMBER 2008

Approval of the thesis:

UNCERTAINTY IN WELL TEST AND CORE PERMEABILITY ANALYSIS

submitted by **CANKAT HAPA** in partial fulfilment of the requirements for the degree of **Master of Science in Petroleum and Natural Gas Engineering, Middle East Technical University** by,

Prof. Dr. Canan Özgen _____
Dean, Graduate School of Natural and Applied Sciences

Prof. Dr. Mahmut Parlaktuna _____
Head of Department, Petroleum and Natural Gas Engineering

Prof. Dr. Serhat Akın _____
Supervisor, Petroleum and Natural Gas Engineering Dept., METU

Examining Committee Members:

Prof. Dr. Mahmut Parlaktuna _____
Petroleum and Natural Gas Engineering Dept., METU

Prof. Dr. Serhat Akın _____
Petroleum and Natural Gas Engineering Dept., METU

Prof. Dr. Mustafa V. Kök _____
Petroleum and Natural Gas Engineering Dept., METU

Assistant Prof. Dr. Evren Özbayoğlu _____
Petroleum and Natural Gas Engineering Dept., METU

Petroleum Engineer Demet Çelebioğlu, M.Sc. _____
TPAO, Production Department

I hereby declare that all information in this document has been obtained and presented in accordance with academic rules and ethical conduct. I also declare that, as required by these rules and conduct, I have fully cited and referenced all material and results that are not original to this work.

Name, Last name: Cankat Hapa

Signature:

ABSTRACT

UNCERTAINTY IN WELL TEST AND CORE PERMEABILITY ANALYSIS

Hapa, Cankat

M.Sc., Department of Petroleum and Natural Gas Engineering

Supervisor: Prof. Dr. Serhat Akın

November 2008, 146 pages

Reservoir permeability is one of the important parameters derived from well test analysis. Small-scale permeability measurements in wells are usually made using core plugs, or more recently, probe permeameter measurements. Upscaling of these measurements for comparisons with permeability derived well tests (Pressure Build-Up) can be completed by statistical averaging methods. Well Test permeability is often compared with one of the core plug averages: arithmetic, geometric and harmonic. A question that often arises is which average does the well test-derived permeability represent and over what region is this average valid? A second important question is how should the data sets be reconciled when there are discrepancies?

In practice, the permeability derived from well tests is often assumed to be equivalent to the arithmetic (in a layered reservoir) or geometric (in a randomly distributed permeability field) average of the plug measures. These averages are known to be members of a more general power-average solution. This pragmatic approach (which may include an assumption on the near-well geology) is often flawed due to a number of reasons, which is tried to be explained in this study. The assessment of in-situ, reservoir permeability requires an understanding of both core

(plug and probe) and well test measurements – in terms of their volume scale of investigation, measurement mechanism, interpretation and integration.

Pressure build-up tests for 26 wells and core plug analysis for 32 wells have valid measured data to be evaluated. Core plug permeabilities are upscaled and compared with pressure build-up test derived permeabilities. The arithmetic, harmonic and geometric averages of core plug permeability data are found out for each facies and formation distribution. The reservoir permeability heterogeneities are evaluated in each step of upscaling procedure by computing coefficient of variation, The Dykstra-Parson's Coefficient and Lorenz Coefficients.

This study compared core and well test measurements in South East of Turkey heavy oil carbonate field. An evaluation of well test data and associated core plug data sets from a single field will be resulting from the interpretation of small (core) and reservoir (well test) scale permeability data. The techniques that were used are traditional volume averaging/homogenization methods with the contribution of determining permeability heterogeneities of facies at each step of upscaling procedure and manipulating the data which is not proper to be averaged (approximately normally distributed) with the combination of Lorenz Plot to identify the flowing intervals. As a result, geometrical average of upscaled core plug permeability data is found to be approximately equal to the well test derived permeability for the goodly interpreted well tests. Carbonates are very heterogeneous and this exercise will also be instructive in understanding the heterogeneity for the guidance of reservoir models in such a system.

Keywords: Permeability, Reservoir Heterogeneity, Facies Modeling, Upscaling.

ÖZ

KUYU TESTİ VE KAROT PERMEABİLİTE ANALİZİNDEKİ BELİRSİZLİKLER

Hapa, Cankat

Yüksek Lisans, Petrol ve Doğal Gaz Mühendisliği Bölümü

Tez Yöneticisi: Prof. Dr. Serhat Akın

Kasım 2008, 146 sayfa

Rezervuar geçirgenliği kuyu testi analizinden elde edilebilen önemli bir parametredir. Kuyularda gerçekleştirilen küçük ölçekli geçirgenlik ölçümleri genellikle karot tapaları, veya son zamanlarda, sonda permeametre ölçümleri ile yapılmaktadır. Bu ölçümlerin kuyu testinden (Basınç Yükselim Testleri) elde edilmiş geçirgenlik ile karşılaştırılması amacı ile ölçeklendirilmesi istatistiki ortalama methodu ile tamamlanabilir. Kuyu testinden elde edilen geçirgenlik değerleri genellikle karot tapalarının analizlerinin aritmetik, geometrik veya harmonik ortalamalarının biriyle karşılaştırılır. Genellikle ortaya çıkan soru kuyu testinden elde edilen geçirgenliğin hangi ortalamayı temsil etttiği ve hangi bölgeden sonra bu ortalamanın geçerli olduğudur. İkinci soru ise veriler arasında uyumsuzluk varken veri kümelerinin nasıl düzenleneceğidir.

Pratikte, kuyu testlerinden elde edilen geçirgenliğin karot tapalarından elde edilen geçirgenlik ölçümlerine aritmetik (tabakalı rezervuarlarda) veya geometrik (rasgele dağılmış geçirgenlik alanlarında) ortalamalarının denk olduğu varsayılır. Bu ortalamalar kuvvet ortalaması çözümünün daha yaygın üyeleri olarak bilinir. Bu faydacı yaklaşım (kuyu civarı jeolojisindeki bir varsayımı de içerebilir) bir çok nedenden ötürü geçersiz kılınmaktadır ve nedenler bu çalışmada belirlenmeye

çalışılacaktır. Rezervuar geçirgenliği değerinin belirlenmesi için hem karotun (tapa ve sonda) hem de kuyu testi ölçümlerinin araştırıldıkları hacim ve ölçüm mekanizmaları doğrultusunda anlaşılması, yorumlanması ve de bütünleştirilmesi gerekmektedir.

Bu çalışmada 32 kuyunun karot geçirgenliği verileri ve 26 kuyunun basınç yükselim testinden elde edilen geçirgenlik verileri kullanılmış olup, karot geçirgenliği verileri ölçeklendirildikten sonra kuyu testi verileri ile karşılaştırılmıştır. Ölçeklendirilmiş karot geçirgenliği verilerinin aritmetik, geometrik ve harmonik ortalamaları her fasiyes ve formasyon için ayrı ayrı bulunmuş ve söz konusu karot verilerinin ölçeklendirilmesi aşamalarının her adımında "coefficient of variation", "The Dysktra Parson's Coefficient" ve "Lorenz Plot" ile rezervuar geçirgenliği heterojenite dağılımları bulunmuştur.

Bu çalışma Türkiye'nin Güney Doğu Anadolu Bölgesi'ndeki bulunan bir ağır petrol sahasında (karbonat rezervuarı) yapılan karot analizlerini ve kuyu test sonuçlarını karşılaştırmıştır. Bir sahadan alınan kuyu testi verilerinin ve birleştirilmiş karot tapa veri kümelerinin değerlendirilmesi küçük (karot) ve rezervuar (kuyu testi) ölçeğinde elde edilen geçirgenlik verilerinin yorumlanması ile gerçekleşmiştir. Bu amaçla kullanılan teknikler geleneksel hacim ortalaması/homojenizasyon metotları ile ölçeklendirmenin her aşamasında geçirgenlik heterojenitelerinin hesaplanarak yaklaşık olarak normal dağılım göstermeyen veya ortalamasının alınması için uygun olmayan verinin düzenlenerek son halinin ise etkin akış birimlerinin de bulunması amacıyla Lorenz Planı metotu ile birleştirilmesidir. Sonuç olarak, yorumlaması iyi yapılmış kuyu testleri için kuyu testi geçirgenliği ölçeklendirilmiş karot testi geçirgenliğinin geometrik ortalamasına yaklaşık olarak eşit çıkmıştır. Karbonatların çok heterojen olması dolayısıyla bu çalışma ayrıca rezervuar modelleme sistemlerinde heterojenitenin anlaşılması açısından da öğretici bir rehber olacaktır.

Anahtar Kelimeler: Geçirgenlik, Rezervuar Heterojenitesi, Fasiyes Modellemesi, Ölçeklendirme.

To My Family

ACKNOWLEDGEMENTS

The author wishes to express his deepest gratitude to his supervisor Prof. Dr. Serhat Akın for guidance, advice, criticism, encouragements and insight throughout the study.

Also Demet Çelebioğlu, Onur Susuz, Uğur Karabakal, Ülker Kalfa, M. Serdar Velioğlu of Turkish Petroleum Corporation are gratefully acknowledged of their help and assistance.

Finally, the author would also like to thank Alper Kahvecioğlu for his companionship, encouragement and invaluable support throughout the study.

TABLE OF CONTENTS

LIST OF FIGURES

LIST OF TABLES

CHAPTER 1

INTRODUCTION

Reservoir permeability is one of the most important flow parameters associated with subsurface production and injection. In many reservoirs, values of permeability are derived from one or as many as four or more sources. However, permeability values from these versatile sources mostly differ from each other. In such cases the question is which value is to be used to represent reservoir performance and well productivity (Haddad et al., 2000). Misinterpretation of reservoir permeability can result in very erroneous results in calculating reservoir productivity index which is depending on permeability thickness product (k.h). Importance of reservoir permeability can also be established by the quantity and versatility of techniques in order to derive it which are well-log evaluation, core analysis methods and well testing methods. Our aim is to find an interrelationship between small-scale permeability measurements that are core measurements within the providence of multi-numbers of local permeability and well test data in which single global value of average reservoir permeability within the area of investigation of the well test is acquired. These will be handled by upscaling of these measurements for comparisons within these data.

The development of an integrated reservoir description is particularly important for low permeability reservoir systems such as fields located in South East of Turkey. Workflows should provide mechanisms, which attempt to correlate and/or scale small-scale reservoir properties into large-scale rock "flow units" which will be incorporated in reservoir characterization study within the integration of geological and engineering data. Discrepancy between the different sources are expected because core permeability (geological data) is static permeability measurement

whereas well test is a dynamic measurement of the in-situ reservoir fluid (Haddad et al., 2000; Haddad et al., 2001).

The objective of this study is to consider the uncertainties in the comparison of core-derived and well-test derived permeability estimates. Well test and core permeability is commonly compared prior to being used in a reservoir model.

While making such a comparison there are many issues, which needed to be considered. To illustrate, when cores are retrieved from the reservoir, the confining forces are removed and the rock can expand in all directions, which could increase the dimensions of the flow paths. If this permeability is to be used in reservoir simulation, it is significant that permeability measured at the laboratory (static framework) be transposed at the confining pressure that represents the overburden pressure of the formation tested.

The core measurements must be upscaled with the well test data for comparison. In this study upscaling will be achieved by using averaging method, which is still commonly applied in the industry. Many core plug measurements exist during the history of the field. The question is to select the correct ones in order to match within near-well geometry of the reservoir in which well test is a function of that.

The well test interpretation is transformed by the introduction of derivative of pressure in 1983. In modern well test interpretation, the identification of certain flow regimes is found by the derivative of the pressure. The basic idea of the derivative is to calculate the slope at each point of the pressure curve on the semi-log (superposition) plot, and display it on the log-log plot.
The expression of the derivative is:

$$\Delta p' = \frac{d\Delta p}{d\,\mathrm{sup}.(\Delta t)} \qquad (1.1)$$

When the well is shut in, the produced build-up pressure which is convex around the wellbore (pressure increasing) and concave everywhere else (pressure still decreasing due to the still-diffusing production signal) should be as follows (in the case of an ideal infinite reservoir) (Figure 1.1):

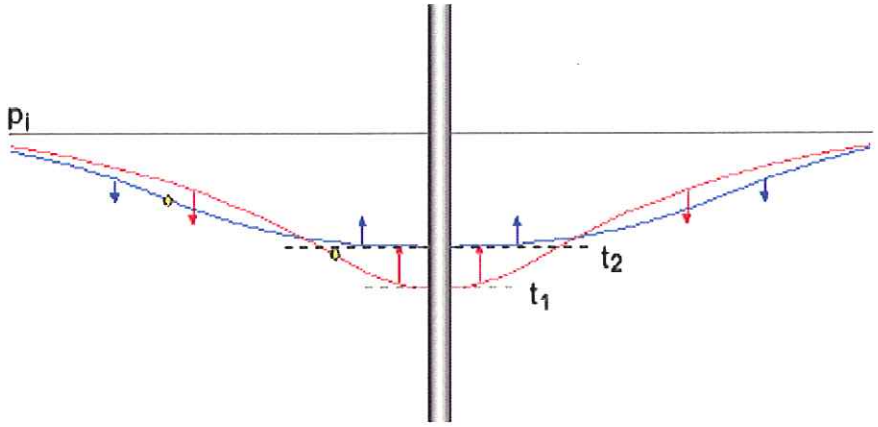

Figure 1-1: Build-Up Pressure (Schlumberger, 1998)

If there is an identification of infinite-acting radial flow, the well test permeability can be easily be derived depending on knowing reservoir thickness.

On infinite-acting radial flow (IARF), fluid flows towards the wellbore equally from all directions. The pressure drop expands radially. The upper and lower bed boundaries are parallel and clearly defined, the reservoir rock between them is homogeneous, and the wellbore is perpendicular to the bed boundaries. IARF is illustrated on Figure 1.2.

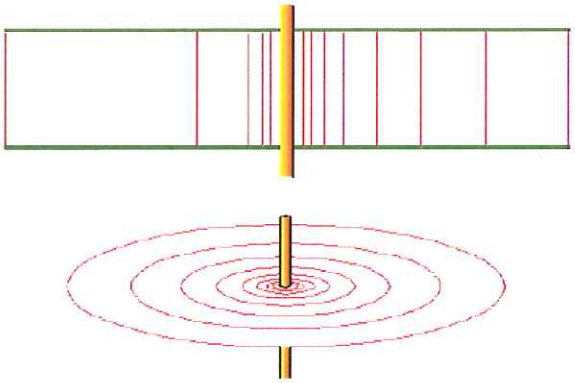

Figure 1-2: IARF (Schlumberger, 1998)

Infinite-acting radial flow is called infinite acting because until the first boundary is reached, the flow pattern and corresponding pressure drop at the wellbore are exactly as would be obtained if the reservoir were truly infinite.

Not only for IARF, but also for other flow regimes (e.g. spherical flow, linear flow) well test permeability can also be derived similarly. The versatility of flow regimes with complex sequence depends upon the heterogeneity and the geometry of the reservoir.

In our study, most of the permeability of the facies is related to the fissure network and it is observed highly in carbonate bodies where channelling is very common. Channelized carbonates are commonly composed of multistoried elements. The combination of composite carbonate bodies of variable thicknesses that are tested as a single element might influence the flow regimes detected in a pressure transient in which the well test interpretation's main objective is to unlock the information contained in pressure transient curves.

All these issues of integrating core and well test permeability could be drawn from different disciplines which are; petrophysics, geology, rock mechanics, statistics and reservoir engineering. In this study, utilization from all these range of disciplines will be realized.

CHAPTER 2

LITERATURE REVIEW

2.1. Permeability and Permeability Measurement Techniques

Permeability of the rock is the measure of the ease with which fluids flow through the rock. It is donated by the symbol k and commonly expressed in units of darcies. Moreover, if a rock is completely saturated with a single fluid, then the permeability is a property of the rock, not the property of the flowing fluid (with the exception of gases at low pressure). This permeability at 100% saturation of a single fluid is termed as the absolute permeability. There is also effective permeability which is the permeability to a particular fluid when there is more than one flowing fluid presented in the rock medium For example, if both oil and water are flowing, the effective permeability to oil is k_o and that to water is k_w. The sum of the effective permeabilities is always less than the absolute permeability. If the effective permeabilities are divided by a base permeability (i.e., the absolute permeability), the dimensionless ratio is referred to as the relative permeability, such as k_{rg} for gas.

2.1.1 Sources of Permeability Data

Various sources of permeability data exists. Generally, permeability data are obtained from core samples, NMR log, formation testers (RFT, MDT etc), and pressure transient tests (DST, mini-DST, well tests, etc.). These permeability data measure different volumes of the reserbvoir and are different in character (absolute or effective permeability) (Shafer and Ezekwe , 2007).

The first technique is the direct measurement of permeability through Darcy's Law in laboratory conditions with a Hassler cell in which the method is described in detailed in 2.3.4 Core Permeability Analysis. Apart from specialized core tests such as thin sections or scanning electron microscopy whole core or core plug are used in laboratory measurement of cores. Thin sections and scanning electron microscopy are available to evaluate the relationship between pore structure and the process being considered. Thin sections are collected from the slab of the core.

There are so many permeameters for measurement of permeability in laboratory conditions except from Hassler cell. To illustrate; Allen, J.C., and Tex, B. (1962) has invented a method for determination of relative gas-oil permeabilities of porous solid materials, such as cores recovered from or representative of underground producing formations. In determining relative gas-oil permeabilities is done by employing live oil a high pressure permeameter and a pressure-volume-temperature (P-V-T) cell are built as a substantially single unit with a flow control means, such as a valve interconnecting the valve and the P-V-T cell. Automated method of determining relative permeability by comprising the steps of injecting known flow rates of water and a hydrocarbon into a core with measuring the differential pressure across said core is firstly introduced by Shen, J.J.S. (1988). Heller, J.P., and Mclemore J.V. (1994) were the first to introduce miniporopermeameter which relates to an apparatus and method for determining the permeability and porosity of small sections at and just below the surface of a slabbed sample of porous rock or other material. Other than these there are still several variations of permeameters developed for measurement of permeability under laboratory conditions.

Hassler cell is the industry standard for laboratory measurement of permeability; however, consistently removing undisturbed rock samples from friable outcrops is difficult. Though, various conventional surface-sealing mini-permeameters are developed as an alternative for permeability measurement. Dinwiddie (2005) introduced and discussed the design and methodology of the small-drillhole minipermeameter probe for a reliable field permeability measurement method to

better achieve small-scale reservoir heterogeneity which plays a substantial role in petroleum migration and reservoir performance.

Starting from the core permeability values, the depth of the investigation for permeability measurement increases with wireline formation tester, which in turn measures permeability at a smaller scale than a well test (Haddad et al., 2000). The constant objective of wireline logging is to obtain a continuous permeability log. However, most of the initial efforts have been directed towards deriving permeability from the combination of porosity with some other log-derived property related to the type of pore geometry. Nuclear Magnetic Resonance (NMR) logging gives excellent results for achieving this in sandstones. However, carbonates the NMR approach sometimes breaks down while managing to generate continuous permeability indicators in complex carbonate formations (Delhomme, J.P.). Yet, the commonly used porosity-permeability transforms often found as inadequate as permeability is also a function of clay distribution, sorting, pore connectivity, turtuosity and variations in other petrophysical properties. The more and more robust permeability estmation could only be evaluated by integrating multiple methods (Taware, S. et al., 2008).

Additionally, in petroleum industry many well testing techniques have been developed and this techniques rapidly became an oilfield standard in order to investigate the rock and the fluid in situ, under actual reservoir flow conditions. By the integration and precise evaluation of well testing methods such as Pressure Drawdown Analysis, Pressure Build-Up Analysis, DST etc. with true flow regime identification global value of permeability can be achieved since the depth of investigation is the biggest in between whole methods.

2.2 Upscaling

Upscaling process is the reverse of scaling. Normally, scaling involves the extrapolation of limited data in order to cover the global behavior. However, upscaling involves in dealing with abundant data within a frame being upscaled and

averages all the values within the frame to a set of representative flow parameters. So, the aim is to reduce the number of gridblocks in a model and represent the reservoir parameters accurately (Novakovic, 2002).

Upscaling can also be described as assigning "effective" properties to coarse scale cells from properties on fine scale grid which is done for reducing CPU time for uncertainty analysis and risk assessment.

2.2.1 Upscaling Methods

In literature, several methodologies have been proposed for upscaling permeability in which some of them are more or less sophisticated depending on the upscaling grid geometry and/or affinity to particular cases (Almeida et al., 1996). Almeida et al. (1996) suggests that upscaling as a concept is treated under several perspectives such as techniques based on the stream tube concept, -study of the turtuosity in porous media -on the renormalization, on means of power *n,* or the formulation of the equation of mass transfer based on mass balance and Darcy's Law.

In broadest terms, the literature regarding upscaling flow parameters in heterogeneous media is enormous. However, methods that are actually used in the development of upscaling can be grouped as following categories: Stochastic (regular perturbation) methods, renormalization theory and volume averaging/homogenization methods.

In upscaling methods two definitions used for upscaled properties: equivalent properties and effective properties.

The term equivalent properties is usually used to indicate a property that has been averaged over a subdomain, where some constraints have been imposed for calculating the property (e.g. permeability). For the example of saturated conductivity, the constraints are that the mean boundary fluxes must be the same and the energy dissipated is equivalent (Renard and Marsily, 1997). Equivalent

parameters are generally sought when upscaling a fine-gird parameter field for calculating a numerical solution on a coarser grid.

The term effective properties is generally reserved for media in which certain statistical constraints have been imposed. Effective parameters are useful because they are functions of only the statistics of the field rather than the particular details of any realization of a field such as in our study.

For some applications, making a division is meaningless because a combination of volume averaging and statistical averaging techniques are both used together (e.g., Kitanidis, 1990).

The first efforts for a stochastic perturbation analysis of unsaturated flow were developed by Yeh et al., (1985a, 1085b, 1985c) for steady flow conditions with anisotropic parameter field statistics. The method involved a conventional linear perturbation analysis that was solved using spectral representation techniques. Russo (1992) was able to combine the theory of Yeh et al. (1985a, 1985b, 1985c) with the concept of the equivalent block permeability to explore how large a heterogeneous domain must be so that the equivalent hydraulic conductivity can be converged into the effective hydraulic conductivity. Finally, Mantolou (1992) was able to extend his previous analysis of unsaturated flow to conditions of nonstationarity statistics. This theory was tested by applying it to field observations (Jensen and Mantoglou, 1992); the stochastic model was able to predict the average system behaviour reasonably well.

In standard normalization technique, a sequential process of upscaling is used to translate fine-grid information up to coarse grids. At each level of upscaling, grid blocks from the previously defined level are grouped, and upscaled parameter properties are determined using finite difference-like techniques. At each step in the upscaling, particular conditions must be imposed at the boundaries of large-scale blocks .

By far the most extensive literature regarding the upscaling of saturated and multiphase flow parameters involves two methods known as volume averaging and homogenization.
The method of spatial homogenization was established as a powerful tool for analyzing multiphase flow systems by the publicationo f monograms by Bensoussan et al., (1978) and more recently by Jikov et al., (1994).

In volume averaging approaches, one seeks to describe the behaviour of a system averaged over a particular volume of porous medium (Whitaker, 1999). The approach can be applied in two distinct modes. In the first mode, the method is used to develop equivalent parameters to upscale structures defined at a fine mesh for use on a coarser mesh. In a second mode, the method is used to develop the effective parameters associated with a representative volume. A representative volume is defined when an effective parameter for a single realization is the same as the effective parameter averaged over the ensemble of all such volumes. The concept of finding the effective permeability which should be the same averaged permeability for whole the reservoir is used in this study.

2.3 Coring and Core Analysis

Coring and core analysis is an application for both qualitative and quantitative interpretation for formation evaluation. Conventional core analyses refer to common procedures that provide information on porosity, permeability, residual fluids, lithology and texture of petroleum reservoirs. On Table 2.1, types of core analyses are listed with the use of their results. On Table 2.2, specialized core analyses with the use of their results are given. Specialized core analysis is done less often, but used for specific applications (Lyons, 1996).

Table 2.1 Types of Routine Core Plug Analysis

Type of Analysis	Use of Results
Porosity	A factor in volume and storage determinations.
Permeability-horizontal and vertical	Defines flow capacity, crossflow, gas and water coning and relative profile capacity of different zones, pay and nonpay zones.
Saturations	Defines presence of hydrocarbons, probable fluid recovery by test, type of recovery, fluid contacts, completion interval
Lithology	Rock type, fractures, vugs, laminations, shale content used in log interpretation, recovery forecasts, capacity estimates.
Core-Gamma Ray Log	Relates core and log depth
Grain Density	Used in log interpretation and lithology

Table 2.2 Types of Specialized Core Plug Analysis

Type of Analysis	Use of Results
Capillary Pressure	Defines irreducible fluid content, contacts.
Rock Compressibility	Volume change caused by pressure change.
Permeability and Porosity vs. Pressure	Corrects to reservoir conditions
Petrographic Studies Mineral Diagenesis Clay Identification Sieve Analysis	 Used in log interpretation. Origin of oil and source bed studies. Origin of oil and log analysis. Selection of screens, sand grain size.
Wettability	Used in capillary pressure interpretation and recovery analysis-relative permeability.
Electrical Formation Factor Resistivity Index	Used in log interpretation.
Acoustic Velocity	Log and seismic interpretation.
Visual Inspection Thin Sections, Slabs	Rock description and geological study.
Air, Water and Other Liquid Permeability	Evaluates completion, workover, fracture and injection fluids; often combined with flood-pot test
Flood-Pot Test and Waterflood Evaluation	Results in values for irreducible saturations, values for final recovery with special recovery fluids such as surfactants, water, and polymers.
Relative Permeability Gas-Oil Gas-Water Water-Oil Oil-Special Fluids Thermal	Relative permeability is used to obtain values for effective permeability to each fluid when two or more fluids flow simultaneously; relative permeability enables the calculation of recovery versus saturation and time while values from flood-pot test give only end-point results.

Routine core analyses can be performed on whole cores or on small plugs that are cut from a larger core. With the exception of petrographic analysis (thin sections, x-ray; scanning electron microscopy, etc.), special core analyses are normally done with core plugs. After a well is drilled and logs are available to identify zones of interest, very small portions of the reservoir can be obtained with percussion sidewall or sidewall drilled cores. Sidewall cores are less expensive and are valuable for petrographic analyses, but are generally not suitable for special core analyses are generally not suitable for special core analyses.

2.3.1 Coring

Well coring refers to the process of obtaining representative samples of the productive formation in order to conduct a variety of laboratory testing. Various techniques are used to obtain core samples: conventional diamond-bit coring, rubber sleeve coring, pressure coring, sidewall coring, and recovery of cuttings generated from the drilling operation. Conventional coring is normally done in competent formations to obtain full-diameter cores. Rubber sleeve coring improves core recovery in softer formations. Pressure coring, although relatively expensive, is used to obtain cores that have not lost any fluids during lifting of the core to the surface.

Core plugs are typically 1 inch to 1 ½ inch (2.5 to 3.8 cm) in diameter and 1 inch to 2 inches (5 cm) long. Core plugs are ordinarily cut perpendicular to the axis of the core, called as horizontal plugs or; parallel to the axis, called as vertical plugs. The terms parallel and vertical are applied for cores cut from a deviated or horizontal wellbore. However until core orientation is measured, the true orientation could not be understood (Schlumberger, 2008).

Besides, a common problem with all of these techniques is to decide when to core. In many instances, cores from the interval of interest are not obtained because of abrupt stratigraphic changes. A second problem is that, typically, non-productive intervals of the desired strata are obtained. These intervals did not initially contain a significant amount of hydrocarbon.

2.3.2 Core Preservation

Preventing wettability changes in core material, after it has been recovered at the surface, can be highly important so that subsequent laboratory measurements are representative of formation conditions. Cores obtained with drilling muds that minimize wettability alteration, and that are protected at the well site to prevent evaporation or oxidation, are called preserved cores. They are also referred to as fresh cores or native state cores. Cores that are cleaned with solvents and re-saturated with reservoir fluids are called restored-state cores or extracted cores. The restoring process is often performed on non-preserved or weathered cores, but the same technique could apply to cores that had been preserved.

There are two methods for preventing conventional cores from changes in wettability after they have been removed from the core barrels. One method consists of immersing the core in deoxygenated formation brine or suitable synthetic brine (i.e., drilling mud filtrate) and keeping the samples in suitable containers that can be sealed to prevent leakage and the entrance of oxygen. In the second method, the cores are wrapped in Saran or polyethylene film and aluminium foil and then coated with wax or strippable plastic.

The second method is preferred for cores that will be used for laboratory determination of residual oil content, but the first method may be preferred for laboratory displacement tests. Plastic bags are often recommended for short- term (24 days) storage of core samples. However, this method will not ensure unaltered rock wettability. Airtight metal cans are not recommended because of the possibility of rust formation and potential leakage. Cores taken with a pressure core barrel are often frozen at the well site for transportation to the laboratory. (Cores are left in the inner core barrel.) Normally, the inner barrel containing the cores is cut into lengths convenient for transport. Because of the complexity of the operation, the pressure core barrel is not used as extensively as the conventional core barrel. An alternate procedure involves bleeding off the pressure in the core and core barrel while the produced liquids are collected and measured. Analysis of the depressurized core is

done by conventional techniques. Fluids collected from the barrel during depressurizing are proportionately added to the volumes of liquid determined from core analysis. In this manner, reconstructed reservoir core saturation is provided (Lyons, 1996).

2.3.3 Core Preparation for Testing

Core samples are cleaned from contaminant hydrocarbons; formation water and drilling fluids with prior aid of "soxhlet extraction" device and using toluene and then waited in vacuum and in alcohol. Cleaned core samples are dried in a temperature-controlled oven at 70 ^{0}C and get prepared for testing after their weights and dimensions are measured.

2.3.4 Core Permeability Analysis

The permeability of core plugs is determined by the flow of a fluid (air, gas, or water) through a core sample of known dimensions. If the absolute permeability is to be determined, the core plug is cleaned so that permeability is-measured at 100% of the saturating fluid. Absolute permeability is a characteristic of the rock and not a function of the flowing fluid. This implies that there is no interaction between the fluid and the rock.

Permeability measurement of a core sample is done by a core sample placed in a Hassler type core cell by flowing a fluid (air, gas or water) through the sample and permeability is calculated with the help of "Darcy Law" and measured permeability values for air, gas or water is corrected via Klinkenberg Slippage and converted to equivalent liquid permeability (k_l) values. When permeabilities to gases are measured, corrections must be made for gas slippage, which occurs when the capillary openings approach the mean free path of the gas. Klinkenberg observed that gas permeability depends on the gas composition and is approximately a linear function of the reciprocal mean pressure. Figure 2.1, shows the variation in permeability as a function of mean pressure for nitrogen, hydrogen and carbon

dioxide. Klinkenberg found that by extrapolating all data to infinite mean pressure, the points converged at an equivalent liquid permeability (k_l), which was the same as the permeability of the porous medium to a non-reactive single-phase fluid. From plots of this type, Klinkenberg showed that the equivalent liquid permeability could be obtained from the slope of the data, m, the measured gas permeability, k_g, a mean flowing pressure p, at which k_g was observed (Lyons, 1996)

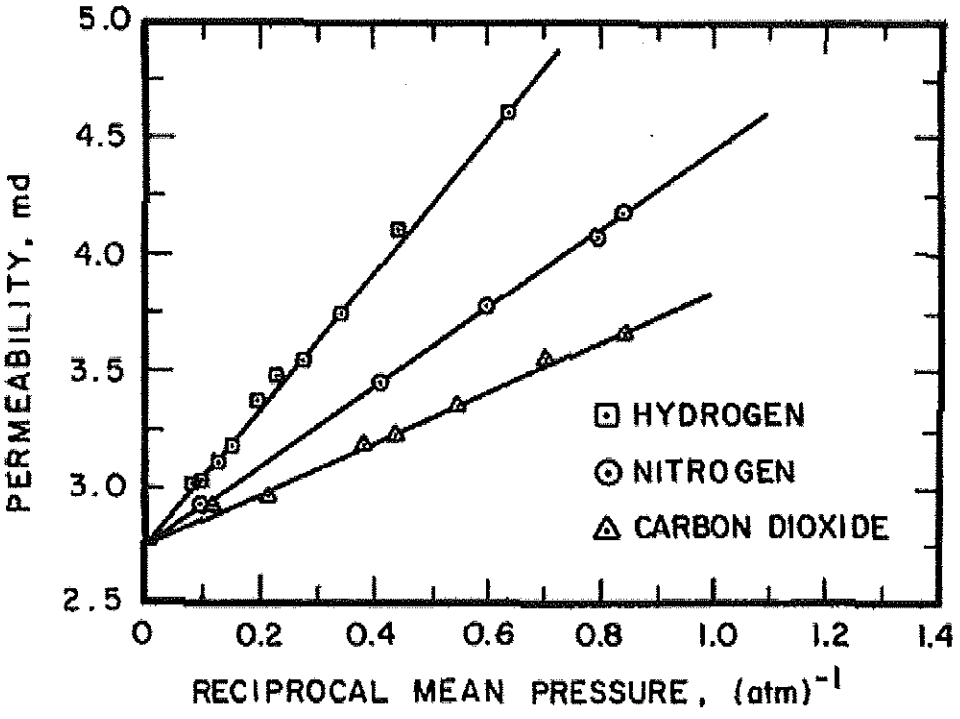

Figure 2-1: Klinkenberg Correction (Lyons, W.C., 1996)

2.3.5 Permeability Measurements under Overburden Pressure

Overburden pressure is the pressure that exists due to the solid mass' weight which is variable but approximately 1.0 psi/foot. Net Overburden pressure is the vectorial sum of the pressures in which the pressures consist of overburden pressure and the formation pressure. Formation pressure (≈0.5 psi/foot), which is the hydrostatic pressure carried out by the fluids in rock pores, acts oppositely to the overburden

pressure. In laboratory conditions, different overburden pressures could be applied (e.g. 800 - 5000) after placing samples in the system.

The production from reservoirs causes decrease in formation pressure with time. So, the net overburden pressure increases and decrease in porosity and permeability values is observed. In our study core plug measurements are taken on unstressed cores. As stated before core plug measurements could also be taken at the confining pressure experience by the rock in situ. At in situ conditions, sandstones are found to have lower permeabilities than at ambient conditions. For good quality sandstones with 15-20% porosity and 200-1000 md permeability, small changes are found up to 10% where stresses are applied parallel to the flow. However, where stresses are applied perpendicular to flow larger changes up to 60% are found. For carbonates, the changes in porosity and permeability with the application of stress are not defined.

Our assumption in our study is that the cores would suffer similarly in permeability from stresses, because the cores to be upscaled are selected within similar depths and similar geometry in this single reservoir.

2.4 Reservoir Heterogeneity

Reservoir heterogeneity is known as a ruling factor for reservoir performance. In literature, there are plentiful studies examining the impact of heterogeneity both theoretically and for actual field data. Heterogeneity is the variation in properties existing everywhere in naturally occurring permeable media and it is one of the most important factors in having a knowledge regarding fluid flow (Lake and Jensen, 1989).

2.4.1 Permeability Heterogeneity

The heterogeneity in reservoir is mostly pronounced in permeability. The measures are in two categories: static and dynamic. In this study, statistical properties of

reservoir heterogeneity by assessing permeability are taken into account by considering the coefficient of variation, The Dysktra-Parsons coefficient and Lorenz coefficient (petrophysical analysis). All three measures are used for permeability heterogeneity but in literature there are examples of including porosity data. In all three measures permeability is assumed to be a scalar quantity. In these measures samples are treated as independent and representative data (Lake and Jensen, 1989).

2.4.2 Coefficient of Variation

Permeability heterogeneity has been defined by the standard deviation of a data set normalized by the arithmetic average (mean) (Corbett and Jensen, 1992; Jensen et al. 1997). This dimensionless ratio is the coefficient of variation (Cv).
Cv is defined to be;

$$C_v = \frac{\sigma}{\mu} \qquad (2.1)$$

σ is standard deviation and μ is mean.
Under this classification, for Cv<0.5, reservoirs are considered to be homogeneous; for 0.5<Cv<1.0, heterogeneous; and for Cv>1.0 very heterogeneous.

The number of measured samples of core plugs taken from the reservoir needed to satisfy the permeability estimation can be calculated within a 95% confidence interval owing to the formation heterogeneity associated with Cv (Hurst and Rosvoll, 1991). The formula is:

$$N_0 = (10.C_v)^2 \qquad (2.2)$$

Oppositely, for a given number (N) of measurements the error tolerance (P) of the permeability estimate can be approximated as follows providing sample numbers exceed 10:

$$P = \frac{(200.C_v)}{\sqrt{N}} \qquad (2.3)$$

2.4.3 The Dysktra-Parsons Coefficient

Original study of Dysktra-Parsons was foreseeing using mini-permeameter measurements, however in general core plug permabilities are used. V_{DP} the Dysktra-Parsons coefficient, which is a measurement of heterogeneity, is also called as "the coefficient of permeability variation", "the varience", or "the variation".

The method consists of plotting assigned log permeability versus probability scale and adding a linear trendline . The trendline is used to determine the 84^{th} percentile and the median 50^{th} percentile, the coefficient estimate then follows from:

$$V_{DP} = \frac{k_{0.50} - k_{0.84}}{k_{0.50}}. \qquad (2.4)$$

2.4.5 The Lorenz Plot

Lorenz coefficient is another measure of reservoir heterogeneity which is defined by Lorenz Plot which is a petrophysical plot (Jensen and Lake, 1988; Jensen et al., 1997). The Lorenz Plot (LP) also called as Lorenz curve is a plot of transmissivity assuming constant viscosity (permeability–thickness product, k.h,) or flow capacity, versus storativity (porosity-thickness product, φ.h, assuming constant compressibility) for each of the petrophysical measurements. Transmissivity and storativity are important elements in the diffusivity equation used in well test interpretation. Thus, the Lorenz Plot becomes a useful plot in the interpretation of core data and well test interpretation.

While creating a Lorenz Plot the core plug data are conventionally ordered by decreasing k/φ so that $k_{(1)}$ is the layer with thickness $h_{(1)}$ and the largest permeability while $k_{(n)}$ is the layer with thickness $h_{(n)}$ and the smallest permeability. In a

homogeneous reservoir, these transmissivity and storativity elements are in a balance, and the data plot is along the diagonal, while in a heterogeneous reservoir, there is a significant departure from the diagonal. The departure from the diagonal defines an area that is quantified as the Lorenz coefficient (Jensen et al., 1997).

When the core plug data are ordered in stratigraphic order rather than decreasing k/φ, the plot of flow capacity will be computed on a flow unit basis and will maintain its stratigraphic position. This plot of flow capacity versus storativity is unlike the traditional Lorenz Plot in which it preserves its stratigraphic information and called as Modified Lorenz Plot (MLP). Corbett et al. (1998) suggests that after combining Lorenz Plot with Modified Lorenz Plot for characterization of reservoir heterogeneity; the integration of core permeability measurements, composite logs and Pressure Logging Tool (PLT) can assist in understanding the entry points of the fluids into the well so that the effective flowing interval can be determined and interpretation of early time transient data in well tests.

CHAPTER 3

GEOLOGICAL BACKGROUND

3.1 Generalities on the B. Field

B. Field is located in South East of Turkey in which the discovery well had started production on 1961. The Initial Oil in Place (IOIP) is about 1.85 billion stock tank barrels (stb) and the recoverable oil amount is 185 million stb. At the end of 2008 the total number of wells drilled would be most probably 355. By June 2008, the number of wells continuing to produce was about 150 and daily average production rate was 7,440.00 bbl.

The structure of the field is an elongated asymmetric anticline, which is about 17 km long and 4 km wide. The produced oil is a heavy oil having 9.5-13.5^0 API in the Upper Crateceous limestone. The gross thickness of the reservoir ranges from 60 m to 80 m and decreasing southward. The total height of the oil column is about 210 m due to tiltings etc.with a 100% water saturated oil water contact at 630 m subsea and the reservoir is limited in the southwest by a reverse fault system and in the southeast by a permeability barrier.

3.2 Regional Geological Framework

B. Field belongs to the folded zone located on south of the Taurus thrust zone. The anticlinal is largely elongated trending W-NW to W-SW show a decrease of the intensity of deformation southwards. Many of the asymmetrical anticline structures are associated with major thrust faults that border the structures. Several major

depositional ages were recognized such as; Cambro-Devonian, Permo-Carboniferous to Upper Jurassic, Lower Crateceous to Lower Eocene and Middle Eocene to Recent.

The Mesozoic was a period of tectonic instability in South East Turkey, thus numerous gaps are present in stratigraphic record.

The Jurassic to Eocene sediments are mostly composed of carbonates occasionally interbedded with shales.

Jurassic deposits are poorly developed and Lower Crateceous sediments are still missing in large parts of South East Turkey. After the deposition of the subreefal M. Formation of Cenomanian-Turonian age, the carbonate platform was tilted and by the end of the Turonian the tectonic began to influence the sedimentation. The varicolored shales and silts of the K. Formation of Campanian to Maastrichtian age unconformably overlay the M. Formation. Table 3.1 illustrates general stratigraphic/lithological units of the B. Field area (Beicip-Franlab, 1994; Beicip-Franlab, 1996).

Table 3.1 General Stratigraphic/Lithological Units of the B. Field (Beicip-Franlab, 1994)

Age	Formation	Lithology	Approximate thickness (m)
Paleocene	Upper Ge.	Shales with sand and carbonate intercalations	ab.650
Maastrichtian	Lower Ge.	Shale with limestone/dolomite intervals	100-160
to	Ga.	Reefal to subreefal limestone	50-85
		(packstone to wackestone)	
Campanian	K.	Shale and Silts with plant debris-coal seams	80-120
Cenon-Turonian	M. Group	Limestone	n. 20
		Limestone or dolomite	

3.3 Structural Model of B. Field

Beicip-Franlab's study in 1994 and 1996 showed that the structure belongs to a series of ranking folds and matches with an asymmetrical anticline trending E-W. Its southern flank is affected by a reverse strike slip fault system. The throw of about 10 m in the central area increases up to more than 100 m in the north-western area.

The northern flank presents a set of W-NW-E-SE trending normal faults with weak throws.

The fold is affected by a tear fault pertaining to the right side roughly oriented NW-SE and shifting the main axis of the structure. Minor normal faults have been interpreted to be parallel to the subjected tear fault. Other trends if the faults could not be estimated. However, the throw of these faults estimated not to exceed 10 to 15 m. They probably do not act as permeability barriers. The NW-SE Schematic Cross-Section of B. Field is illustrated in Figure 3.1. Additionally, N-S Structural Cross-Section of Western Area (Figure 3.2) and Central Area (Figure 3.3) of B. Field are given in here.

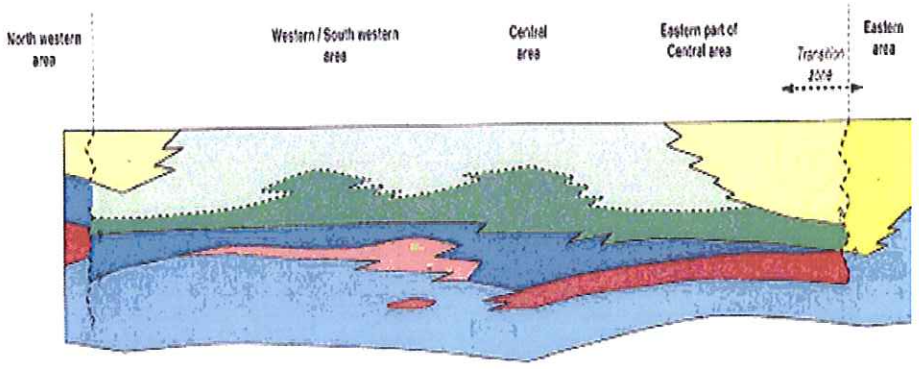

Figure 3-1: NW-SE Schematic Cross Section of B. Field (Beicip-Franlab, 1994)

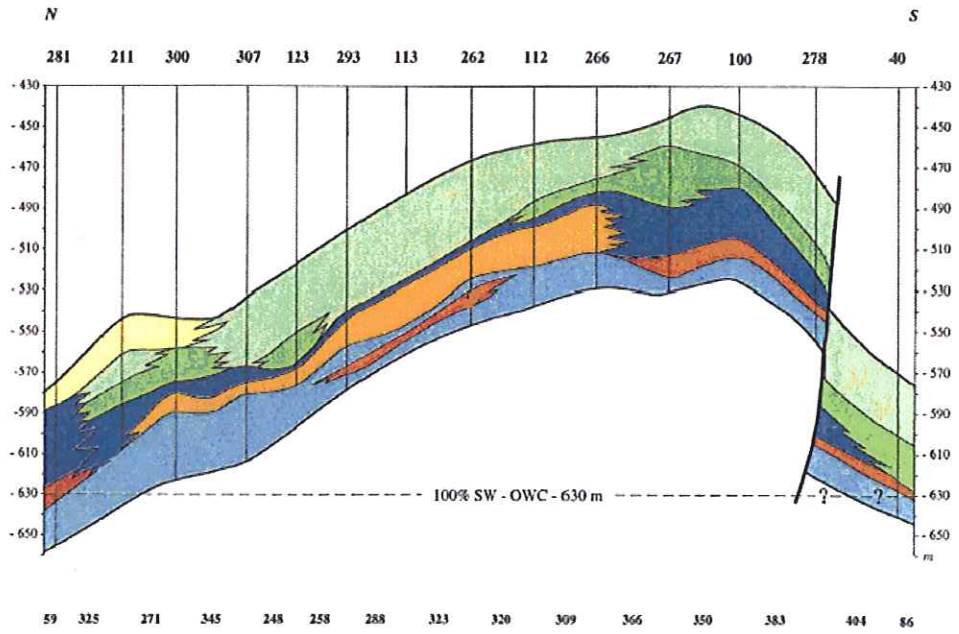

Figure 3-2: N-S Structural Cross Section of B. Field (Western Area)
(Beicip-Franlab, 1994)

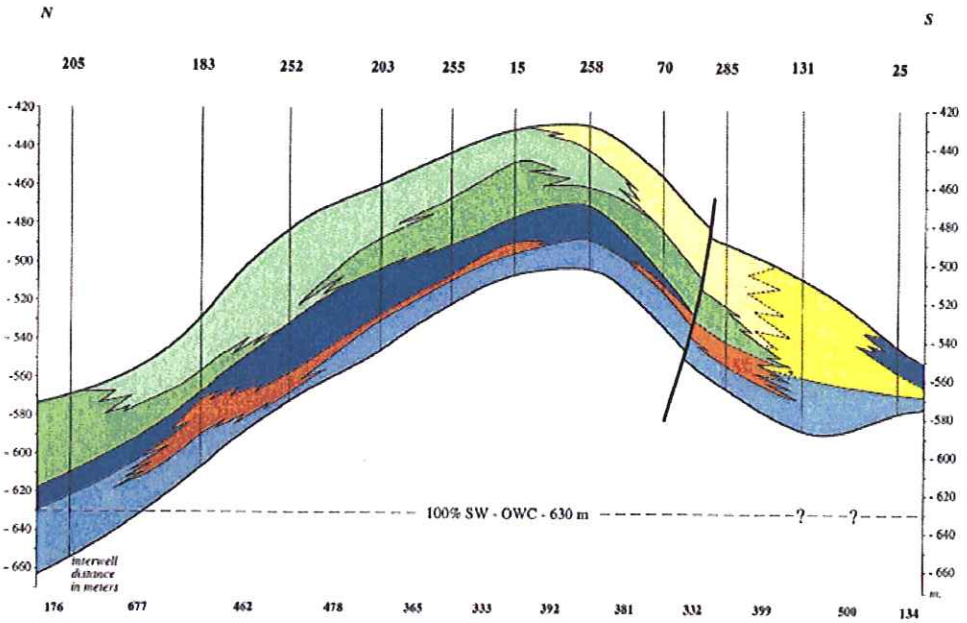

Figure 3-3: N-S Structural Cross Section of B. Field (Central Area)
(Beicip-Franlab, 1994)

3.4 Lithology and Depositional Environment

Due to the rapid lateral variations of facies which can be observed frequently in this type of environment Ga. limestone shows a very heterogeneous mixture of facies. Also, diagenetic processes of the sedimentary rock which are compaction, dissolution, precipitation and re-crystallization strongly modified the original characteristics of these sediments

3.5 Diagenesis

Owing to the repeated sub-aerial exposures during sedimentation on the unstable shelf, the physical and chemical changes taking place in the sediments or sedimentary rock between deposition and either metamorphism, or uplift and weathering took place strongly, which affected the original packstone/wackestone. Ga. limestone was raised into the upper part of the fresh water subterranean zones where dissolution of the material occurred. The dissolution caused mouldy and vuggy porosity. Vugs and molds were partly or completely cemented by sparry calcite resulting in a more or less erratic distribution of tight cemented packstone and soft porous packstone. This resulted in a very heterogeneous distribution of facies/reservoir units (Beicip-Franlab, 1994).

3.6 Distribution of the Reservoir Units

Geographical zonation of the Ga. limestone reservoir, excluding the lower non-reservoir unit E is given in Figure 3.4. These zones are as flows from Southeast to Northwest which are basically described depending mostly on the properties of the porous media, not exactly the sedimentological classification since the reservoir is highly heterogeneous.

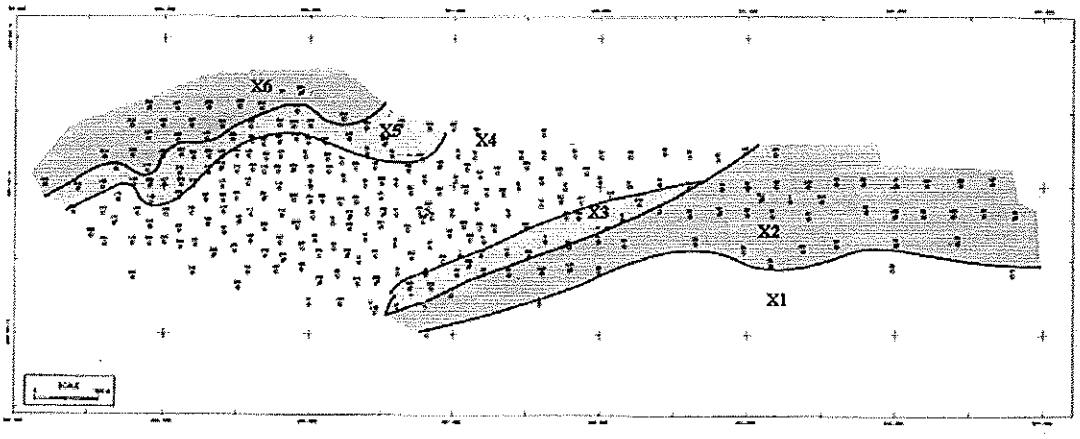

Figure 3-4: Geographical Zonation of B. Field
(Beicip-Franlab, 1994)

Zone X1: Intercalation of tight and porous limestones with low permeability decreasing southwards.

Zone X2: Mostly represented by a thick homogeneous porous/permeable and weakly fissured .

Zone X3: Porous/permeable matricial reservoir is largely dominant. A few tight fissured layers are interbedded.

Zone X4: Characterized by a thick section made up of tight fissured facies and porous/permeable facies in variable proportions. From top to the bottom the units are: B, D, F, G.

Zone X5: Upper homogeneous thick porous matricial section overlying a heterogeneous matricial/tight fissured section. Units represented are: A, B, D (G)

Zone X6: Mostly characterized by two porous/permeable sections weakly fissured (Units A and E) separated by a poorly fissured tight unit C.

3.7 Updates on Geological Model

The introduction of 2D and 3D seismic survey studies helped in redefining the major and minor fault systems which there had been too many uncertainties relating to them since they were defined depending on the well test and log interpretations. With

the indication of the fractured regions, the structural elements of the field has been updated, including the new assumptions incorporating the 2D seismic volumes and production behaviours. However, a recently dominated hybrid model has been developed with 3D seismic survey, which has been carried out in the western part of the field covering approximately one-third of the field (Arslan, 2007).

For a comparison the structural map before the 2D and 3 D seismic surveys is given in Figure 3.5 and the new structural map of Ga. Formation using 2D and 3D seismic surveys is given in Figure 3.6. In Figure 3.5 the divided sections correspond to the gathering stations' zone of production. Additionally, the new cross section showing lateral and vertical extensions of facies, from the central part of B. is given in Figure 3.7.

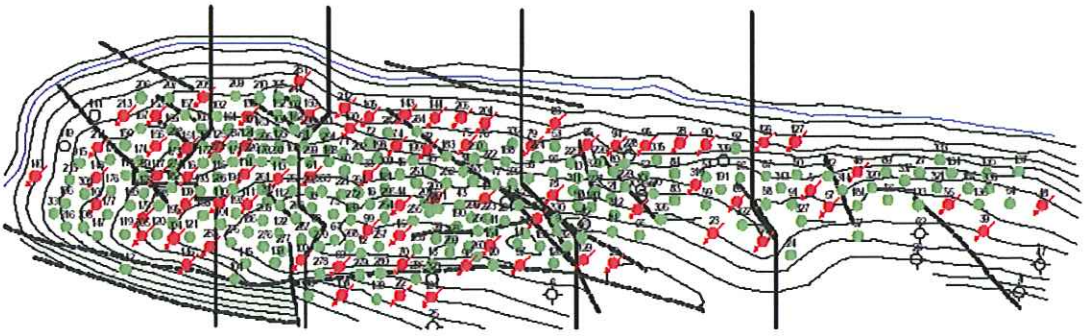

Figure 3-5: NW-SE Structural Map (Old Version) (Sahin, S., et al., 2007))

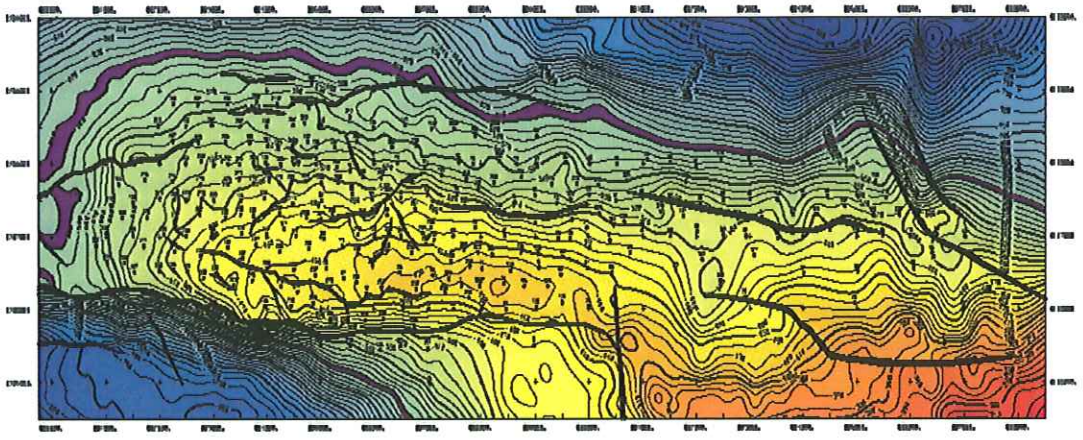

Figure 3-6 NW-SE Structural Map (New Version) (Arslan et al., 2007)

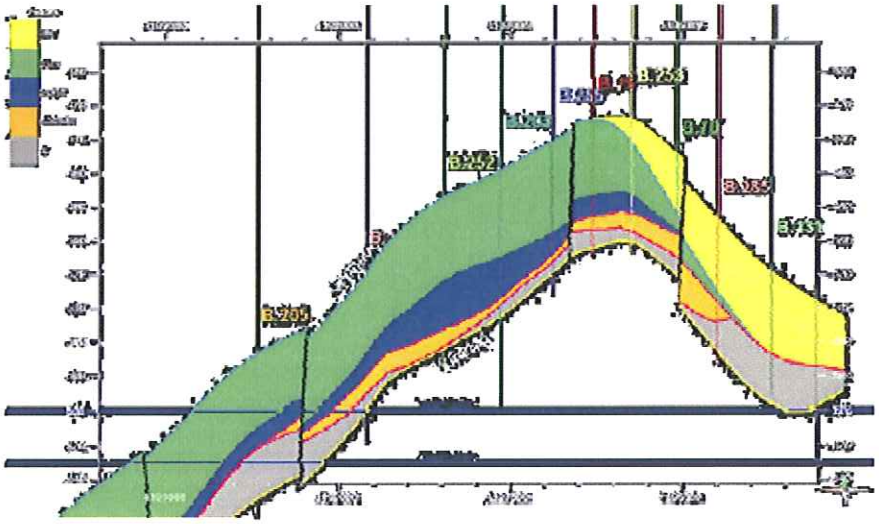

Figure 3-7 Structural Cross-Section (Cental Area-New Version) (Arslan et al., 2007)

CHAPTER 4

STATEMENT OF THE PROBLEM

The main aim of the study is to highlight the uncertainties in reservoir permeability by making a comparison in between core plug measurements (static data) and well test data (dynamic data). To achieve this challenging task geological, statistical and engineering issues will be considered. As a result, necessary information on the near well geological architecture of the field could be gained and contributed for the assessment of reservoir simulation.

CHAPTER 5

METHODOLOGY AND APPLICATIONS

The first step is to explore the inventory of both well test and core plug measurements and consider them with respect to their scales of measurement. After exhibiting the history of core plug measurements and tested wells; the depth interval of the core plug measurements will be documented and they will be compared with the producing interval acknowledged in well tests.

After matching the core plug measurements and well test data regarding well numbers and depths of measurement; in order to expand the variety of data sets in this study, the possibility of interrelating non-overlapping different wells' data within themselves according to their geology (distribution of the reservoir units etc.) and petrophysical properties will be investigated.

Formerly, the statistical methods will be used to comprehend the reservoir heterogeneity by evaluating core plug data concerning the density of the measurements. The reservoir heterogeneity will be examined by practising diverse methods. Determining the reservoir heterogeneity will lead to understand the ruling factor for reservoir performance. Petrophysical analysis methods will be combined with these studies, so that the flowing interval could be determined clearly.

Subsequently, representative well test measurements will be interpreted primarily for identification of flow regimes which appears as characteristic patterns displayed by the pressure derivative data. A regime is the geometry of the flow streamlines in the tested formation by using only the portion of the transient data. This will be also

contributing to understanding the near wellbore geology and effective flowing interval.

After that, integration of core plug measurements and well test interpretations will be executed by using averaging methods within the frame to a set of representative reservoir permeability values. So as to integrating these static and dynamic (performance) data, the aggregate permeability of the system will be tried to fit in a averaging solution. In the case of flaws in the approach, the reasons of the flaws will be further investigated.

5.1 Available Data

Pressure Build Up Tests for 26 wells and core plug analysis for 32 wells have valid data in order to be used. Total number of core plug permeability data used in this study is 1198. and the total number of available pressure build-up tests used in this study, which were previously interpreted by Turkish Petroleum Corporation (TPAO) Production Department staff, is 45. After having a look to the core plug and well test permeability data it is seen that only two wells have both measured well test data and core plug permeability data which are well#2 and well#172. Pressure build-up test results are given in Appendix A with their identified flow regimes and boundary types.

The wells which have permeability analysis results from core plugs and pressure build-up tests are marked on both structural maps (old version-Figure 3.5 and updated version –Figure 3.6). The wells that have core plug permeability measurements are marked with the diamond shaped arrow and projected to the updated version of structure map with the dotted lines. The wells that have well test permeability measurements are marked with the oval-shaped arrow and projected to the updated version of structure map with the constant lines. The figure is given in Figure 5.1.

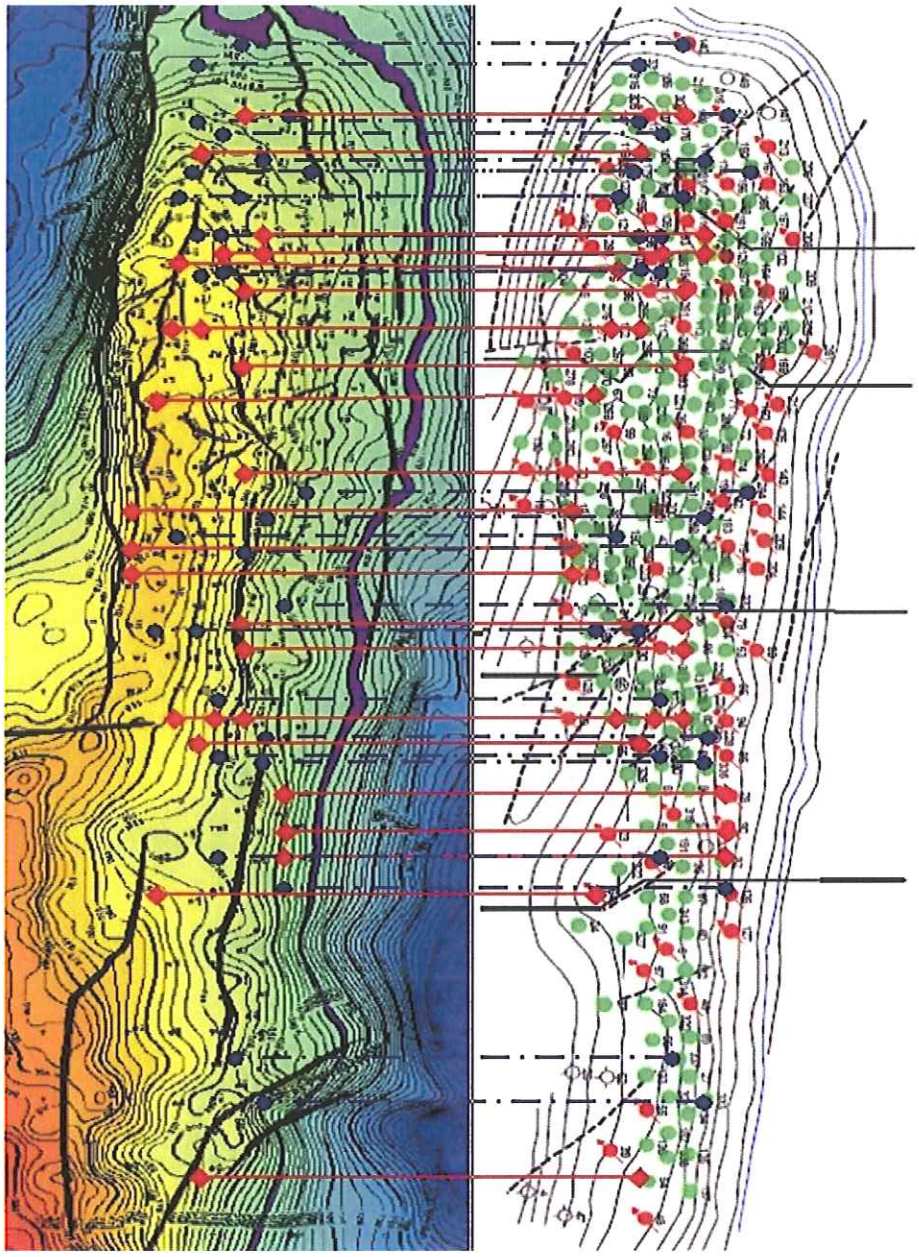

Figure 5-1 Comparison of Structural Maps

The projection resulted in identification of the wells in new structure map. So that while interrelating the core permeability and well test measurements -related both of the structure maps could be taken into the account for comparison.

5.2 Descriptive Statistics of Raw Core Plug Data

The equivalent liquid permeability data available for core plugs are investigated as statistical measures so that statistical properties are reviewed here. The first attempt is to identify basic statistical properties of core plug permeability data for each well such as median, mean, standard error, mode, standard deviation, kurtosis, skewness etc.

In probability theory and statistics, median is described as the number separating the higher half of the sample, a population, or a probability distribution from the lower half.

The standard deviation is a measure of the dispersion of a collection of numbers. It is applied in our table to a data set.

The standard deviation is usually denoted with the letter σ (lowercase sigma). The standard error of a method of measurement or estimation is the estimated standard deviation of the error in that method. Specifically, it estimates the standard deviation of the difference between the measured or estimated values and the true values. True value of the standard deviation is usually unknown and the use of the term standard error carries with it the idea that an estimate of this unknown quantity is being used. It also carries with it the idea that it measures not the standard deviation of the estimate itself but the standard deviation of the error in the estimate.

The mode is the mostly occurrent frequency in a data set.

Skewness is described as a measure of the deviation of a distribution from symmetry. The skewness of a normal distribution is zero, so that a positive value for this parameter indicates a distribution with a positive skew (Sahin, A., et al., 2007). Sahin, A., et al., (2007) also describes kurtosis as the measure of the flatness or peakedness of a distribution, relative to a normal distribution. Higher kurtosis means more of the variance is due to infrequent extreme deviatians, as opposed to

frequently modestly-sized distributions. The kurtosis can be positive without a limit exceptionally it can be negative for a point distribution or degenerate distribution in which supporting data consists of only from a single or insufficient data. When a distribution is more peaked than the normal results in a positive value it is called as leptokurtic and when the distribution is more flat than the normal results in a negative one called as platykurtic.

In descriptive statistics, the range is defined as an indication of statistical dispersion which is the difference between the highest and the lowest value.

As the assessment of descriptive statistics is done, the assortion and the variances in statistical measures of the data set in this study could have been seen.

5.2.1 Heterogeneity Analysis of Raw Core Plug Data

Preliminary heterogeneity analysis of raw core plug data is done by finding out the coefficients of variation (C_v).

Error tolerances (P), and ideal sample numbers needed to precisely define reservoir heterogeneities without an error tolerance are introduced. However in this stage, it could be apprehended that it is too early to interpret the reservoir heterogeneities and reservoir permeability.

5.3 Facies Determination

Before introducing the averaged data to represent the reservoir permeability , the reservoir heterogeneities must be understood more clearly. In order to achieve this, the error to be introduced within the averaged data could be minimized using the appropriate averaging scheme for identified facies types and layering (Jackson et al., 2003).

Thus, the thicknesses of facies are introduced which were deduced from the latest geological and reservoir modeling of B. Field by using Petrel 2008-1, Schlumberger Information Solutions (SIS) software. The depths of the facies and the thicknesses of these facies for each well having whether core plug or well test data are given in Appendix B.

5.3.1 Facies Discrimination of Raw Core Plug Data

Afterwards, core plug data are sorted for their depths. Next, the facies they are belonging to are determined. The arithmetic mean permeabilities of the facies of wells and the number of core plug data in each facies of the wells are determined. Some of the facies in wells' profiles do have insufficient data for understanding the heterogeneities. While calculating the Cv's, the error tolerance could be understood for sample numbers exceeding 10, the number of the core plug data for facies to be evaluated should have been at least 10. However, since the data set is limited, core plug data for facies having sample numbers exceeding 5 are only evaluated, the rest is trimmed.

Since the variety of distinct facies and their layout is characterized, the main aim is to define permeabilities' diversity with facies structure, relating to the depositional and post-deposional environments. In order to achieve this, an empirical approach will be used and modeled through following up core permeability data. By previous reservoir heterogeneity calculations, it is observed that it is not sensible to make a single statistical analysis on permeability values taken from a mix of distinct facies (Lu et al., 2002).

5.4 Trimming of Noise Data

The range and the distributions of core plug permeability data were investigated empirically by forming a bin of data which is constituted by observing the intervals of frequently existing core permeability data.

After empirically observing the core permeability data distribution; it can be seen that most of the increment distributions of the facies of wells which are having sufficient data, show similar peaked frequency distributions except from untrimmed noise data. Since upscaling involves in dealing with abundant data and averages all the values within the frame to a set of representative flow parameters; the process of trimming noise data is also a part of permeability upscaling (Novakovic, 2002).

The data pertaining to the margins are trimmed and the outlying core plug data is refined. No more data to evaluate Facies C and Facies F existed after noise data cleaning.

The point in doing that is to look for resemblance for each facies to implement the general trend of permeability frequency distributions for each facies of wells which should be anologous to probability density functions reflecting Gaussian distribution.

By refinement of noise data using symmetrizing method which was used before for probability density functions; it is known that good results can be achieved (Emerson and Stoto, 1982). However, it is also a fact that a symmetrical histogram approach is not necessasily giving Gaussian distribution (Jensen et al., 1987).

5.5 Descriptive Statistics and Heterogeneity Analysis of Trimmed Core Plug Data

Furthermore, descriptive statistics are computed again and new C_v's are found for the refined data.

Error tolerances (P), and ideal sample numbers needed define reservoir heterogeneities are introduced again, but this time for the trimmed data.

After statistically analysing the data set and determining the coefficients of variation it is seen that refinement of core permeability data decreased uncertainties up to a level. However heterogeneities still vary too much, and there is still no possibility for

averaging permeabilities for finding facies permeabilities and global permeability values for each well.

In order to step forward and scale up the core plug data; the trimmed core plug permeability data sets of facies are further eliminated and refined due to having error tolerance (P) more than 75% and N_0/Count above 11.

5.6 Normality Check and Normalization of Trimmed Core Plug Data

Next step is the normality check of the data sets. Probability density functions and histograms of core permeability data are plotted via using Easy Fit 5.0 Professional software. The distribution of the data are checked for their goodness of fit to a normally distribution.

Goodness of fit tests measure the compatibility of a random sample with a theoretical probability density function. In other words, these tests show how well the distribution fits to the data.

Three measurement methods as Kolmogorov-Smirnov, Anderson-Darling and Chi-Squared are used in this study.

Kolmogorov-Smirnov statistic (D) is based on the largest vertical difference between the theoretical and the empirical cumulative distribution function:

$$D=\max_{1\le i\le n}\left(F(x_i)-\frac{i-1}{n},\frac{i}{n}-F(x_i)\right) \qquad (5.1)$$

The hypothesis regarding the distributional form is rejected at the chosen significance level (α) if the test statistic, D, is greater than the critical value obtained from a table. The fixed values of α (0.01, 0.05 etc.) are generally used to evaluate the null hypothesis (H_0) at various significance levels. The standard tables of critical values used in tihis test are valid for only testing whether a data set is from a normal

distribution. The P-value in contrast to fixed α values, is calculated based on the test statistic, and denotes the threshold value of the significance level in the sense that the null hypothesis (H_0) will be accepted for all value of α less than the P-value. For example, if P-0.025, the null hypothesis will be accepted att all significance levels less than P(i.e. 0.01 and 0.02) and rejected at higher levels, including 0.05 and 0.1.

In other words, if Statistic,D<Critical values and P-value>α the hypothesis should be accepted for stated significance level.

The Anderson-Darling statistic (A^2) is defined as:

$$A^2 = -n - \frac{1}{n}\sum_{i=1}^{n}(2i-1).[\ln F(X_i) + \ln(1 - F(X_{n-i+1}))] \quad (5.2)$$

Likewise Kolmogorov-Smirnov Test, the fixed values of α (0.01, 0.05 etc.) are generally used to evaluate the null hypothesis (H_0) at various significance levels.

In The Anderson-Darling Test, if Statistic, A^2<Critical values; then the hypothesis should be accepted.

The Chi-Squared Test is also used to determine if a sample comes from a population with a specific distribution. The Chi-Squared statistic is defined as:

$$x^2 = \sum_{i=1}^{k}\frac{(O_i - E_i)^2}{E_i} \quad (5.3)$$

Where O_i is the observed frequency for bin i, and E_i is the expected frequency for bin calculated by;

$$E_i = F(x_2) - F(x_1) \quad (5.4)$$

Where F is the cumulative distribution function of the probability distribution being tested, and x_1, x_2 are the limits for bin i.

The hypothesis regarding the distributional form is rejected at the chosen significance level (α) if the test statistic is greater than the critical value defined as:

$$X^{2}_{1-\alpha,k-1} \qquad (5.5)$$

Meaning the Chi-Squared inverse CDF with k-1 degrees of freedom and a significance level of α. Though the number of degrees of freedom can be calculated as k-c-1 (where c is the number of estimated parameters).

In the same way to the Kolmogorov-Smirnov Test, if Statistic,X^2<Critical values and P-value>α the hypothesis should be accepted for stated significance level.

5.6.1 Normalization of Core Plug Data Using Box-Cox Power Transformation

After searching for the distributions of the core plug data if they are normally distributed or not; normalization using Box-Cox Power Transformation method is applied for the ones which are not normally distributed. Box and Cox presented the method for normalization of data based on maximum likehood (Jensen et al., 1987). Data transformation, and particularly the Box-Cox power transformation, is one of the remedial actions that may help to make data normal. Transforming data means performing the same mathematical operation on each piece of original data.

The statisticians George Box and David Box developed a procedure to identify an appropriate exponent (Lambda=λ) to use to transform data into a "Gaussian Shape". The lambda value indicates the power to which all data should be raised (Box and Cox, 1964). In order to achieve this, the Box-Cox power transformation searches from Lambda= -2 to Lambda= +2 to find the optimum value.

The normalization procedure is applied by using Statgraphics Centurion XV software.

5.7 Reservoir Heterogeneities for the Normalized Core Plug Data

5.7.1 Coefficient of Variation

After the normalization of the data, again coefficients of variation are calculated for determining the last level of reservoir heterogeneities for the refined and normalized data sets.

5.7.2 The Dysktra-Parson's Coefficient

To further investigate and crosscheck the reservoir heterogeneities, The Dysktra-Parson's coefficients are calculated. The semi-log plots, constituting from core plug permeabilities vs. probability of these permeabilities in data sets, are formed.

5.7.3 The Lorenz Plot & The Lorenz Coefficient

The next step is to find out Lorenz coefficients for each facies. To achieve this, equivalent liquid permeabilities are ordered in decreasing k/φ. The transmissivities and storativities for the ordered data are calculated and listed. The transmissivity is also named as fluid flow capacity and storativity is named as storage capacity. The sum of the sequence of these terms are calculated with addition operations between them. Then, these ordered series data are proportioned to the sum of the series. Thus, fractions of total fluid flow capacity and total storage capacity are found out for the facies interval. Fractions of fluid capacity vs. storage capacity is plotted. Hence, Lorenz Plot is formed. By figuring Lorenz Plot, the reservoir heterogeneities could be further investigated and the flowing intervals for the range of data could be understood.

In Lorenz plot, a curvature forms, which will determine the Lorenz coefficient. Additionally, a diagonal is plotted from the origin of the x,y axis. The departure of the curve from the diagonal is the indication of the reservoir heterogeneity. Additionally, sharp deflections are also an indication of particular effective flowing intervals. The Lorenz Plots can also be figured by ignoring the porosity of the interval and can be ordered within that context. However, the difference between other statistical measurements to identify reservoir heterogeneity is the contribution of porosities into the system and making a comparison in the increase of total fluid flow capacity and total fluid storage capacity.

Lorenz coefficients are determined by calculating two times the area underlying the curve subtracted by the area underlying the diagonal. The stated area is found by identifying the most fitting polynomial trendline and determining this polynomial function's equation. The equations of polynomial functions are also given in the Lorenz Plots. The integrals of the polynomial functions are calculated. Resultedly, the Lorenz coefficients are easily found out.

5.8 Comparison of Well Test Permeability & Upscaled Core Plug Permeability Data

Lastly, the pressure build-up test results in this study's inventory (Appendix A) are used for comparing with upscaled core plug permeability data. The arithmetic, geometric and harmonic averages of the upscaled core plug permeability data for each facies of wells are formed. Additionally, overall facies means are found out.

The wells having consistent pressure build-up test results are selected by seeking for having considerable test durations, well determined flow regimes, ETR, MTR. Also, facies distributions of the wells are taken into account since the after refining and normalization procedure for some facies (Facies C, E and F) no data to be evaluated is left.

The remaining pressure build-up tested wells' facies distribution and thickness of the facies' are identified. After normalization and refinement procedure the most reliable and accountable data to be representative for whole reservoir system is the upscaled data. In comparison of well test permeability data with core plug data, the whole depth of well section is taken into account as the interval contributing to the production in order to derive permeability from transmissivity, however for core plug permeabilities facies thickness of pressure build-up tested wells' are taken into account and overall facies average permeabilities are taken since they are the most representative and upscaled data amongst all and each facies' transmissivity is added and total transmissivity is divided by the overall thickness of facies and averaged permeability is found. The results are proportioned and the beginning question which was asking which average does the well test-derived permeability represent and over what region this average is valid is tried to be answered.

CHAPTER 6

RESULTS AND DISCUSSION

6.1 Available Data

The available data is found out to be really consistent and the sample numbers for core plug permeability measurements is really sufficient to be upscaled and understand the heterogeneity level and the distribution of the permeability for each facies. However, for core plug data some facies could not be evaluated. However, their contribution to the flow is regarded as the coincidence to the data regarding these facies in this large data set is very small and this assumption is crosschecked with the literature (Beicip-Franlab, 1996).

6.2 Descriptive Statistics of Raw Core Plug Data

The first attempt is to identify basic statistical properties of core plug permeability data for each well. In Table 6.1, the count of the samples (sample number) and basic statistical measures which are mean, standard error, median, mode, sample variance, standard deviation are given. All of these measuremements are very dispersed and varying and there are significant variances in median and mean of these distributions. Wells which do have more sample numbers do also have bigger standard deviation, sample variance and standard error. The uncertainty deepens as the number of the core plug data increases. This can be an indication of the content of the noise data and the outlying data due to measured core plug samples which were taken from fissured highly permeable points or etc.

Table 6.1 Descriptive Statistics of Raw Core Plug Data

Well Number	Mean	Standard Error	Median	Mode	Standard Deviation.	Sample Variance	Count
2	118.80	0.00	118.80	N/A	-	-	**1**
24	3.74	0.00	3.74	N/A	-	-	**1**
86	63.23	41.21	44.49	N/A	71.37	5093.56	**3**
126	14.05	9.51	5.03	N/A	16.48	271.46	**3**
140	53.51	0.00	53.51	N/A	-	-	**1**
155	66.91	22.94	69.73	N/A	60.69	3683.10	**7**
167	0.65	0.00	0.65	N/A	-	-	**1**
172	51.14	17.48	11.45	0.03	172.14	29632.12	**97**
174	39.78	11.86	2.64	0.03	70.15	4921.50	**35**
176	10.86	3.76	1.82	0.01	28.17	793.35	**56**
177	3.78	0.31	3.78	N/A	0.44	0.19	**2**
179	2.46	1.26	0.13	0.02	7.43	55.20	**35**
180	35.42	5.97	20.61	1.61	45.44	2064.42	**58**
182	10.01	2.06	3.86	1.40	17.94	321.82	**76**
183	3.02	0.00	3.02	N/A	-	-	**1**
185	31.74	6.16	31.36	N/A	27.53	757.73	**20**
190	36.76	9.87	8.47	N/A	63.96	4091.25	**42**
192	1.09	0.35	0.80	N/A	0.61	0.37	**3**
193	41.01	21.73	5.05	0.02	220.52	48629.93	**103**
194	6.16	2.61	1.46	N/A	6.91	47.70	**7**
195	27.63	9.92	13.05	N/A	35.77	1279.22	**13**
196	34.90	8.60	24.67	N/A	36.50	1332.10	**18**
197	28.76	8.34	15.65	N/A	22.06	486.61	**7**
214	25.81	7.22	3.15	0.05	50.00	2500.07	**48**
284	29.42	9.84	6.83	N/A	56.53	3195.43	**33**
331	44.87	8.09	13.38	N/A	70.50	4969.59	**76**
332	54.79	22.35	9.80	N/A	116.13	13485.08	**27**
333	40.44	16.45	3.81	N/A	75.39	5683.18	**21**
334	27.35	7.70	5.22	0.01	100.07	10013.88	**169**
335	15.45	2.77	4.97	N/A	26.74	715.29	**93**
337	92.06	48.43	52.31	N/A	96.87	9383.79	**4**
341	22.56	3.55	2.99	N/A	41.53	1724.41	**137**

In Table 6.2, basic statistical measurements such as kurtosis, skewness, range, sum, minimum and maximum are introduced. In Table 6.2., it can be seen that most of the data set for wells have positive skewness ranging dispersedly other than the wells having very few data in count. The minimum, maximum and the range of the data is also an indicative of how the permeability data varies and how the geological distribution is random since the core plug permeability data is pertained to the certain depths.

Table 6.2 Descriptive Statistics of Raw Core Plug Data (2)

Well Number	Kurtosis	Skewness	Range	Minimum	Maximum	Sum	Count
2	-	-	0.00	118.80	118.80	118.80	**1**
24	-	-	0.00	3.74	3.74	3.74	**1**
86	-	1.10	139.00	3.11	142.10	189.70	**3**
126	-	1.73	29.01	4.06	33.07	42.16	**3**
140	-	-	0.00	53.51	53.51	53.51	**1**
155	-1.60	0.49	140.32	6.68	147.00	468.39	**7**
167	-	-	0.00	0.65	0.65	0.65	**1**
172	71.97	8.04	1,611.36	0.01	1,611.37	4,960.99	**97**
174	5.58	2.29	308.50	0.01	308.51	1,392.17	**35**
176	17.60	4.11	154.37	0.01	154.38	608.14	**56**
177	-	-	0.62	3.47	4.09	7.56	**2**
179	14.51	3.88	34.59	0.01	34.60	86.10	**35**
180	3.11	1.90	182.00	0.10	182.10	2,054.46	**58**
182	16.20	3.64	114.18	0.01	114.19	760.74	**76**
183	-	-	0.00	3.02	3.02	3.02	**1**
185	3.85	1.62	116.78	0.34	117.12	634.84	**20**
190	5.21	2.35	273.90	0.04	273.94	1,543.96	**42**
192	-	1.66	1.11	0.68	1.79	3.27	**3**
193	96.24	9.68	2,220.98	0.02	2,221.00	4,223.53	**103**
194	-2.23	0.53	15.13	0.09	15.22	43.13	**7**
195	1.71	1.66	111.35	0.85	112.20	359.20	**13**
196	2.75	1.70	135.84	0.08	135.92	628.16	**18**
197	-1.46	0.70	53.79	9.70	63.49	201.31	**7**
214	7.42	2.67	216.32	0.01	216.33	1,238.71	**48**
284	11.33	3.22	272.35	0.01	272.36	970.85	**33**
331	4.02	2.18	289.10	0.09	289.19	3,409.90	**76**
332	8.62	2.94	495.33	0.13	495.46	1,479.22	**27**
333	6.61	2.61	291.10	0.03	291.13	849.19	**21**
334	101.36	9.28	1,165.59	0.01	1,165.60	4,622.18	**169**
335	21.19	3.95	192.16	0.01	192.17	1,436.65	**93**
337	2.98	1.74	204.32	29.66	233.97	368.26	**4**
341	14.74	3.44	285.44	0.06	285.50	3,091.15	**137**

6.2.1 Heterogeneity Analysis of Raw Core Plug Data

By the assessment of data for each well regarding descriptive statistics the coefficients of variation (C_v) are found out for the raw core permeability data. The results can be seen in Table 6.3. The coefficients of variation are one of the guidance in understanding the level of these heterogeneities. Thus, other than the wells having

insufficient but by chance consistent data most of the wells permeabilities are strictly heterogeneous.

Table 6.3 Coefficient of Variation of Raw Core Plug Data

Well Number	C_v	N_o	*P*	Heterogeneity	Count	N_o/Count
2	-	-	-	-	**1**	-
24	-	-	-	-	**1**	-
86	1.13	127	130	Very Heterogeneous	**3**	**42**
126	1.17	137	234	Very Heterogeneous	**3**	**46**
140	-	-	-	-	**1**	-
155	0.91	82	181	Heterogeneous	**7**	**12**
167	-	-	-	-	**1**	-
172	3.37	1,133	673	Very Heterogeneous	**97**	**12**
174	1.76	311	353	Very Heterogeneous	**35**	**9**
176	2.59	673	519	Very Heterogeneous	**56**	**12**
177	0.12	1	23	Homogeneous	**2**	**1**
179	3.02	912	604	Very Heterogeneous	**35**	**26**
180	1.28	165	257	Very Heterogeneous	**58**	**3**
182	1.79	321	358	Very Heterogeneous	**76**	**4**
183	-	-	-	-	**1**	-
185	0.87	75	173	Heterogeneous	**20**	**4**
190	1.74	303	-	Very Heterogeneous	**42**	**7**
192	0.56	31	-	Slightly Het.	**3**	**10**
193	5.38	2,892	-	Very Heterogeneous	**103**	**28**
194	1.12	126	0	Very Heterogeneous	**7**	**18**
195	1.29	168	0	Very Heterogeneous	**13**	**13**
196	1.05	109	-	Heterogeneous	**18**	**6**
197	0.77	59	0	Heterogeneous	**7**	**8**
214	1.94	375	-	Very Heterogeneous	**48**	**8**
284	1.92	369	-	Very Heterogeneous	**33**	**11**
331	1.57	247	-	Very Heterogeneous	**76**	**3**
332	2.12	449	-	Very Heterogeneous	**27**	**17**
333	1.86	348	6	Very Heterogeneous	**21**	**17**
334	3.66	1,339	-	Very Heterogeneous	**169**	**8**
335	1.73	300	-	Very Heterogeneous	**93**	**3**
337	1.05	111	0	Heterogeneous	**4**	**28**
341	1.84	339	-	Very Heterogeneous	**137**	**2**

The wells 177 and 192 which are having only 2 and 3 core plug data seems to be homogeneous due to lack of sufficient data. Besides, the distributions in the rest of the wells are highly heterogeneous. Error tolerances (*P*) which are given in percentage of the data sets are also extremely high.

6.3 Facies Determination

The depths of the facies and the thicknesses of these facies for each well having whether core plug or well test data are given in Appendix B.

6.3.1 Facies Discrimination of Raw Core Plug Data

The highlighted boxes in Table 6.4 and Table 6.5 are given to illustrate the eliminated core plug data having less than or equal to 5 sample numbers.

Table 6.4 The Eliminated Core Plug Data for Facies A, B, C, D

The Core Plug Data for Facies								
Well Number	A		B		C		D	
	k_{ar}	Data#	k_{ar}	Data#	k_{ar}	Data#	k_{ar}	Data#
2								
24	3.74	1						
86	63.23	3						
126	14.05	3						
140					53.51	1		
155			76.95	6			6.68	1
167					0.65	1		
172			32.75	72			17.53	9
174	57.93	24			0.16	11		
176			20.28	13			7.06	13
177			3.78	2				
179			4.97	16			1.14	5
180	48.01	24	50.04	10			8.42	8
182	12.09	47	5.38	14			9.14	2
183			3.02	1				
185	35.56	12	29.66	5				
190	45.16	23					15.55	6
193			53.76	76			5.11	27
194			6.16	7				
195			27.63	13				
196			34.90	18				
197			28.76	7				
214	6.91	20			39.31	28		
284			31.45	30			9.08	3
331	65.74	21	36.90	55				
332			54.79	27				
333	40.44	21						
334	114.57	1	35.24	114			9.65	6
335	8.16	1	21.04	47			20.25	6
337	92.06	4						
341	34.22	88	1.62	49				

Table 6.5 The Eliminated Core Plug Data for Facies F, G, H

The Core Plug Data for Facies								
Well Number	F		G		H		Overall k_{ar}	Total Data #
	k_{ar}	Data#	k_{ar}	Data#	k_{ar}	Data#		
2					118.80	1	118.80	1
24							3.74	1
86							63.23	3
126							14.05	3
140							53.51	1
155							66.91	7
167							0.65	1
172	10.00	3	185.78	13			51.14	97
174							39.78	35
176					8.42	30	10.86	56
177							3.78	2
179					0.06	14	2.46	35
180			15.97	11	31.75	5	35.42	58
182			0.47	3	9.73	10	10.01	76
183							3.02	1
185			19.93	3			31.74	20
190			49.33	8	3.49	5	36.76	42
193							41.01	103
194							6.16	7
195							27.63	13
196							34.90	18
197							28.76	7
214							25.81	48
284							29.42	33
331							44.87	76
332							54.79	27
333							40.44	21
334			23.29	11	4.76	37	27.35	169
335			16.01	19	0.69	20	15.45	93
337							92.06	4
341							22.56	137

6.4 Descriptive Statistics and Heterogeneity Analysis of Trimmed Core Plug Data

New C_v's are found for the refined data. The newly found are presented in Table 6.6, Table 6.7, Table 6.8, Table 6.9 and Table 6.10.

Table 6.6 The New C_v's for Facies A

Well Number	FACIES A					
	C_v	N_o	*P*	Heterogeneity	Count	N_o/Count
174	0.91	83	**50**	Heterogeneous	13	**6**
180	0.69	47	**30**	Heterogeneous	21	**2**
182	1.62	262	**49**	Very Heterogeneous	43	**6**
185	0.83	69	**48**	Heterogeneous	12	**6**
190	1.48	218	**64**	Very Heterogeneous	21	**10**
331	1.04	108	**48**	Heterogeneous	19	**6**
333	1.25	157	**63**	Very Heterogeneous	16	**10**
341	1.25	157	**27**	Very Heterogeneous	85	**2**

Table 6.7 The New C_v's for Facies B

Well Number	FACIES B					
	C_v	N_o	*P*	Heterogeneity	Count	N_o/Count
155	0.78	60	**63**	Heterogeneous	6	**10**
172	1.69	286	**44**	Very Heterogeneous	59	**5**
176	1.74	304	**110**	Very Heterogeneous	10	**30**
180	0.94	89	**60**	Heterogeneous	10	**9**
193	1.36	184	**39**	Very Heterogeneous	49	**4**
195	1.05	110	**66**	Heterogeneous	10	**11**
196	0.99	98	**48**	Heterogeneous	17	**6**
197	0.77	59	**58**	Heterogeneous	7	**8**
284	1.57	248	**66**	Very Heterogeneous	23	**11**
331	1.65	272	**48**	Very Heterogeneous	48	**6**
332	1.79	320	**78**	Very Heterogeneous	21	**15**
334	1.96	384	**41**	Very Heterogeneous	92	**4**
335	1.41	200	**45**	Very Heterogeneous	39	**5**

Table 6.8 The New C_v's for Facies D

Well Number	FACIES D					
	C_v	N_o	*P*	Heterogeneity	Count	N_o/Count
176	1.20	145	76	Very Heterogeneous	10	14
180	0.50	25	**38**	Homogeneous	7	**4**
193	1.23	152	68	Very Heterogeneous	13	12

Table 6.9 The New C_v's for Facies G

Well Number	FACIES G					
	C_v	N_o	*P*	Heterogeneity	Count	N_o/Count
172	1.00	100	76	Heterogeneous	7	14
180	0.79	63	71	Heterogeneous	5	13
190	0.89	79	89	Heterogeneous	4	20
334	0.74	54	**44**	Heterogeneous	11	**5**
335	0.67	45	**37**	Heterogeneous	13	**3**

Table 6.10 The New C_v's for Facies H

Well Number	FACIES H					
	C_v	N_o	*P*	Heterogeneity	Count	N_o/Count
176	1.40	197	**54**	Very Heterogeneous	27	**7**
334	1.80	325	**62**	Very Heterogeneous	34	**10**
335	1.70	290	76	Very Heterogeneous	20	14

6.5 Normality Check and Normalization of Trimmed Core Plug Data

The selected data sets for further evaluation of core permeability analysis are given as bold characters for the specified features of P and N_0/Count in Tables 6.6-10. The selected well numbers for Facies A are 174, 180, 182, 185, 190, 331, 333 and 341. For Facies B they are 155, 172, 180, 193, 195, 196, 197, 284, 331, 334 and 335. For

Facies D Well#180 is selected for further evaluation. For Facies G wells 334 and 335 survived. For Facies H wells 176 and 334 stood.

The results of the goodness of fit tests of Kolmogorov-Smirnov, Anderson-Darling and Chi-Squared for normal distribution is exhibited in Appendix C1 and Probability Density Functions with Histograms in Appendix C2.

Well # 182, 190, 341 for Facies A, 172, 193, 284, 331, 334 and 335 for Facies B and 176, 334 for Facies H found not to be fitting to the Gaussian (Normal) Distribution. Other data sets for facies of wells are fitting to the normal distribution.

6.5.1 Normalization of Core Plug Data Using Box-Cox Power Transformation

Box-Cox power transformation and normalization procedure is given in Appendix D.

After normalization, the data sets of Well#190 for Facies A and Well#331 for Facies B which are having the most sophisticated data are checked for illustration whether the normalized data sets fits to the normal distribution or not. In Table 6.11 and Table 6.12, results of the normality tests are given. In Figure 6.1 and Figure 6.2 probability density functions with their histograms are exhibited.

Table 6.11 Goodness of Fit Test Results for Well#190 Facies A

Normal					
Kolmogorov-Smirnov					
Sample Size Statistic P-Value Rank	21 0,1618 0,58586 24				
α	0,2	0,1	0,05	0,02	0,01
Critical Value	0,22617	0,25858	0,28724	0,32104	0,34427
Reject?	No	No	No	No	No
Anderson-Darling					
Sample Size Statistic Rank	21 0,61875 23				
α	0,2	0,1	0,05	0,02	0,01
Critical Value	1,3749	1,9286	2,5018	3,2892	3,9074
Reject?	No	No	No	No	No
Chi-Squared					
Deg. of freedom Statistic P-Value Rank	2 1,4877 0,47528 9				
α	0,2	0,1	0,05	0,02	0,01
Critical Value	3,2189	4,6052	5,9915	7,824	9,2103
Reject?	No	No	No	No	No

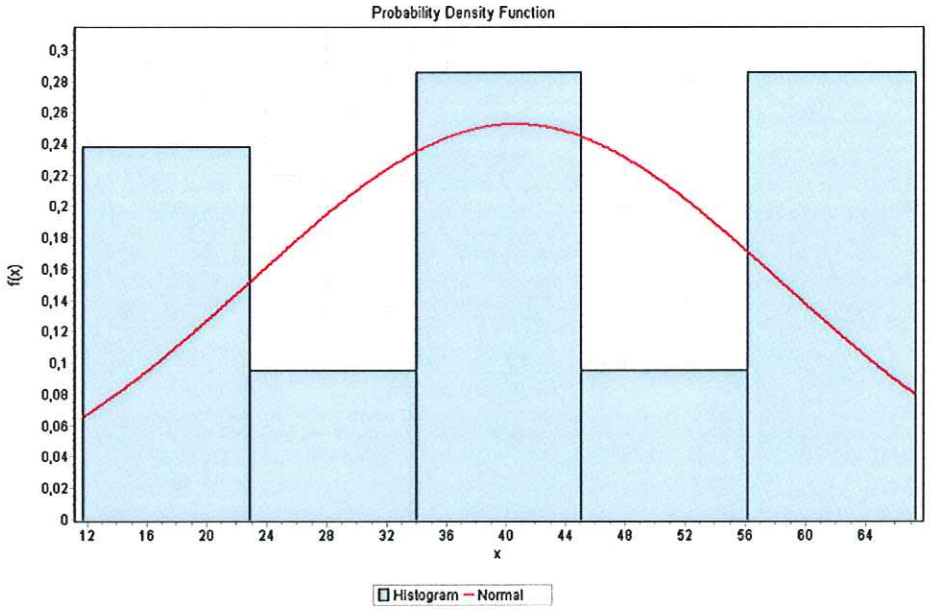

Figure 6-1: PDF & Histogram for Well#190 Facies A

Table 6.12 Goodness of Fit Test Results for Well#331 Facies B

Normal					
Kolmogorov-Smirnov					
Sample Size Statistic P-Value Rank	48 0,10115 0,67232 22				
α	0,2	0,1	0,05	0,02	0,01
Critical Value	0,1513	0,17302	0,19221	0,21493	0,23059
Reject?	No	No	No	No	No
Anderson-Darling					
Sample Size Statistic Rank	48 0,41775 10				
α	0,2	0,1	0,05	0,02	0,01
Critical Value	1,3749	1,9286	2,5018	3,2892	3,9074
Reject?	No	No	No	No	No
Chi-Squared					
Deg. of freedom Statistic P-Value Rank	4 1,6248 0,80433 10				
α	0,2	0,1	0,05	0,02	0,01
Critical Value	5,9886	7,7794	9,4877	11,668	13,277
Reject?	No	No	No	No	No

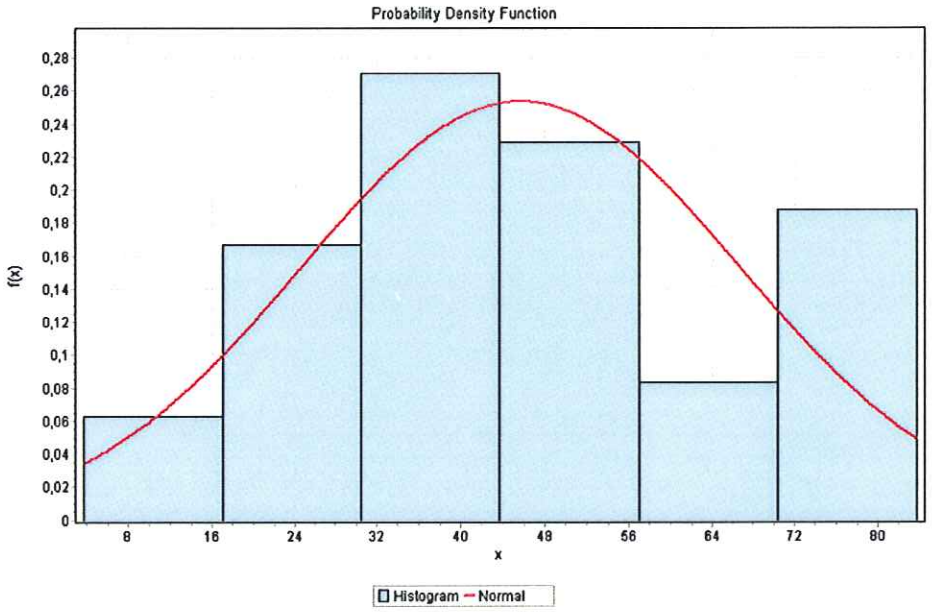

Figure 6-2: PDF & Histogram for Well#331 Facies B

6.6 Reservoir Heterogeneities for the Normalized Core Plug Data

As it can be seen from the probability density functions given in Appendix C; the ones which were not normalized are Approximately Normally Distributed (AND). However, since the objective isto find an exponent that makes the observations AND (Jensen et al., 1987), the AND data is also just sufficient in order to use for averaging.

6.6.1 Coefficient of Variation

The latest coefficients of variation are given in Table 6.13, Table 6.14, Table 6.15, Table 6.16 and Table 6.17.

After the normalization and the refinement of the data it can be seen that the permeability distributions are still heterogeneous but the heterogeneities are reduced down to a good level. The distribution of coefficients of variation for each wells of a particular facies is consistent with each other. That means the finally derived permeability measurements can be representative in order to make a comparison with well test derived permeability.

Table 6.13 C_v's for Normalized and Refined Data Facies A

Well Number	FACIES A					
	C_v	N_o	*P*	Heterogeneity	Count	N_o/Count
174	0.91	83	50	Heterogeneous	13	6
180	0.69	47	30	Heterogeneous	21	2
182	0.60	36	18	Heterogeneous	43	1
185	0.83	69	48	Heterogeneous	12	6
190	0.43	19	19	Homogeneous	21	1
331	1.04	108	48	Heterogeneous	19	6
333	1.25	157	63	Very Heterogeneous	16	10
341	0.50	25	11	Homogeneous	85	0

Table 6.14 C_v's for Normalized and Refined Data Facies B

Well Number	FACIES B					
	C_v	N_o	*P*	Heterogeneity	Count	N_o/Count
155	0.78	60	**63**	Heterogeneous	6	**10**
172	0.52	27	**13**	Slightly Heterogeneous	59	**0**
180	0.94	89	**60**	Heterogeneous	10	**9**
193	0.37	14	**11**	Homogeneous	49	**0**
195	1.05	110	**66**	Heterogeneous	10	**11**
196	0.99	98	**48**	Heterogeneous	17	**6**
197	0.77	59	**58**	Heterogeneous	7	**8**
284	0.50	25	**21**	Homogeneous	23	**1**
331	0.46	21	**13**	Homogeneous	48	**0**
334	0.47	22	**10**	Homogeneous	92	**0**
335	0.43	18	**14**	Homogeneous	39	**0**

Table 6.15 C_v's for Normalized and Refined Data Facies D

Well Number	FACIES D					
	C_v	N_o	*P*	Heterogeneity	Count	N_o/Count
180	0.50	25	**38**	Homogeneous	7	**4**

Table 6.16 C_v's for Normalized and Refined Data Facies G

Well Number	FACIES G					
	C_v	N_o	*P*	Heterogeneity	Count	N_o/Count
334	0.74	54	**44**	Heterogeneous	11	**5**
335	0.67	45	**37**	Heterogeneous	13	**3**

Table 6.17 C_v's for Normalized and Refined Data Facies H

Well Number	FACIES H					
	C_v	N_o	*P*	Heterogeneity	Count	N_o/Count
176	0.83	69	**32**	Heterogeneous	27	**3**
334	0.79	63	**27**	Heterogeneous	34	**2**

The bold characterized well numbers in the tables indicate the normalized data sets. After investigating the latest coefficients of variation, it can be observed there is a large remediation of data and consistency in the coefficients of variation.

6.6.2 The Dysktra-Parson's Coefficient

The semi-log plots to identify The Dysktra Parson's coefficients are given in Appendix E. Also the calculated coefficients are given in Table 6.18.

The coefficients of variation and The Dysktra Parson's coefficients are very close to each other and in line.

As it can be seen, the normalized data are found to be more homogeneous both for coefficient of variation and The Dysktra-Parson's coefficient. However, the aim is to find the most representative global permeability values with the least possible data manipulation.

Table 6.18 The Dysktra Parson's Coefficients for Normalized and Refined Data

Well #	$k_{0,50}$	$k_{0,84}$	V_{DP}
FACIES A			
174	15.99	4.81	0.70
180	24.65	10.78	0.56
182	8.96	3.06	0.66
185	26.58	11.65	0.56
190	36.66	21.94	**0.40**
331	25.76	6.87	0.73
333	9.15	2.05	0.78
341	33.17	15.63	0.53

Well #	$k_{0,50}$	$k_{0,84}$	V_{DP}
FACIES D			
180	2.78	1.78	**0.36**

Well #	$k_{0,50}$	$k_{0,84}$	V_{DP}
FACIES G			
334	19.72	11.63	**0.41**
335	18.59	9.65	**0.48**

Well #	$k_{0,50}$	$k_{0,84}$	V_{DP}
FACIES B			
155	50.46	18.52	0.63
172	34.64	15.23	0.56
180	31.11	10.06	0.68
193	52.60	31.32	**0.40**
195	22.68	8.83	0.61
196	23.19	7.54	0.67
197	21.94	10.66	0.51
284	39.03	19.56	**0.50**
331	38.66	19.58	**0.49**
334	24.61	12.31	**0.50**
335	31.78	18.03	**0.43**

Well #	$k_{0,50}$	$k_{0,84}$	V_{DP}
FACIES H			
176	0.10	0.01	0.87
334	0.41	0.14	0.66

6.6.3 The Lorenz Plot & The Lorenz Coefficient

Lorenz Plots for the specified facies are given in Appendix F.

In Table 6.19 computed Lorenz coefficients are presented.

Table 6.19 Lorenz Coefficients for Normalized and Refined Data

Well #	L_c
FACIES A	
174	0.46
180	0.32
182	0.29
185	0.36
190	0.21
331	0.43
333	0.46
341	0.25

Well #	L_c
FACIES B	
155	0.38
172	0.32
180	0.41
193	0.22
195	0.55
196	0.47
197	0.36
284	0.20
331	0.33
334	0.25
335	0.30

Well #	L_c
FACIES D	
180	0.28

Well #	L_c
FACIES G	
334	0.3
335	0.32

Well #	L_c
FACIES H	
176	0.31
334	0.16

In our plots, it is seen that the heterogeneities predetermined can be confirmed again with the crosschecking of a petrophysical plot which is also giving the indications of effective flowing interval in between the searched interval. However, since in our study of interest only every single facies' of each well is examined the whole profile cannot be seen. However, the aim is to see in if there is an abrupt peak and/or changes in flowing interval in a specified facies to see the change in flow capacity with the storage capacity in order to further understand the reservoir permeability heterogeneities. However, the trend for each facies is sufficiently close and the pre-determined heterogeneities are confirmed.

6.7 Comparison of Well Test Permeability & Upscaled Core Plug Permeability Data

In Table 6.20, Table 6.21, Table 6.22, Table 6.23 and Table 6.24 the core plug permeabilities which will be used for comparison with the well test derived permeability as the overall facies permeabilities are taken as representative permeabilities.

Table 6.20 Averages for Core Permeability Data Facies A

Well Number	Equivalent Liquid Permeabilities for Facies A		
	k_{ar} (md)	k_{geo} (md)	k_{har} (md)
174	26.40	15.98	8.14
180	31.76	24.65	17.47
182	12.70	8.93	2.60
185	35.56	26.55	18.98
190	40.61	36.66	32.54
331	45.89	25.71	9.97
333	21.57	9.13	4.39
341	40.07	33.10	20.61
OVERALL	**31.82**	**20.10**	**7.81**

Table 6.21 Averages for Core Permeability Data Facies B

Well Number	Equivalent Liquid Permeabilities for Facies B		
	k_{ar} (md)	k_{geo} (md)	k_{har} (md)
155	76.95	50.46	27.64
172	43.30	34.60	20.30
180	50.04	31.06	14.53
193	58.61	52.57	38.63
195	35.61	22.66	16.10
196	36.95	23.18	13.31
197	28.76	21.93	17.24
284	46.29	39.00	30.02
331	45.67	38.63	26.18
334	28.97	24.57	18.05
335	35.71	31.76	26.58
OVERALL	**44.26**	**32.20**	**20.37**

Table 6.22 Averages for Core Permeability Data Facies D

Well Number	Equivalent Liquid Permeabilities for Facies D		
	k_{ar} (md)	k_{geo} (md)	k_{har} (md)
180	3.07	2.78	2.53
OVERALL	**3.07**	**2.78**	**2.53**

Table 6.23 Averages for Core Permeability Data Facies G

Well Number	Equivalent Liquid Permeabilities for Facies G		
	k_{ar} (md)	k_{geo} (md)	k_{har} (md)
334	23.29	19.72	17.44
335	22.40	18.58	15.42
OVERALL	**22.84**	**19.14**	**16.37**

Table 6.24 Averages for Core Permeability Data Facies H

Well Number	Equivalent Liquid Permeabilities for Facies H		
	k_{ar} (md)	k_{geo} (md)	k_{har} (md)
176	0.72	0.15	0.00
334	0.63	0.37	0.18
OVERALL	**0.68**	**0.23**	**0.00**

The selected wells which have fairly consistent well test data are given in Table 6.25. The selected wells' pressure derivative log-log plots are exhibited in Appendix G. The overall transmissivities of wells have been found for core plug data by using overall facies permeabilities in which comparison is made by taking well tested wells facies thicknesses. It is exhibited in Table 6.26.

Table 6.25 Selected Well Test Results

Well no.	Test no.	Test dura.	Pi (psi)	k (md)	k.h (md.ft)	S	Reservoir	Boundary
21	1	295	429.831	1150	93400	-4.26	Two Por. PSS	One fault
28	1	72	1469.91	2130	1.60E+05	11.3	Two Por. PSS	One fault
35	1	72	1529.59	1750	1.15E+05	-0.331	Two Por. PSS	Intersecting faults-Any Angle
80	1	216	956.017	2480	3.54E+05	-4.11	Two Por. PSS	One fault
148	3	169	613.615	2110	1.46E+05	-0.535	Two Por. PSS	One fault
148	4	169	573.612	2050	1.41E+05	-0.725	Two Por. PSS	Infinite
148	5	813	536.301	1790	1.24E+05	-3.4	Two Por. PSS	Circle, No flow
172	1	214.5	928.025	295	4.65E+04	-4.43	Two Por. PSS	One fault

Table 6.26 Transmissivities of Averaged Core Plug Data by Using Well Tested Well's Thicknesses

WELL # W.T.		Transmissivity - Flow Capacity of Wells -k.h (md.m)									
		Facies Overall Core Plug Permeabilities Correlated For Well Tested Wells' Thicknesses									
		A	B	C	D	E	F	G	H	∑h	∑k.h
172	μ_{ar}.h	0.00	2,787.02	0.00	8.44	0.00	0.98	148.49	5.49	80.33	2,950
	μ_{geo}.h		2,027.69		7.63			124.39	1.88		2,162
	μ_{har}.h		1,282.89		6.96			106.40	0.01		1,396
35	μ_{ar}.h	0.00	2,345.76	0.00	12.27	0.00	0.00	228.44	8.12	79.00	2,595
	μ_{geo}.h		1,706.64		11.10			191.38	2.78		1,912
	μ_{har}.h		1,079.77		10.12			163.69	0.02		1,254
21	μ_{ar}.h	977.21	1,074.18	0.00	0.00	0.00	0.00	183.44	12.22	81.08	2,247
	μ_{geo}.h	617.19	781.51					153.67	4.19		1,557
	μ_{har}.h	239.96	494.45					131.44	0.03		866
28	μ_{ar}.h	0.00	2,212.98	0.00	58.30	0.00	0.00	32.90	7.14	81.00	2,311
	μ_{geo}.h		1,610.04		52.74			27.56	2.45		1,693
	μ_{har}.h		1,018.65		48.07			23.57	0.02		1,090
80	μ_{ar}.h		2,360.80	0.00	12.18	0.00	0.00	193.95	0.00	65.80	2,567
	μ_{geo}.h		1,717.59		11.02			162.48			1,891
	μ_{har}.h		1,086.70		10.04			138.97			1,236
148	μ_{ar}.h	0.00	1,599.98	0.00	33.91	0.00	0.00	0.00	0.00	47.20	1,634
	μ_{geo}.h		1,164.06		30.67						1,195
	μ_{har}.h		736.48		27.96						764

Compared permeability values are given in Table 6.27. For wells 35, 21 and 148 the geometric mean of core permeability data is nearly equal to the well test derived permeability data. This results and proportions for these stated wells are also given in Figure 6.3, Figure 6.4 and Figure 6.5.

Table 6.27 Compared Permeability Values

			WELLS	∑k.h (md.m)	h (meter)	k (md)	$k_{welltest}/k_{corepbg}$
1	Core Plug	k_{har}	172	2,950	80.33	36.73	**0.29**
		k_{geo}		2,162		26.91	**0.39**
		k_{dhar}		1,396		17.38	**0.60**
	Well Test	$k_{overall}$	172	14,173	1,348.94	10.51	
2	Core Plug	k_{har}	35	2,595	79.00	32.84	**0.75**
		k_{geo}		1,912		24.20	**1.02**
		k_{dhar}		1,254		15.87	**1.56**
	Well Test	$k_{overall}$	35	35,052	1,419.00	24.70	
3	Core Plug	k_{har}	21	2,247	81.08	27.71	**0.73**
		k_{geo}		1,557		19.20	**1.06**
		k_{dhar}		866		10.68	**1.90**
	Well Test	$k_{overall}$	21	28,468	1,404.31	20.27	
4	Core Plug	k_{har}	28	2,311	81.00	28.53	**1.25**
		k_{geo}		1,693		20.90	**1.70**
		k_{dhar}		1,090		13.46	**2.64**
	Well Test	$k_{overall}$	28	48,768	1,372.00	35.55	
5	Core Plug	k_{har}	80	2,567	65.80	39.01	**1.98**
		k_{geo}		1,891		28.74	**2.68**
		k_{dhar}		1,236		18.78	**4.11**
	Well Test	$k_{overall}$	80	107,899	1,399.00	77.13	
6	Core Plug	k_{har}	148	1,634	47.20	34.62	**0.92**
		k_{geo}		1,195		25.31	**1.26**
		k_{dhar}		764		16.20	**1.97**
	Well Test	$k_{overall}$	148	41,758	1,310.00	31.88	

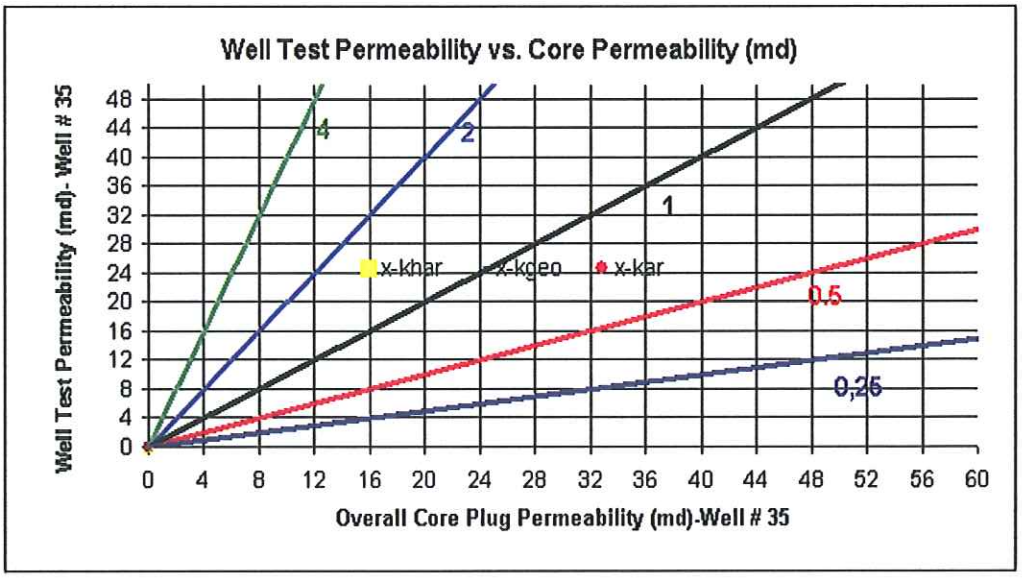

Figure 6-3: Well Test Permeability vs. Core Permeability Well#35

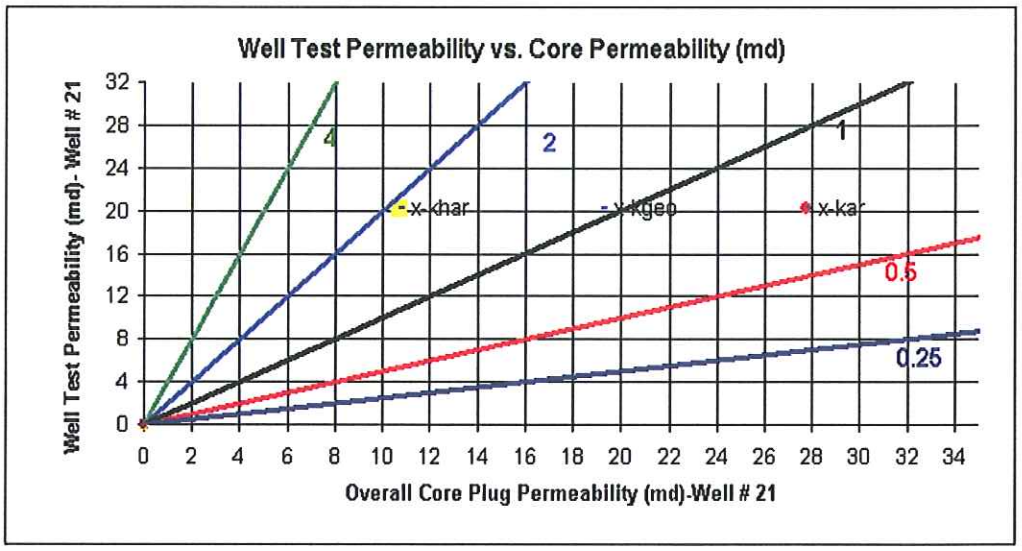

Figure 6-4: Well Test Permeability vs. Core Permeability Well#21

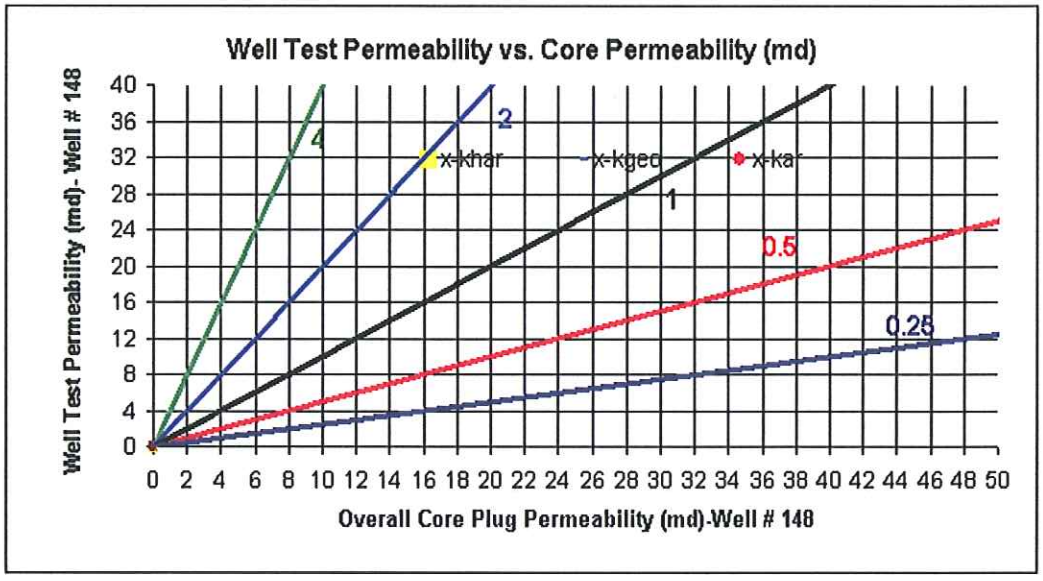

Figure 6-5: Well Test Permeability vs. Core Permeability Well#148

The 6 well test permeability derived wells which have been found proper for comparing with upscaled core plug permeability data did tend to be equal to the geometrical mean which is an indicative of random distribution for 50% of the compared wells. For the rest of the wells which are wells#172, 28 and 80 are the

averaged core permeability data and well test derived permeability data are also similar, however the points illustrated in Figures 6.3-5 are shifted leftwards or rightwards. Since there is no certain trend for unmatched data, it can be stated that well tests are misinterpreted such as ETR and MTR are misidentified or the flowing intervals cannot be always taken as the whole well section. However, it is understood that for the well tests which are interpreted as having similar transmissivities, do match with the geometric mean of the upscaled and refined core plug permeability data for this heavy oil carbonate B. Field.

CHAPTER 7

CONCLUSIONS

After this study, it is highlightened that the comparison of core data and well test data are influenced by so many issues (physical, statistical, geological and engineering issues). This study proved that putting simple relationships between static and dynamic measurements is really difficult to justify but not impossible. Effective properties can be found by taking data as they are only functions of the statistics of the field rather than particular details of any realization of a field if significant number data to be evaluated is available.

As stated, high density of measurements is a must, however cleaning and pressure corrections for core plug data is also essential. However, in our study the errors introduced within permeability variations due to overburden pressure and core plug cleaning is not taken into account since these measurements are readily gathered from TPAO Production Technologies Department.

After that, well test data should be re-organized by considering that well tests are showing effective balance withdrawals, confirming the contribution of secondary porosity. Furthermore, while averaging core plug measurements; not only power averaging methods, but also other methods could be used or combined

Moreover, depth matching and knowledge of reservoir units' distribution is essential. In heterogeneous reservoirs, the effective flow interval which can be determined on the Lorenz Plot; could be considered thoroughly by additionally taking the perforated intervals into account. The permeabilities derived from core and well test

permeabilities should be expressed as range, to account for uncertainties in core and test data, rather than as single values.

To conclude, the evaluated core plug permeability data from 32 wells and pressure build-up test permeabilities from 26 wells are compared. In order to compare these statistical and dynamic data, the noise data within the core plug permeability data set is trimmed by discriminating the core plug permeability data regarding the facies and formation distribution. While doing that permeability heterogeneities are calculated with C_V, V_{DP} and L_C to see if the upscaled data is consistent or not. Then, the arithmetic, geometric and harmonic averages of the upscaled core plug facies permeability data is found and these overall facies permability data is used while making a comparison with the well test derived permeability data.

Thus, it is understood that if sufficient well test interpretation is valid, and the results and flow regimes are consistent within each other, the well test permeability data can be matched with the geometric mean of upscaled core permeability data in which these processes are actualized with regarding the reservoir units' distribution for a randomly distributed heavy oil carbonate field. In our method, homogenization and normalization of data is used in order to upscale core plug permeabilities.

In the results, the geometric mean permeability of the core plug data, in which the facies permeabilities are proportioned to the thickness of well tested well's thicknesses, is found out to be approximately equal to the pressure build-up test derived permeabilites. Since, B. Field's layering seems to be random; the rule of geometric mean's being representative for randomly distributed reservoirs seem to be valid for upscaled and normalized data. Thus, the overall facies permeability values given in Table 6.20 to Table 6.24 can be used as representative facies permeability.

REFERENCES

Allen, J.C., and Tex, B., "Method for Permeability Measurements ", US Patent#3,030,801, 24 April 1962.

Almeida, J.A., Soares, A., and Pereira M.J., 1996. "Upscaling of Permeability: Implementation of a Conditional Approach to Improve the Performance in Flow Simulation", SPE 35490, presented at the 3-D Reservoir Modeling Conference, Stavanger, Norway, 16-17 April.

Arslan, I, Akın, S., Karakeçe, Y., and Korucu, Ö., 2007. "Is Batı Raman Heavy Oil a Triple Porosity System?", SPE 111146, Presented at the 2007 SPE/EAGE Reservoir Characterization and Simulation Conference, Abu Dhabi, U.A.E., 28th-31th October.

Beicip-Franlab Petroleum Consultants, 1994. "TPAO Batı Raman Field EOR Project Phase II Geological Model by Beicip-Franlab", Beicip-Franlab Petroleum Consultants, pp. 13-27.

Beicip-Franlab Petroleum Consultants, 1996. "Batı Raman Field Enhanced Oil Recovery Project Final Report by Beicip-Franlab", Beicip-Franlab Petroleum Consultants, pp. 8-32.

Bensoussan, A., Lions, J.L., and Papanicolaou, G., 1978. "Asymptotic Analysis for Periodic Structures", North-Holland Publishing Company, Amsterdam, The Netherlands.

Box, G.E.P., and Cox, D.R., 1964. "An analysis of ,Transformations", *Journal of the Royal Statistical Society*, **Series B26**, pp. 211-246.

Corbett, P.V.M., and Jensen, J.L., 1992. "Estimating the mean permeability-how many measurements do you need?", *First Break*, **Vol. 10**, pp. 89-94, 1992.

Corbett, P.V.M., Zheng, S.-Y., Pinisetti, M., Mesmari, A., and Stewart, G., 1998. "The Integration of Geology and Well Testing for Improved Fluvial Reservoir Characterization", SPE 48880, Proceedings of the Society of Petroleum Engineers Annual and Technical Conference and Exhibition, Beijing, China, pp. 471-488.

Delhomme, J.P. "The Quest for Permeability Evaluation in Wireline Logging", Schlumberger Water Services.

Dinwiddie, C.L., 2005. "The Small-Drillhole Minipermeameter Probe for In-Situ Permeability Measurement", SPE 84595, *Reservoir Evaluation & Engineering*, pp. 491-501, December 2005.

Haddad S., Cribbs M., Sagar R., Viro E., and Casteljins, K., 2000. "So What is the Reservoir Permeability?", SPE 63138, Presented at the 2000 SPE Annual Technical Conference and Exhibition, Dallas, Texas, U.S.A.,1st-4th October.

Haddad S., Cribbs, M., Sagar, R. Tang, Y., Viro, E., and Casteljins, K., 2001. "Integrating Permeabilities from NMR, Formation Tester, Well Test and Core Data", SPE 71722, Presented at the 2001 SPE Annual Technical Conference and Exhibition, New Orleans, Lousiana, U.S.A., 30th September-3rd October.

Heller, J.P., and Mclemore J.V., "Miniporopermeameter", US Patent#5,373,727, 20 December 1994.

Hurst, A. and Rosvoll, 1991. Permeability Variations in Sandstones and Their Relationship to Sedimentary Structures", in Lake, L.W., Carroll Jr. H.B. and Wesson T.C., eds., Reservoir Characterization II: San Diego, California, Academic Pres, p. 315-338.

Emerson, J.D., and Stoto, M.A., 1982. "Explanatory Methods for Choosing Power Transformations", J. *Am. Stat. Assoc.*, **Vol 77**, pp. 103-108, March 1982.

Jackson, M.D., Muggeridge, A.H., Yoshida, S., and Johnson H.D., 2003. "Upscaling Permeability Measurements Within Complex Heterolithic Tidal Sandstones", *Mathematical Geology*, **Vol. 35(5)**, pp. 499-520, July 2003.

Jensen, J.L., Hinkley, D.W., and Lake, L.W., 1987. "A Statistical Study of Reservoir Permeability: Distributions, Correlations, and Averages", SPE 14270, *SPE Formation Evaluation*, **Vol. 2**, pp. 461-468, December 1987.

Jensen, J.L., and Lake, L.W., 1988. "The Influence of Sample Size and Permeability Distribution Upon Heterogeneity Measures", SPE 15434, *SPE Reservoir Engineering*, Vol. 2, pp. 629-637, May 1988.

Jensen, J.L., Lake, L.W., Corbett, P.V.M. and Goggin, D.J., 1997. "Statistics for Petroleum Engineers and Geoscientists", Prentice Hall, Englewood Cliffs, New Jersey, p. 390.

Jensen, K.H., and Mantoglou, A., 1992. "Application of Stochastic Unsaturated Flow Theory, Numerical Simulations, and Comparison to Field Observations, *Water Resources Research*, **Vol. 28**, pp. 269-284.

Jikov, V.V., Kozlov, S.M., and Oleinik, O.A., 1994. "Homogenization of Differential Operators and Integral Functionals, Springer-Verlag, New York.

Kitanidis, P.K., 1990. "Effective Hydraulic Conductivity for Gradually Varying Flow", *Water Resources Research*, **Vol 26**, pp. 1197-1208.

Lake, L.W. and Jensen, J.L., 1989. "A Review of Heterogeneity Measures Used in Reservoir Characterization", SPE 20156.

Lyons, W.C. "Standard Handbook of Petroleum & Natural Gas Engineering Volume 2", Gulf Publishing Company, Houston, Texas, pp.73-91, 1996.

Lu, S., Molz, F.J., Fogg, G.E., and Castle J.W., 2002. "Combining Stochastic Facies and Fractal Models for representing Natural Heterogeneity", *Hydrogeology Journal*, **Vol 10**, pp. 475-482, 2002.

Mantoglou, A., 1992. "A Theoretical Approach for Modeling Unsaturated Flow in Saptially Variable Soils: Effective Flow Modles in Finite Domains and Nonstatitonarity", *Water Resources Research*, **Vol 28**, pp. 251-267.

Noetinger, B. and Haas, A., 1996. "Permeability Averaging for Well Tests in 3D Stochastic Reservoir Models", SPE 36653, Proceedings of the Society of Petroleum Engineers Annual and Technical Conference and Exhibition, *Formation Evaluation and Reservoir Geology*, 379-387.

Novakovic, D., 2002. "Numerical Reservoir Characterization Using Dimensionless Scale Numbers With Application In Upscaling", A Ph.D Thesis in Petroleum Engineering Department of Lousiana State University and Agricultural and Mechanical College, p. 21.

Renard, P., and Marsily, G. de, 1997. "Calculating Equivalent Permeability: A Review", *Advances in Water Resources*, **Vol20(5-6)**, pp. 253-278,

Russo, D., 1992. "Upscaling of Hydraulic Conductivity in Partially Saturated Heterogeneous Porous Formation", *Water Resouces. Research*, **Vol 28**, pp. 397-409.

Sahin, A., Ali, A.Z., and Menouar, H., 2007. "Permeability Anisotropy Distributions in an Upper Jurassic Carbonate Reservoir, Eastern Saudi Arabia", *Journal of Petroleum Geology*, **Vol 30(2)**, pp. 147-158, April 2007.

Sahin, S., Kalfa, U., and Celebioglu, D., 2007 "Batı Raman Field Immiscible CO2 Application: Status Quo and Future Plans", SPE 106575, Presented at the 2007 SPE Latin American and Caribbean Petroleum Engineering Conference, Buenos Aires, Argentina, 15th-18th April.

Schlumberger, Introduction to Well Testing, Schlumberger Wireline & Testing, Bath, England, 1998.

Schlumberger, Well Test Interpretation, Schlumberger Educational Services, U.S.A., 2002.

Schlumberger (2008), "Oilfield Glossary: Core Plug", http://www.glossary.oilfield.slb.com/Display.cfm?Term=core%20plug (accessed in 05 August, 2008)

Shafer, J.L., and Ezekwe, N.J., 2007. "Methods for Upscaling Diverse Rock Permeability Data for Reservoir Characterization and Modeling", SPE 109128, Presented at the 2007 SPE Annual Technical Conference and Exhibition, Anaheim, California, U.S.A.,11th -4th November.

Shen, J.J.S., "Automated Steady State Relative Permeability Measurement System", US Patent#4,77,254, 27 September 1988.

Taware, S., Taware, A., Sinha, A., Jamkhindikar, A., Talukdar, R., and Gupta A.D., 2008. "Integrated Permeability Modeling Using Wireline Logs, Core and DST Data in a Deepwater Reservoir", SPE 113599, Presented at the 2008 Indian Oil and Gas Technical Conference abd Exhibition, Mumbai, India, 4th -6th March.

Whitaker, S., 1999. "The Method of Volume Averaging", Kluwer, Dordrecht.

Yeh, T.C.J., Gelhar, L., and Gutjahr A., 1985a. "Stochastic Abalysis of Unsaturated Flow in Heterogeneous Soils, 1, Statistically Isotropic Media", *Water Resources*, **Vol 21**, pp. 447-456.

Yeh, T.C.J., Gelhar, L., and Gutjahr A., 1985b. "Stochastic Abalysis of Unsaturated Flow in Heterogeneous Soils, 2, Statistically Anisotropic Media with Variable x", *Water Resources*, **Vol 21**, pp. 457-464.

Yeh, T.C.J., Gelhar, L., and Gutjahr A., 1985c. "Stochastic Abalysis of Unsaturated Flow in Heterogeneous Soils, 3, Observation and Application", *Water Resources*, **Vol 21**, pp. 465-471.

APPENDIX A

AVAILABLE WELL TEST RESULTS

Table A.1 Pressure Build-Up Tests Results

Well #	Test #	Test duration	Pi (psi)	k.h (md.ft)	S	Reservoir	Boundary
2	1	72	83.8507	5.09E+05	8.99	Two Porosity PSS	One fault
18	1	984	368	3730			
18	2	984	1898.7	792	7.08	Two Porosity PSS	One fault
20	1	72	280.27	15300	60.7	Two Porosity Slab	One fault
21	1	295	429.831	93400	-4.26	Two Porosity PSS	One fault
28	1	72	1469.91	1.60E+05	11.3	Two Porosity PSS	One fault
35	1	72	1529.59	1.15E+05	-0.331	Two Porosity PSS	Intersecting faults-Any Angle
45	1	72	1197.47	4.16E+05	-0.176	Two Porosity PSS	One fault
54	1	72	1140.14	3.35E+04	0.836	Two Porosity PSS	Infinite
54	2	720	1091.21	8.09E+03	1.91	Two Porosity PSS	One fault
54	3	11400	1414.86	2.01E+01	-3.36	Two Porosity Slab	Circle, No flow
61	1	552	377.301	4.46E+04	-7.31	Two Porosity PSS	One fault
64	1	18	795.171	90100	-2.07	Two Porosity PSS	One fault
64	2	18	762.266	3.03E+05	7.74	Two Porosity PSS	One fault
64	3	194	1083.99	35000	-3.17	Two Porosity PSS	One fault
64	4	2134	1086.32	36.8	-7.87	Two Porosity PSS	One fault
67	1	72	420.23	40000	-7.5	Two Porosity PSS	One fault
67	2	288	287.805	93600	0.431	Two Porosity PSS	One fault
80	1	216	956.017	3.54E+05	-4.11	Two Porosity PSS	One fault
81	1	72	2126.77	1690	-5.79	Two Porosity PSS	One fault
90	1	72	1448.47	18400	-2.9	Two Porosity PSS	One fault
92	1	72	2501.73	64600	-1.65	Two Porosity PSS	Homogeneous
96	1	72	1207.8	3.13E+05	-2.67	Two Porosity PSS	Circle, No flow
96	2	72	1433.36	1.07E+05	-4.98	Two Porosity PSS	One fault
96	3	168	1262.79	4.47E+05	-3.14	Two Porosity PSS	One fault
96	4	337	1625.42	6.72E+04	-5.24	Two Porosity PSS	One fault
98	1	6094	1060.44	5.57E+03	-6.02	Two Porosity PSS	One fault
101	1	72	495.876	7.32E-01	-12.6	Two Porosity Sphere	Infinite
101	2	1341	479.888	2.39E+03	-6.89	Two Porosity PSS	One fault
103	1	1301	696.195	1.16E+05	1.65	Two Porosity PSS	One fault

Table A.1 (cont'd)

Well #	Test #	Test duration	Pi (psi)	k.h (md.ft)	S	Reservoir	Boundary
110	1	72	220.204	2.87E+07	129	Two Porosity PSS	One fault
110	2	963	161	2.04E+06	-24.5	Two Porosity Sphere	Infinite
114	1	476	243.417	1.30E+05	-2.18	Two Porosity PSS	Infinite
115	1	72	236.92	1.04E+06	20.5	Homogeneous	One fault
122	1	668	310.469	9.45E+06	46.1	Two Porosity Sphere	One fault
133	1	72	333.451	4.47E+04	-2.59	Two Porosity PSS	One fault
133	2	96	267.128	3.03E+05	0	Homogeneous	One fault
133	3	1416	474.258	3.97E+04	25.2	Two Porosity PSS	One fault
133	4	2712	593.23	8.14E+03	0.0769	Two Porosity Slab	One fault
148	1	72	475	6.97E+04	0		
148	2	96	654.61	1.24E+06	-2.96	Two Porosity PSS	Infinite
148	3	169	613.615	1.46E+05	-0.535	Two Porosity PSS	One fault
148	4	169	573.612	1.41E+05	-0.725	Two Porosity PSS	Infinite
148	5	813	536.301	1.24E+05	-3.4	Two Porosity PSS	Circle, No flow
172	1	214.5	928.025	4.65E+04	-4.43	Two Porosity PSS	One fault
172	2	1128	13723.3	5.60E+01	0	Two Porosity PSS	Infinite

APPENDIX B

FACIES LAYOUT

Table B.1 Facies Layout for Wells' Section

WELLS	FACIES LAYOUT (m)															
	A		B		C		D		E		F		G		H	
	TOP	BASE	TOP	BASE	TOP	BASE	TOP	BASE	TOP	BASE	TOP	BASE	TOP	BASE	TOP	BASE
2	1342.8	1388.1	1388.1	1399.2									1399.2	1404.4	1404.4	1423.5
18	1335.0	1369.0	1369.0	1383.0			1383.0	1383.8					1383.8	1395.0	1395.0	1409.0
20	1321.0	1373.0	1373.0	1373.7			1373.7	1374.6					1374.6	1377.2	1377.2	1398.7
21	1323.2	1353.9	1353.9	1378.2									1378.2	1386.2	1386.2	1404.3
24	1337.0	1365.0													1365.0	1383.0
28			1291.0	1341.0			1341.0	1360.0					1360.0	1361.4	1361.4	1372.0
35			1340.0	1393.0			1393.0	1397.0					1397.0	1407.0	1407.0	1419.0
45			1280.4	1331.3			1331.3	1332.1					1332.1	1332.5	1332.5	1339.2
54	1207.3	1247.6													1247.6	1278.7
61			1303.8	1346.4			1346.4	1363.8			1363.8	1364.3	1364.3	1365.3	1365.3	1379.0
64	1309.2	1342.6													1342.6	1360.0
67			1257.0	1301.0			1301.0	1322.7					1322.7	1325.6	1325.6	1335.0
80			1333.2	1386.5			1386.5	1390.5					1390.5	1399.0		
81	1291.9	1349.7	1349.7	1350.1									1350.1	1350.4	1350.4	1361.3
86	1299.0	1346.8													1346.8	1365.7
90			1313.0	1376.4			1376.4	1390.0								
92	1293.6	1300.4	1300.4	1368.6			1368.6	1380.0								

Table B.1 (cont'd.)

WELLS	FACIES LAYOUT (m)															
	A		B		C		D		E		F		G		H	
	TOP	BASE	TOP	BASE	TOP	BASE	TOP	BASE	TOP	BASE	TOP	BASE	TOP	BASE	TOP	BASE
96			1338.2	1394.1									1394.1	1394.5	1394.5	1400.0
98	1331.2	1367.1	1367.1	1367.7			1367.7	1373.9					1373.9	1382.2	1382.2	1385.0
101			1294.9	1340.4			1340.4	1358.0					1358.0	1358.5	1358.5	1367.5
103	1248.8	1253.8	1253.8	1293.7			1293.7	1311.0							1311.0	1320.9
110			1296.0	1323.3			1323.3	1342.6			1342.6	1347.0				
112			1261.0	1296.0			1296.0	1303.1			1303.1	1304.1	1304.1	1319.1	1319.1	1341.0
114			1269.0	1303.1			1303.1	1307.1			1307.1	1329.1			1329.1	1349.1
115			1289.8	1320.0												
122			1306.0	1346.0			1346.0	1380.0					1380.0	1387.0	1387.0	1394.0
126	1338.6	1370.5	1370.5	1420.0												
133	1253.0	1309.0													1309.0	1330.0
140	1311.0	1317.2			1317.2	1325.0			1325.0	1354.0					1354.0	1379.0
148			1262.8	1299.0			1299.0	1310.0								
155			1243.0	1290.0			1290.0	1295.0					1295.0	1304.0	1304.0	1319.0
167	1266.1	1279.5			1279.5	1309.8			1309.8	1318.0					1318.0	1328.1
172			1267.6	1330.6			1330.6	1333.4			1333.4	1334.3	1334.3	1340.8	1340.8	1348.9
174	1286.5	1302.3			1302.3	1320.4	1320.4	1322.4	1322.4	1348.5					1348.5	1365.5
176			1243.0	1258.0			1258.0	1283.0							1283.0	1315.0
177			1242.0	1268.0			1268.0	1301.0					1301.0	1305.0	1305.0	1313.0
179			1289.9	1330.8			1330.8	1335.9					1335.9	1340.8	1340.8	1364.0
180	1326.2	1355.6	1355.6	1364.9			1364.9	1374.0					1374.0	1386.1	1386.1	1401.9

Table B.1 (cont'd.)

WELLS	FACIES LAYOUT (m)															
	A		B		C		D		E		F		G		H	
	TOP	BASE	TOP	BASE	TOP	BASE	TOP	BASE	TOP	BASE	TOP	BASE	TOP	BASE	TOP	BASE
182	1268.0	1290.0	1290.0	1301.0			1301.0	1308.0			1308.0	1308.8	1308.8	1317.0	1317.0	1342.9
183			1330.0	1367.0			1367.0	1372.0					1372.0	1390.0	1390.0	1407.0
185	1295.3	1326.2	1326.2	1338.0			1338.0	1339.6					1339.6	1357.3	1357.3	1373.4
190	1292.0	1339.0					1339.0	1346.0					1346.0	1352.0	1352.0	1367.9
192																
193			1285.2	1326.5			1326.5	1351.4			1351.4	1351.5			1351.5	1360.6
194			1267.4	1308.5			1308.5	1314.5			1314.5	1322.9			1322.9	1344.2
195			1269.0	1302.0			1302.0	1307.0							1307.0	1342.0
196			1259.0	1285.0			1285.0	1325.0							1325.0	1335.0
197			1266.0	1298.0			1298.0	1303.0			1303.0	1311.0	1311.0	1311.8	1311.8	1343.0
214	1280.4	1307.8			1307.8	1320.7	1320.7	1324.0								
284			1342.0	1384.0			1384.0	1393.0							1393.0	1422.8
331	1261.8	1277.5	1277.5	1294.6			1294.6	1319.7					1319.7	1323.6	1323.6	1331.4
332			1272.0	1320.0			1320.0	1332.0							1332.0	1354.7
333	1296.0	1345.0													1345.0	1380.8
334	1331.2	1335.1	1335.1	1383.2			1383.2	1388.1					1388.1	1396.3	1396.3	1425.3
335	1332.0	1337.0	1337.0	1378.0			1378.0	1386.0					1386.0	1392.0	1392.0	1418.4
337	1242.0	1280.0													1280.0	1316.0
341	1345.0	1379.0	1379.0	1400.0									1400.0	1409.0	1409.0	1428.6

Table B.2 Thickness of Facies for Wells' Section

WELLS	Thickness of Facies (m)								TOTAL
	A	B	C	D	E	F	G	H	
2	45.29	11.08	0	0	0	0	5.26	19.09	80.72
18	33.99	14.01	0	0.83	0	0	11.17	14	74
20	52	0.71	0	0.87	0	0	2.57	21.51	77.66
21	30.71	24.27	0	0	0	0	8.03	18.07	81.08
24	28	0	0	0	0	0	0	18	46
28	0	50	0	19	0	0	1.44	10.56	81
35	0	53	0	4	0	0	10	12	79
45	0	50.89	0	0.77	0	0	0.43	6.68	58.77
54	40.33	0	0	0	0	0	0	31.04	71.37
61	0	42.62	0	17.4	0	0.53	0.98	13.69	75.22
64	33.41	0	0	0	0	0	0	17.37	50.78
67	0	44	0	21.7	0	0	2.87	9.43	78
80	0	53.34	0	3.97	0	0	8.49	0	65.8
81	57.89	0.31	0	0	0	0	0.33	10.92	69.45
86	47.75	0	0	0	0	0	0	18.96	66.71
90	0	63.46	0	13.57	0	0	0	0	77.03
92	6.78	68.19	0	11.44	0	0	0	0	86.41
96	0	55.92	0	0	0	0	0.44	5.49	61.85
98	35.94	0.59	0	6.17	0	0	8.31	2.83	53.84
101	0	45.45	0	17.65	0	0	0.5	8.96	72.56
103	5.01	39.88	0	17.35	0	0	0	9.83	72.07
110	0	27.25	0	19.32	0	4.43	0	0	51
112	0	34.92	0	7.1	0	1.02	14.99	21.95	79.98
114	0	34.08	0	4.03	0	21.95	0	19.97	80.03
115	0	30.23	0	0	0	0	0	0	30.23
122	0	40	0	34	0	0	7	7	88
126	31.94	49.51	0	0	0	0	0	0	81.45
133	56	0	0	0	0	0	0	21	77
140	6.16	0	7.84	0	29	0	0	25	68
148	0	36.15	0	11.05	0	0	0	0	47.2
155	0	47	0	5	0	0	9	15	76
167	13.4	0	30.31	0	8.21	0	0	10.12	62.04
172	0	62.97	0	2.75	0	0.98	6.5	8.11	81.31
174	15.81	0	18.11	2.01	26.16	0	0	16.94	79.03
176	0	15	0	25	0	0	0	32	72
177	0	26	0	33	0	0	4	8	71
179	0	40.96	0	5.03	0	0	4.94	23.17	74.1
180	29.44	9.28	0	9.07	0	0	12.09	15.84	75.72
182	22.02	10.98	0	7.01	0	0.8	8.2	25.89	74.9
183	0	37	0	5	0	0	18	17	77
185	30.94	11.75	0	1.62	0	0	17.66	16.08	78.05

Table B.2 (cont'd)

WELLS	Thickness of Facies (m)								TOTAL
	A	B	C	D	E	F	G	H	
190	47	0	0	7	0	0	6	15.88	75.88
192	0	0	0	0	0	0	0	0	0
193	0	41.31	0	24.92	0	0.12	0	9.02	75.37
194	0	41.13	0	6.03	0	8.4	0	21.23	76.79
195	0	33	0	5	0	0	0	34.99	72.99
196	0	26.01	0	39.99	0	0	0	10	76
197	0	32	0	5	0	8	0.83	31.17	77
214	27.39	0	12.96	3.27	0	0	0	0	43.62
284	0	42	0	9	0	0	0	29.8	80.8
331	15.7	17.05	0	25.1	0	0	3.92	7.78	69.55
332	0	48	0	12	0	0	0	22.66	82.66
333	49	0	0	0	0	0	0	35.75	84.75
334	3.93	48.09	0	4.91	0	0	8.2	28.96	94.09
335	5	41	0	8	0	0	6	26.39	86.39
337	38	0	0	0	0	0	0	36	74
341	34	21	0	0	0	0	9	19.6	83.6

APPENDIX C

NORMAL DISTRIBUTION CHECK

C.1. Goodness of Fit Test Results

Table C.1.1 Goodness of Fit Test Results for Well#174 Facies A

Normal					
Kolmogorov-Smirnov					
Sample Size Statistic P-Value Rank	13 0,19838 0,61683 29				
α	0,2	0,1	0,05	0,02	0,01
Critical Value	0,2847	0,32549	0,36143	0,40362	0,43247
Reject?	No	No	No	No	No
Anderson-Darling					
Sample Size Statistic Rank	13 0,54327 24				
α	0,2	0,1	0,05	0,02	0,01
Critical Value	1,3749	1,9286	2,5018	3,2892	3,9074
Reject?	No	No	No	No	No
Chi-Squared					
Deg. of freedom Statistic P-Value Rank	1 0,55056 0,45809 28				
α	0,2	0,1	0,05	0,02	0,01
Critical Value	1,6424	2,7055	3,8415	5,4119	6,6349
Reject?	No	No	No	No	No

Table C.1.2 Goodness of Fit Test Results for Well#180 Facies A

Normal					
Kolmogorov-Smirnov					
Sample Size Statistic P-Value Rank	21 0,1789 0,45957 40				
α	0,2	0,1	0,05	0,02	0,01
Critical Value	0,22617	0,25858	0,28724	0,32104	0,34427
Reject?	No	No	No	No	No
Anderson-Darling					
Sample Size Statistic Rank	21 0,72952 33				
α	0,2	0,1	0,05	0,02	0,01
Critical Value	1,3749	1,9286	2,5018	3,2892	3,9074
Reject?	No	No	No	No	No
Chi-Squared					
Deg. of freedom Statistic P-Value Rank	2 3,8536 0,14561 45				
α	0,2	0,1	0,05	0,02	0,01
Critical Value	3,2189	4,6052	5,9915	7,824	9,2103
Reject?	Yes	No	No	No	No

Table C.1.3 Goodness of Fit Test Results for Well#182 Facies A

Normal					
Kolmogorov-Smirnov					
Sample Size Statistic P-Value Rank	43 0,27742 0,00204 41				
α	0,2	0,1	0,05	0,02	0,01
Critical Value	0,15974	0,18257	0,20283	0,22679	0,24332
Reject?	Yes	Yes	Yes	Yes	Yes
Anderson-Darling					
Sample Size Statistic Rank	43 5,9523 44				
α	0,2	0,1	0,05	0,02	0,01
Critical Value	1,3749	1,9286	2,5018	3,2892	3,9074
Reject?	Yes	Yes	Yes	Yes	Yes
Chi-Squared					
Deg. of freedom Statistic P-Value Rank	3 7,9557 0,04694 27				
α	0,2	0,1	0,05	0,02	0,01
Critical Value	4,6416	6,2514	7,8147	9,8374	11,345
Reject?	Yes	Yes	Yes	No	No

Table C.1.4 Goodness of Fit Test Results for Well#185 Facies A

Normal					
Kolmogorov-Smirnov					
Sample Size Statistic P-Value Rank	12 0,23953 0,42948 37				
α	0,2	0,1	0,05	0,02	0,01
Critical Value	0,29577	0,33815	0,37543	0,41918	0,44905
Reject?	No	No	No	No	No
Anderson-Darling					
Sample Size Statistic Rank	12 0,86045 34				
α	0,2	0,1	0,05	0,02	0,01
Critical Value	1,3749	1,9286	2,5018	3,2892	3,9074
Reject?	No	No	No	No	No

Table C.1.5 Goodness of Fit Test Results for Well#190 Facies A

Normal					
Kolmogorov-Smirnov					
Sample Size Statistic P-Value Rank	21 0,36736 0,00476 40				
α	0,2	0,1	0,05	0,02	0,01
Critical Value	0,22617	0,25858	0,28724	0,32104	0,34427
Reject?	Yes	Yes	Yes	Yes	Yes
Anderson-Darling					
Sample Size Statistic Rank	21 2,9881 33				
α	0,2	0,1	0,05	0,02	0,01
Critical Value	1,3749	1,9286	2,5018	3,2892	3,9074
Reject?	Yes	Yes	Yes	No	No
Chi-Squared					
Deg. of freedom Statistic P-Value Rank	1 8,2702 0,00403 36				
α	0,2	0,1	0,05	0,02	0,01
Critical Value	1,6424	2,7055	3,8415	5,4119	6,6349
Reject?	Yes	Yes	Yes	Yes	Yes

Table C.1.6 Goodness of Fit Test Results for Well#331 Facies A

Normal					
Kolmogorov-Smirnov					
Sample Size Statistic P-Value Rank	19 0,22335 0,2584 30				
α	0,2	0,1	0,05	0,02	0,01
Critical Value	0,23735	0,27136	0,30143	0,33685	0,36117
Reject?	No	No	No	No	No
Anderson-Darling					
Sample Size Statistic Rank	19 1,2257 27				
α	0,2	0,1	0,05	0,02	0,01
Critical Value	1,3749	1,9286	2,5018	3,2892	3,9074
Reject?	No	No	No	No	No
Chi-Squared					
Deg. of freedom Statistic P-Value Rank	2 6,0572 0,04838 42				
α	0,2	0,1	0,05	0,02	0,01
Critical Value	3,2189	4,6052	5,9915	7,824	9,2103
Reject?	Yes	Yes	Yes	No	No

Table C.1.7 Goodness of Fit Test Results for Well#333 Facies A

Normal					
Kolmogorov-Smirnov					
Sample Size Statistic P-Value Rank	16 0,24752 0,23813 30				
α	0,2	0,1	0,05	0,02	0,01
Critical Value	0,25778	0,29472	0,32733	0,36571	0,39201
Reject?	No	No	No	No	No
Anderson-Darling					
Sample Size Statistic Rank	16 1,6079 25				
α	0,2	0,1	0,05	0,02	0,01
Critical Value	1,3749	1,9286	2,5018	3,2892	3,9074
Reject?	Yes	No	No	No	No
Chi-Squared					
Deg. of freedom Statistic P-Value Rank	1 0,97628 0,32312 19				
α	0,2	0,1	0,05	0,02	0,01
Critical Value	1,6424	2,7055	3,8415	5,4119	6,6349
Reject?	No	No	No	No	No

Table C.1.8 Goodness of Fit Test Results for Well#341 Facies A

Normal					
Kolmogorov-Smirnov					
Sample Size Statistic P-Value Rank	85 0,21949 4,4685E-4 42				
α	0,2	0,1	0,05	0,02	0,01
Critical Value	0,11442	0,13072	0,1452	0,16236	0,17421
Reject?	Yes	Yes	Yes	Yes	Yes
Anderson-Darling					
Sample Size Statistic Rank	85 7,1461 42				
α	0,2	0,1	0,05	0,02	0,01
Critical Value	1,3749	1,9286	2,5018	3,2892	3,9074
Reject?	Yes	Yes	Yes	Yes	Yes
Chi-Squared					
Deg. of freedom Statistic P-Value Rank	5 12,146 0,03284 27				
α	0,2	0,1	0,05	0,02	0,01
Critical Value	7,2893	9,2364	11,07	13,388	15,086
Reject?	Yes	Yes	Yes	No	No

Table C.1.9 Goodness of Fit Test Results for Well#155 Facies B

Normal					
Kolmogorov-Smirnov					
Sample Size Statistic P-Value Rank	6 0,20876 0,91072 7				
α	0,2	0,1	0,05	0,02	0,01
Critical Value	0,41037	0,46799	0,51926	0,57741	0,61661
Reject?	No	No	No	No	No
Anderson-Darling					
Sample Size Statistic Rank	6 0,36704 8				
α	0,2	0,1	0,05	0,02	0,01
Critical Value	1,3749	1,9286	2,5018	3,2892	3,9074
Reject?	No	No	No	No	No

Table C.1.10 Goodness of Fit Test Results for Well#172 Facies B

Normal					
Kolmogorov-Smirnov					
Sample Size Statistic P-Value Rank	59 0,28238 1,1793E-4 44				
α	0,2	0,1	0,05	0,02	0,01
Critical Value	0,13686	0,15639	0,17373	0,19427	0,20844
Reject?	Yes	Yes	Yes	Yes	Yes
Anderson-Darling					
Sample Size Statistic Rank	59 8,0637 46				
α	0,2	0,1	0,05	0,02	0,01
Critical Value	1,3749	1,9286	2,5018	3,2892	3,9074
Reject?	Yes	Yes	Yes	Yes	Yes
Chi-Squared					
Deg. of freedom Statistic P-Value Rank	4 8,2859 0,08165 26				
α	0,2	0,1	0,05	0,02	0,01
Critical Value	5,9886	7,7794	9,4877	11,668	13,277
Reject?	Yes	Yes	No	No	No

Table C.1.11 Goodness of Fit Test Results for Well#180 Facies B

Normal					
Kolmogorov-Smirnov					
Sample Size Statistic P-Value Rank	10 0,20433 0,72628 26				
α	0,2	0,1	0,05	0,02	0,01
Critical Value	0,3226	0,36866	0,40925	0,45662	0,48893
Reject?	No	No	No	No	No
Anderson-Darling					
Sample Size Statistic Rank	10 0,61454 31				
α	0,2	0,1	0,05	0,02	0,01
Critical Value	1,3749	1,9286	2,5018	3,2892	3,9074
Reject?	No	No	No	No	No
Chi-Squared					
Deg. of freedom Statistic P-Value Rank	1 0,77564 0,37848 28				
α	0,2	0,1	0,05	0,02	0,01
Critical Value	1,6424	2,7055	3,8415	5,4119	6,6349
Reject?	No	No	No	No	No

Table C.1.12 Goodness of Fit Test Results for Well#193 Facies B

Normal					
Kolmogorov-Smirnov					
Sample Size Statistic P-Value Rank	49 0,29107 3,5877E-4 46				
α	0,2	0,1	0,05	0,02	0,01
Critical Value	0,14987	0,17128	0,19028	0,21277	0,22828
Reject?	Yes	Yes	Yes	Yes	Yes
Anderson-Darling					
Sample Size Statistic Rank	49 6,179 42				
α	0,2	0,1	0,05	0,02	0,01
Critical Value	1,3749	1,9286	2,5018	3,2892	3,9074
Reject?	Yes	Yes	Yes	Yes	Yes
Chi-Squared					
Deg. of freedom Statistic P-Value Rank	3 12,394 0,00615 29				
α	0,2	0,1	0,05	0,02	0,01
Critical Value	4,6416	6,2514	7,8147	9,8374	11,345
Reject?	Yes	Yes	Yes	Yes	Yes

Table C.1.13 Goodness of Fit Test Results for Well#195 Facies B

Normal					
Kolmogorov-Smirnov					
Sample Size Statistic P-Value Rank	10 0,35729 0,11973 41				
α	0,2	0,1	0,05	0,02	0,01
Critical Value	0,3226	0,36866	0,40925	0,45662	0,48893
Reject?	Yes	No	No	No	No
Anderson-Darling					
Sample Size Statistic Rank	10 1,1478 25				
α	0,2	0,1	0,05	0,02	0,01
Critical Value	1,3749	1,9286	2,5018	3,2892	3,9074
Reject?	No	No	No	No	No

Table C.1.14 Goodness of Fit Test Results for Well#196 Facies B

Normal					
Kolmogorov-Smirnov					
Sample Size Statistic P-Value Rank	17 0,1953 0,47673 39				
α	0,2	0,1	0,05	0,02	0,01
Critical Value	0,25039	0,28627	0,31796	0,35528	0,38086
Reject?	No	No	No	No	No
Anderson-Darling					
Sample Size Statistic Rank	17 1,1222 37				
α	0,2	0,1	0,05	0,02	0,01
Critical Value	1,3749	1,9286	2,5018	3,2892	3,9074
Reject?	No	No	No	No	No
Chi-Squared					
Deg. of freedom Statistic P-Value Rank	1 1,3519 0,24495 30				
α	0,2	0,1	0,05	0,02	0,01
Critical Value	1,6424	2,7055	3,8415	5,4119	6,6349
Reject?	No	No	No	No	No

Table C.1.15 Goodness of Fit Test Results for Well#197 Facies B

Normal					
Kolmogorov-Smirnov					
Sample Size Statistic P-Value Rank	7 0,29525 0,48567 32				
α	0,2	0,1	0,05	0,02	0,01
Critical Value	0,38148	0,43607	0,48342	0,53844	0,57581
Reject?	No	No	No	No	No
Anderson-Darling					
Sample Size Statistic Rank	7 0,57792 19				
α	0,2	0,1	0,05	0,02	0,01
Critical Value	1,3749	1,9286	2,5018	3,2892	3,9074
Reject?	No	No	No	No	No

Table C.1.16 Goodness of Fit Test Results for Well#284 Facies B

Normal					
Kolmogorov-Smirnov					
Sample Size Statistic P-Value Rank	23 0,28896 0,03404 42				
α	0,2	0,1	0,05	0,02	0,01
Critical Value	0,21645	0,24746	0,2749	0,30728	0,32954
Reject?	Yes	Yes	Yes	No	No
Anderson-Darling					
Sample Size Statistic Rank	23 3,1592 38				
α	0,2	0,1	0,05	0,02	0,01
Critical Value	1,3749	1,9286	2,5018	3,2892	3,9074
Reject?	Yes	Yes	Yes	No	No
Chi-Squared					
Deg. of freedom Statistic P-Value Rank	1 2,1097 0,14637 16				
α	0,2	0,1	0,05	0,02	0,01
Critical Value	1,6424	2,7055	3,8415	5,4119	6,6349
Reject?	Yes	No	No	No	No

Table C.1.17 Goodness of Fit Test Results for Well#331 Facies B

Normal					
Kolmogorov-Smirnov					
Sample Size Statistic P-Value Rank	48 0,33644 2,3870E-5 41				
α	0,2	0,1	0,05	0,02	0,01
Critical Value	0,1513	0,17302	0,19221	0,21493	0,23059
Reject?	Yes	Yes	Yes	Yes	Yes
Anderson-Darling					
Sample Size Statistic Rank	48 7,6604 41				
α	0,2	0,1	0,05	0,02	0,01
Critical Value	1,3749	1,9286	2,5018	3,2892	3,9074
Reject?	Yes	Yes	Yes	Yes	Yes
Chi-Squared					
Deg. of freedom Statistic P-Value Rank	2 14,452 7,2730E-4 29				
α	0,2	0,1	0,05	0,02	0,01
Critical Value	3,2189	4,6052	5,9915	7,824	9,2103
Reject?	Yes	Yes	Yes	Yes	Yes

Table C.1.18 Goodness of Fit Test Results for Well#334 Facies B

Normal					
Kolmogorov-Smirnov					
Sample Size Statistic P-Value Rank	92 0,34082 6,1277E-10 42				
α	0,2	0,1	0,05	0,02	0,01
Critical Value	0,11005	0,12572	0,13965	0,15616	0,16755
Reject?	Yes	Yes	Yes	Yes	Yes
Anderson-Darling					
Sample Size Statistic Rank	92 17,057 43				
α	0,2	0,1	0,05	0,02	0,01
Critical Value	1,3749	1,9286	2,5018	3,2892	3,9074
Reject?	Yes	Yes	Yes	Yes	Yes
Chi-Squared					
Deg. of freedom Statistic P-Value Rank	3 30,149 1,2840E-6 32				
α	0,2	0,1	0,05	0,02	0,01
Critical Value	4,6416	6,2514	7,8147	9,8374	11,345
Reject?	Yes	Yes	Yes	Yes	Yes

Table C.1.19 Goodness of Fit Test Results for Well#335 Facies B

Normal					
Kolmogorov-Smirnov					
Sample Size Statistic P-Value Rank	39 0,2516 0,01159 43				
α	0,2	0,1	0,05	0,02	0,01
Critical Value	0,16753	0,19148	0,21273	0,23786	0,25518
Reject?	Yes	Yes	Yes	Yes	No
Anderson-Darling					
Sample Size Statistic Rank	39 4,3988 43				
α	0,2	0,1	0,05	0,02	0,01
Critical Value	1,3749	1,9286	2,5018	3,2892	3,9074
Reject?	Yes	Yes	Yes	Yes	Yes
Chi-Squared					
Deg. of freedom Statistic P-Value Rank	3 8,3145 0,03994 36				
α	0,2	0,1	0,05	0,02	0,01
Critical Value	4,6416	6,2514	7,8147	9,8374	11,345
Reject?	Yes	Yes	Yes	No	No

Table C.1.20 Goodness of Fit Test Results for Well#180 Facies D

Normal					
Kolmogorov-Smirnov					
Sample Size Statistic P-Value Rank	7 0,17775 0,95234 15				
α	0,2	0,1	0,05	0,02	0,01
Critical Value	0,38148	0,43607	0,48342	0,53844	0,57581
Reject?	No	No	No	No	No
Anderson-Darling					
Sample Size Statistic Rank	7 0,35863 24				
α	0,2	0,1	0,05	0,02	0,01
Critical Value	1,3749	1,9286	2,5018	3,2892	3,9074
Reject?	No	No	No	No	No

Table C.1.21 Goodness of Fit Test Results for Well#334 Facies G

Normal					
Kolmogorov-Smirnov					
Sample Size Statistic P-Value Rank	11 0,3089 0,19812 39				
α	0,2	0,1	0,05	0,02	0,01
Critical Value	0,30829	0,35242	0,39122	0,4367	0,4677
Reject?	Yes	No	No	No	No
Anderson-Darling					
Sample Size Statistic Rank	11 1,3364 32				
α	0,2	0,1	0,05	0,02	0,01
Critical Value	1,3749	1,9286	2,5018	3,2892	3,9074
Reject?	No	No	No	No	No
Chi-Squared					
Deg. of freedom Statistic P-Value Rank	1 0,1579 0,6911 16				
α	0,2	0,1	0,05	0,02	0,01
Critical Value	1,6424	2,7055	3,8415	5,4119	6,6349
Reject?	No	No	No	No	No

Table C.1.22 Goodness of Fit Test Results for Well#335 Facies G

Normal					
Kolmogorov-Smirnov					
Sample Size Statistic P-Value Rank	13 0,17546 0,7572 32				
α	0,2	0,1	0,05	0,02	0,01
Critical Value	0,2847	0,32549	0,36143	0,40362	0,43247
Reject?	No	No	No	No	No
Anderson-Darling					
Sample Size Statistic Rank	13 0,64002 36				
α	0,2	0,1	0,05	0,02	0,01
Critical Value	1,3749	1,9286	2,5018	3,2892	3,9074
Reject?	No	No	No	No	No
Chi-Squared					
Deg. of freedom Statistic P-Value Rank	1 0,68675 0,40727 41				
α	0,2	0,1	0,05	0,02	0,01
Critical Value	1,6424	2,7055	3,8415	5,4119	6,6349
Reject?	No	No	No	No	No

Table C.1.23 Goodness of Fit Test Results for Well#176 Facies H

Normal					
Kolmogorov-Smirnov					
Sample Size Statistic P-Value Rank	27 0,26115 0,04104 32				
α	0,2	0,1	0,05	0,02	0,01
Critical Value	0,2003	0,22898	0,25438	0,28438	0,30502
Reject?	Yes	Yes	Yes	No	No
Anderson-Darling					
Sample Size Statistic Rank	27 2,8385 21				
α	0,2	0,1	0,05	0,02	0,01
Critical Value	1,3749	1,9286	2,5018	3,2892	3,9074
Reject?	Yes	Yes	Yes	No	No
Chi-Squared					
Deg. of freedom Statistic P-Value Rank	2 4,2975 0,11663 25				
α	0,2	0,1	0,05	0,02	0,01
Critical Value	3,2189	4,6052	5,9915	7,824	9,2103
Reject?	Yes	No	No	No	No

Table C.1.24 Goodness of Fit Test Results for Well#334 Facies H

Normal					
Kolmogorov-Smirnov					
Sample Size Statistic P-Value Rank	34 0,36322 1,5855E-4 35				
α	0,2	0,1	0,05	0,02	0,01
Critical Value	0,17909	0,20472	0,22743	0,25429	0,27279
Reject?	Yes	Yes	Yes	Yes	Yes
Anderson-Darling					
Sample Size Statistic Rank	34 5,7028 20				
α	0,2	0,1	0,05	0,02	0,01
Critical Value	1,3749	1,9286	2,5018	3,2892	3,9074
Reject?	Yes	Yes	Yes	Yes	Yes
Chi-Squared					
Deg. of freedom Statistic P-Value Rank	1 12,47 4,1346E-4 25				
α	0,2	0,1	0,05	0,02	0,01
Critical Value	1,6424	2,7055	3,8415	5,4119	6,6349
Reject?	Yes	Yes	Yes	Yes	Yes

C.2 Probability Density Functions & Histograms

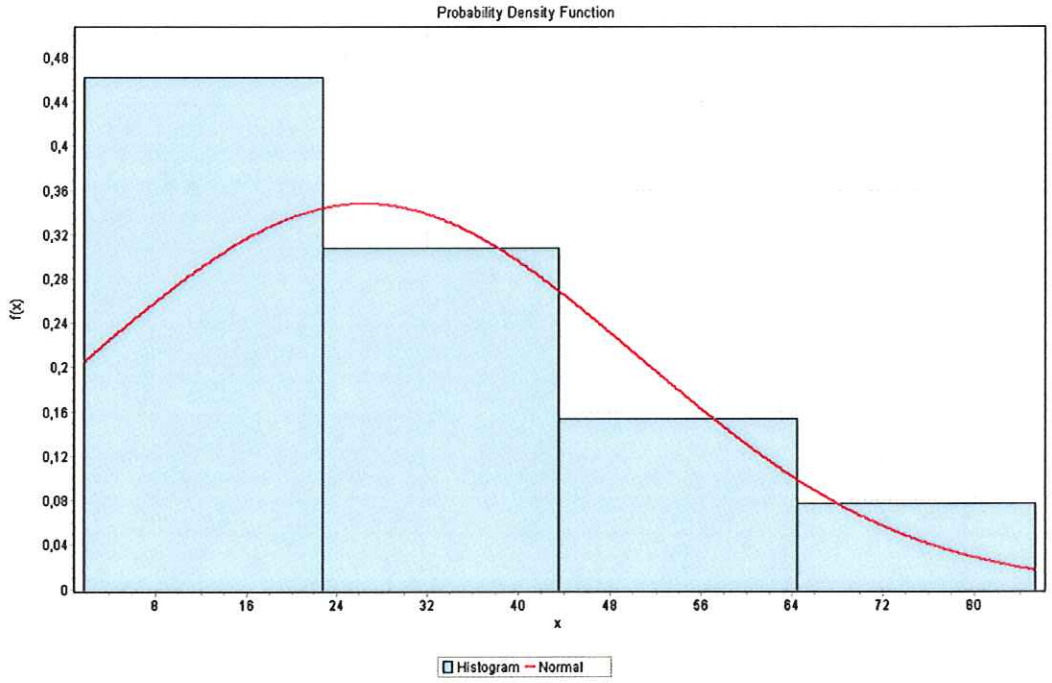

Figure C.2.1 PDF & Histogram Well#174 Facies A

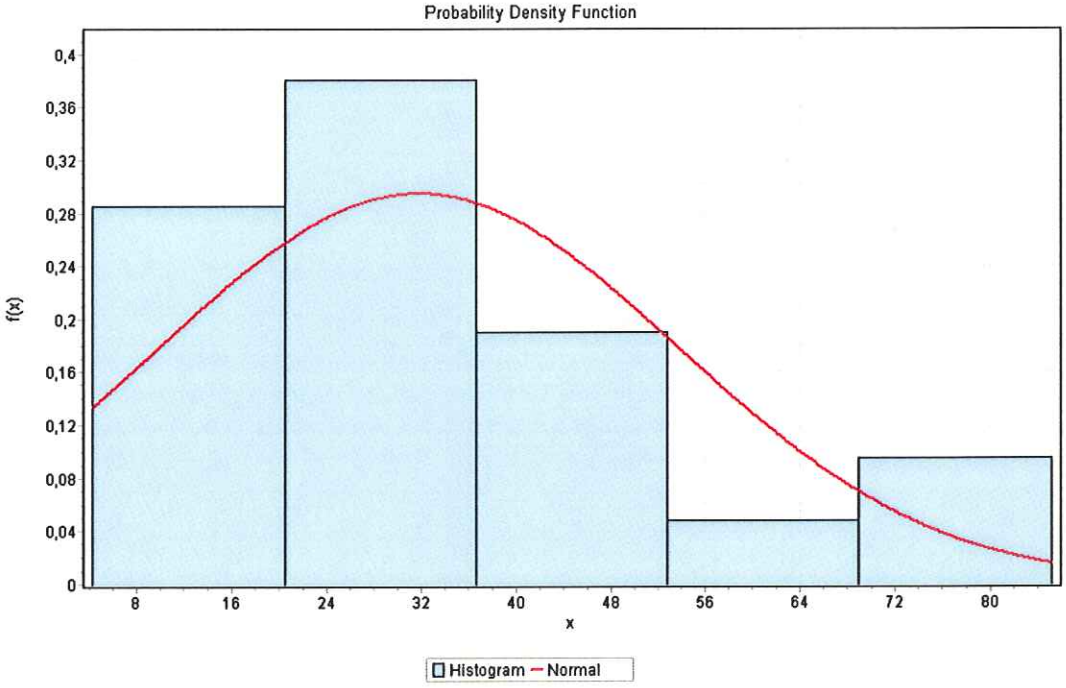

Figure C.2.2 PDF & Histogram Well#180 Facies A

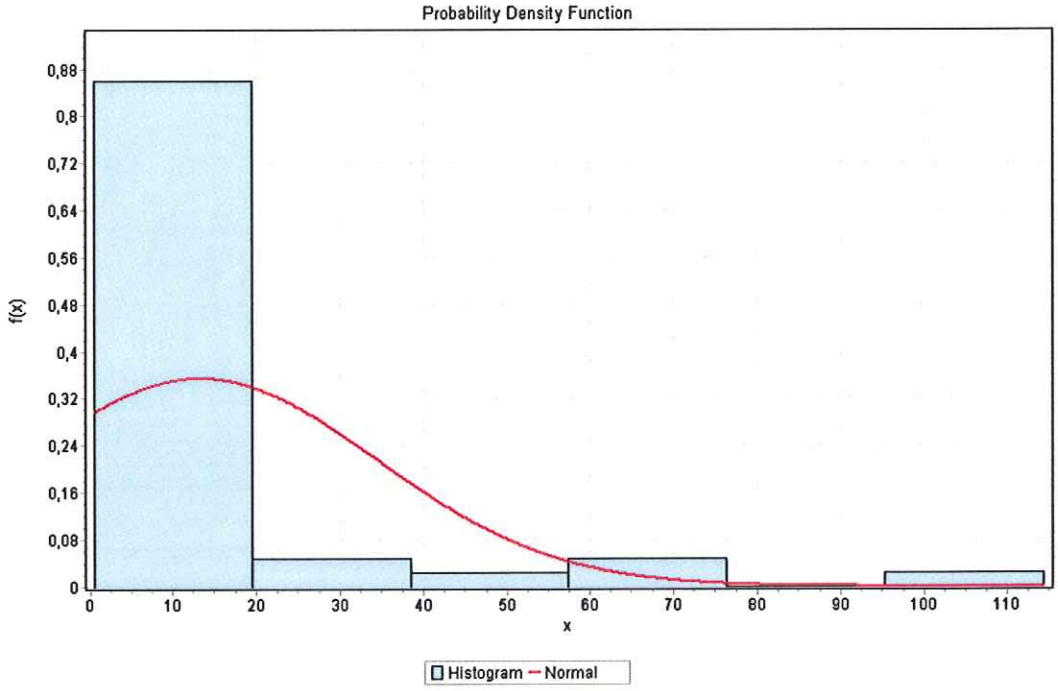

Figure C.2.3 PDF & Histogram Well#182 Facies A

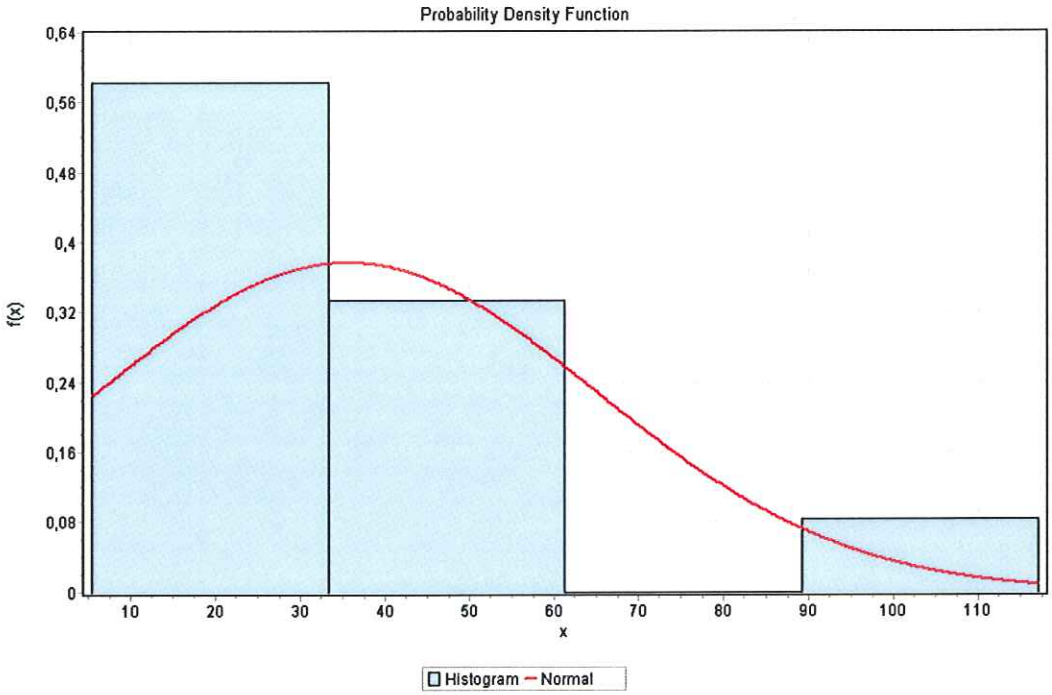

Figure C.2.4 PDF & Histogram Well#185 Facies A

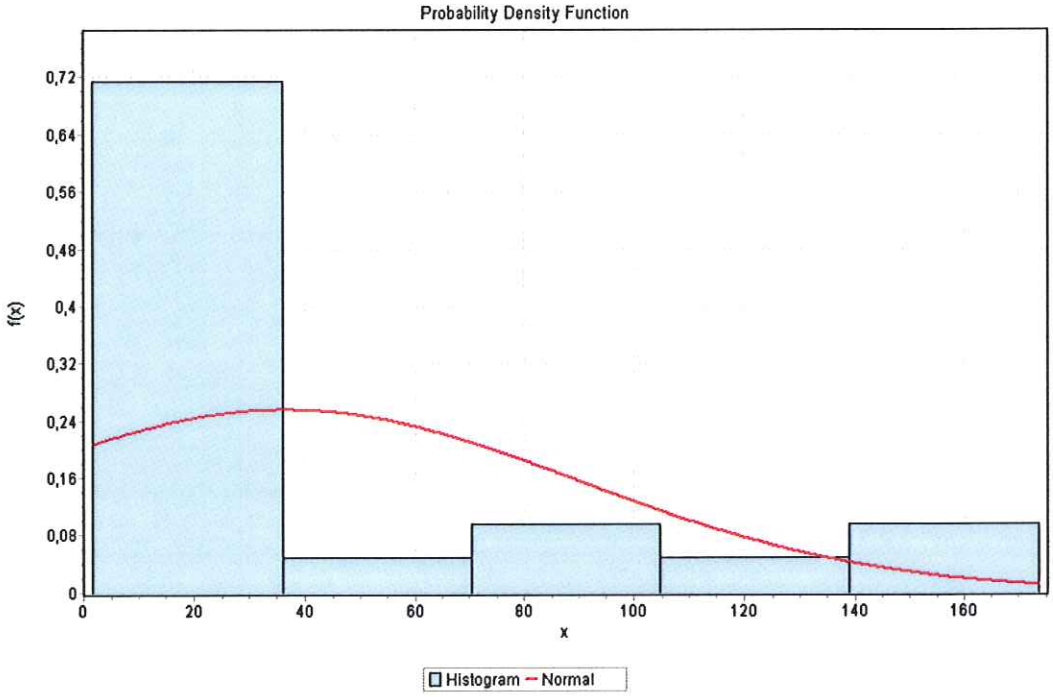

Figure C.2.5 PDF & Histogram Well#190 Facies A

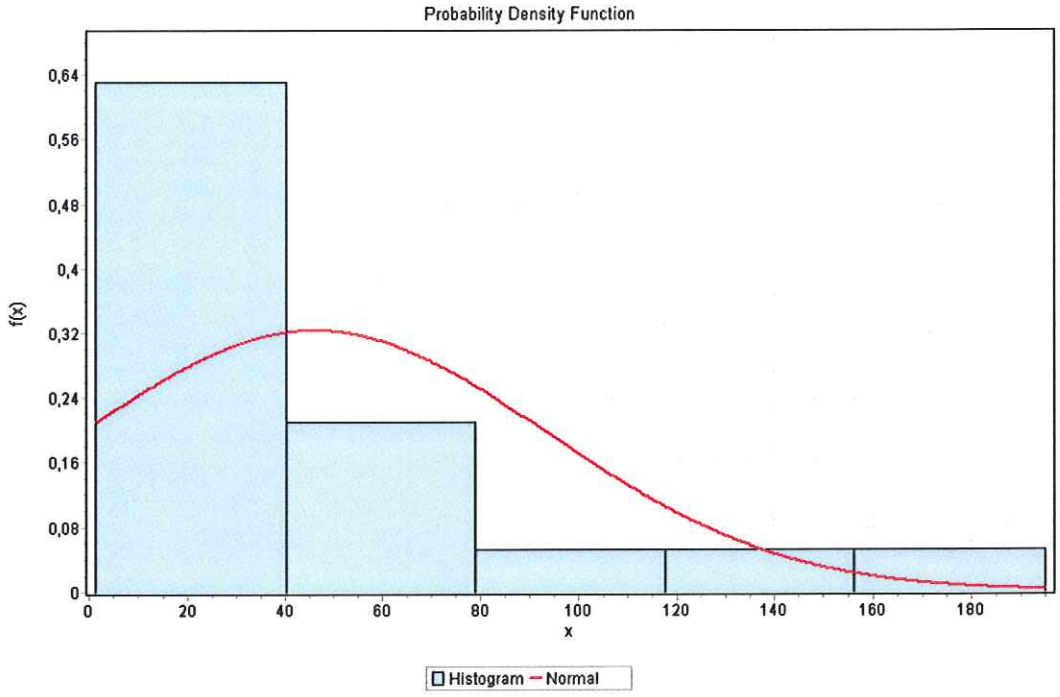

Figure C.2.6 PDF & Histogram Well#331 Facies A

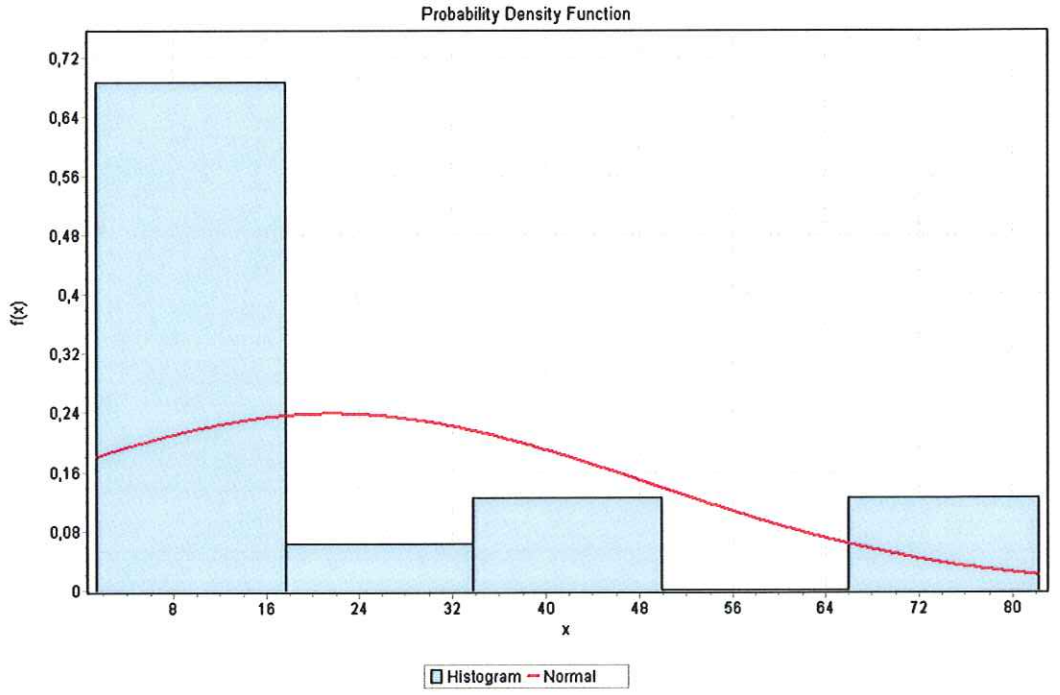

Figure C.2.7 PDF & Histogram Well#333 Facies A

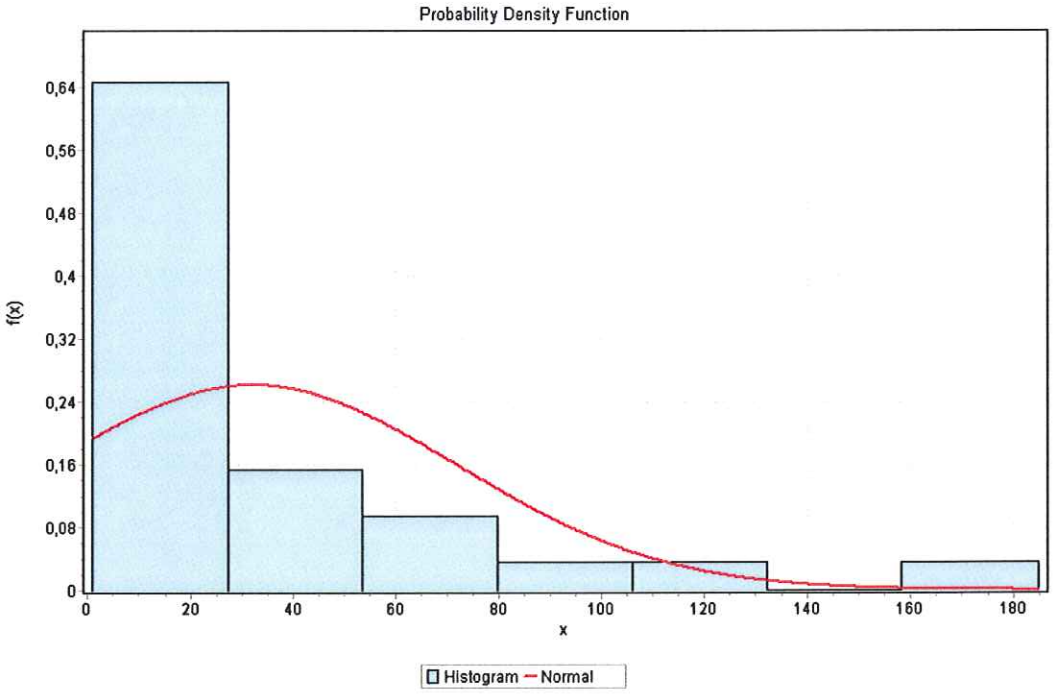

Figure C.2.8 PDF & Histogram Well#341 Facies A

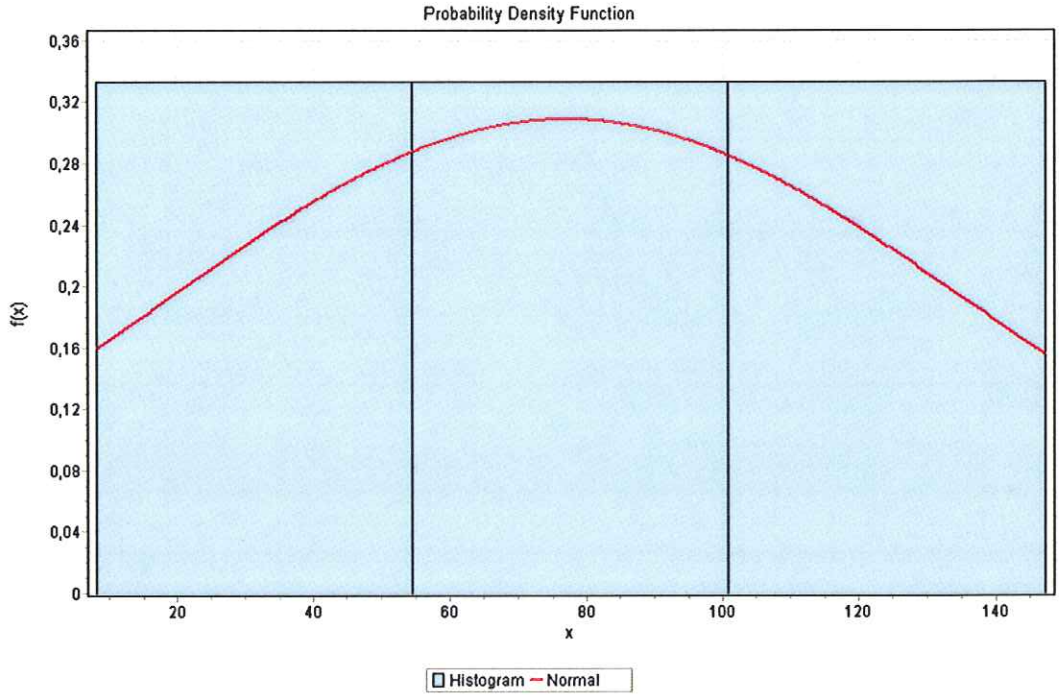

Figure C.2.9 PDF & Histogram Well#155 Facies B

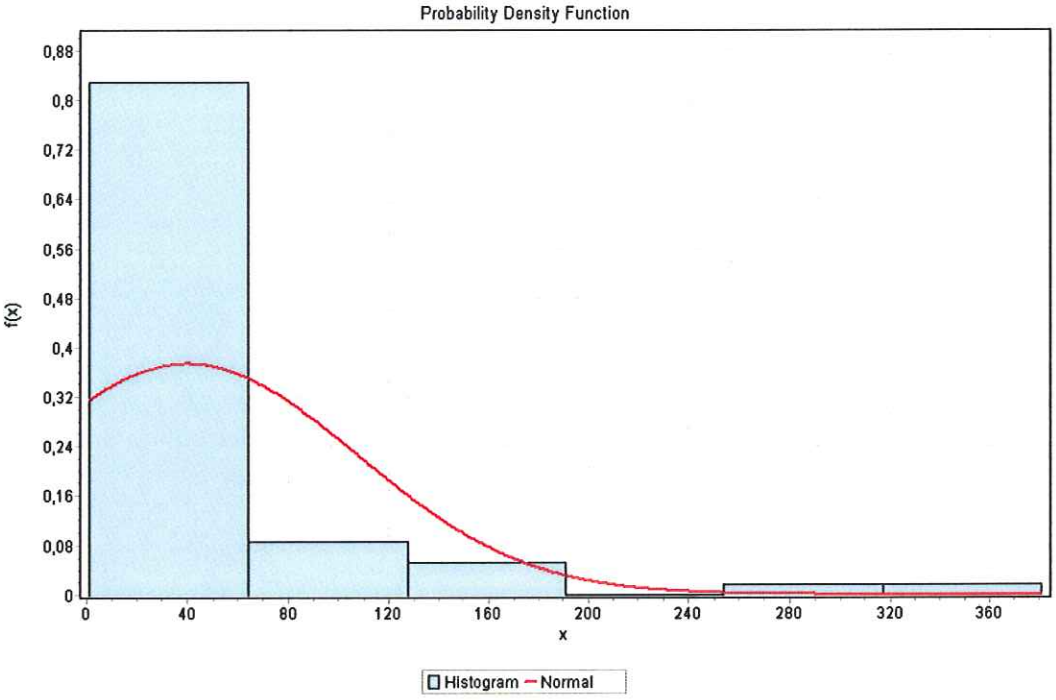

Figure C.2.10 PDF & Histogram Well#172 Facies B

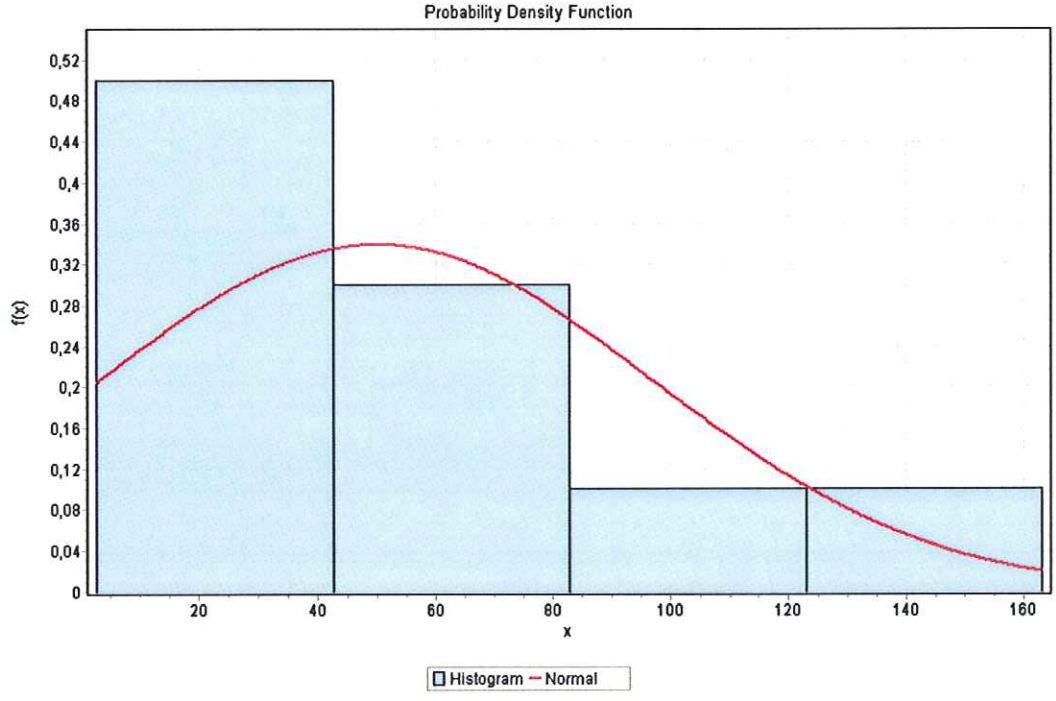

Figure C.2.11 PDF & Histogram Well#180 Facies B

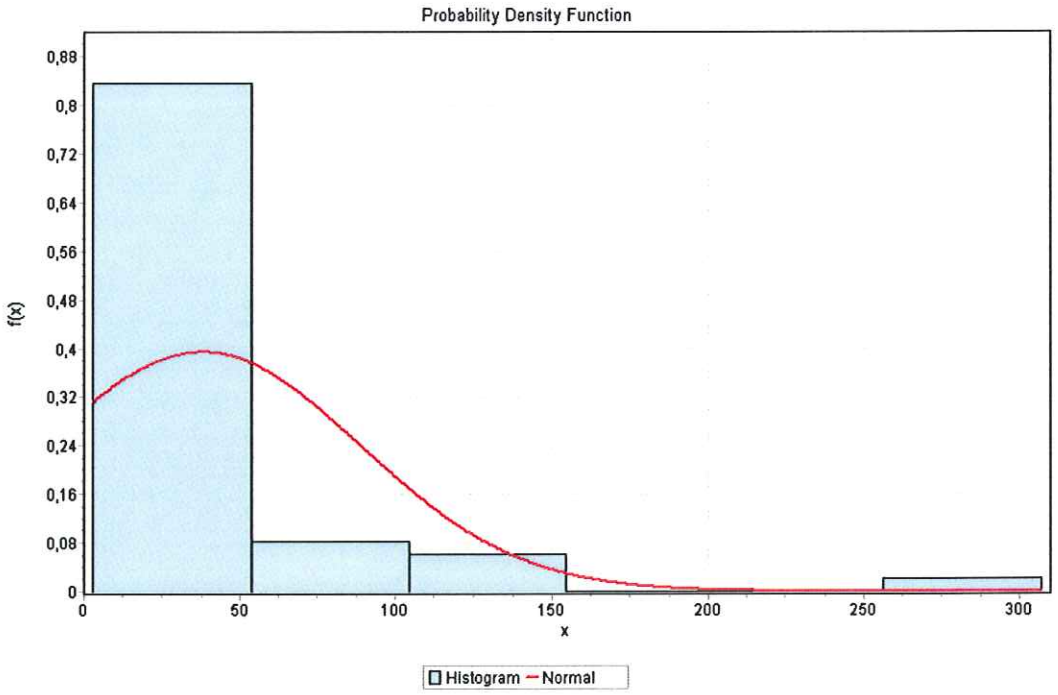

Figure C.2.12 PDF & Histogram Well#193 Facies B

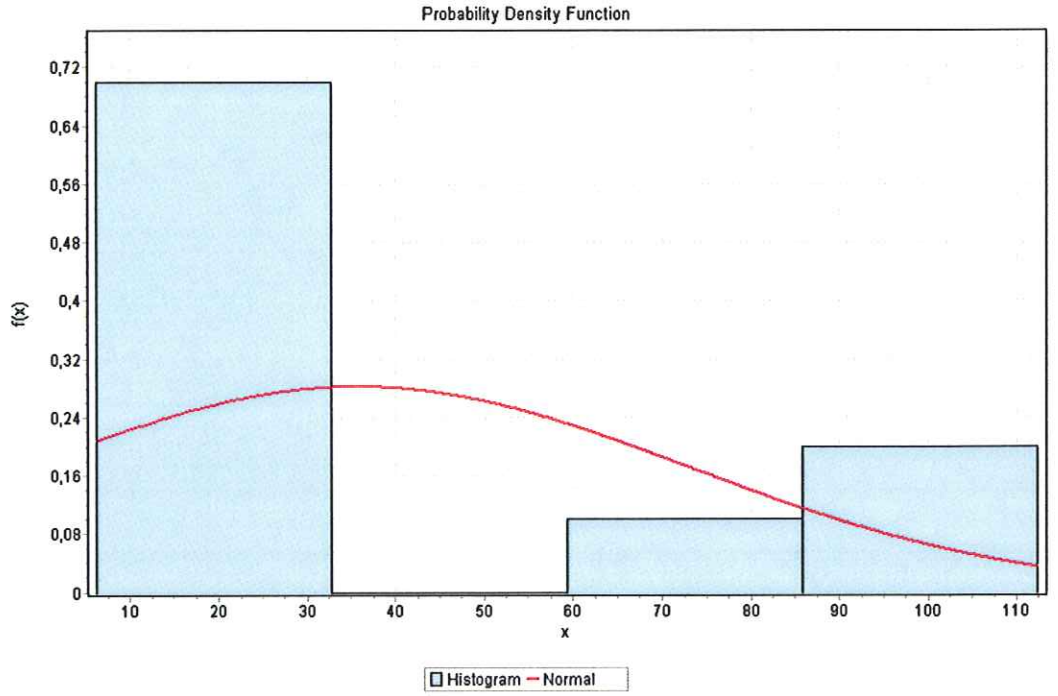

Figure C.2.13 PDF & Histogram Well#195 Facies B

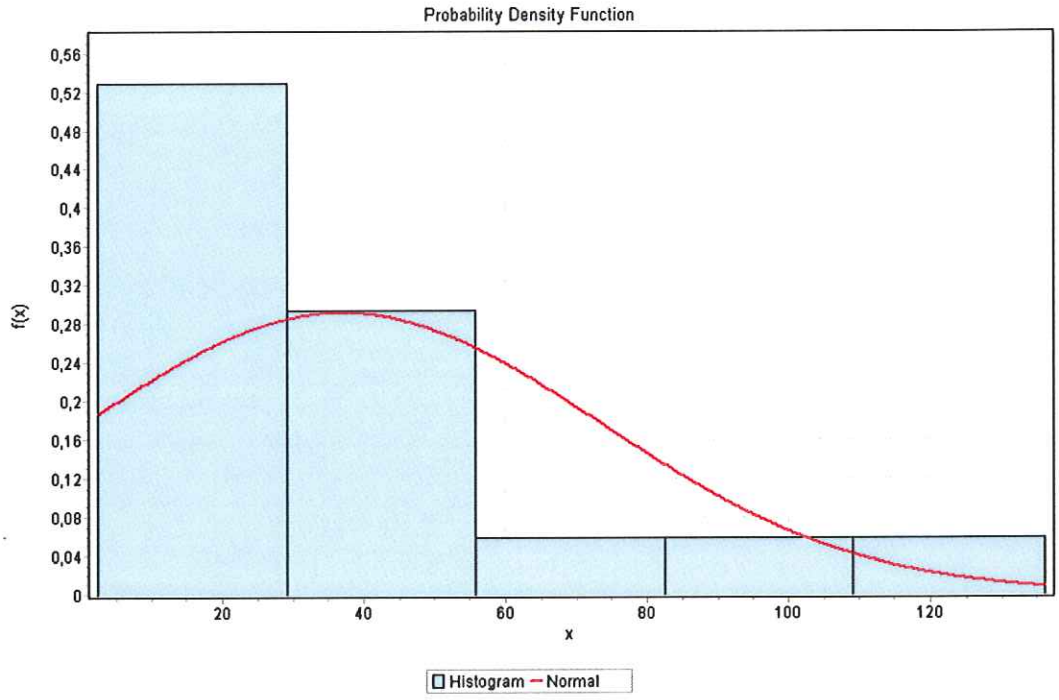

Figure C.2.14 PDF & Histogram Well#196 Facies B

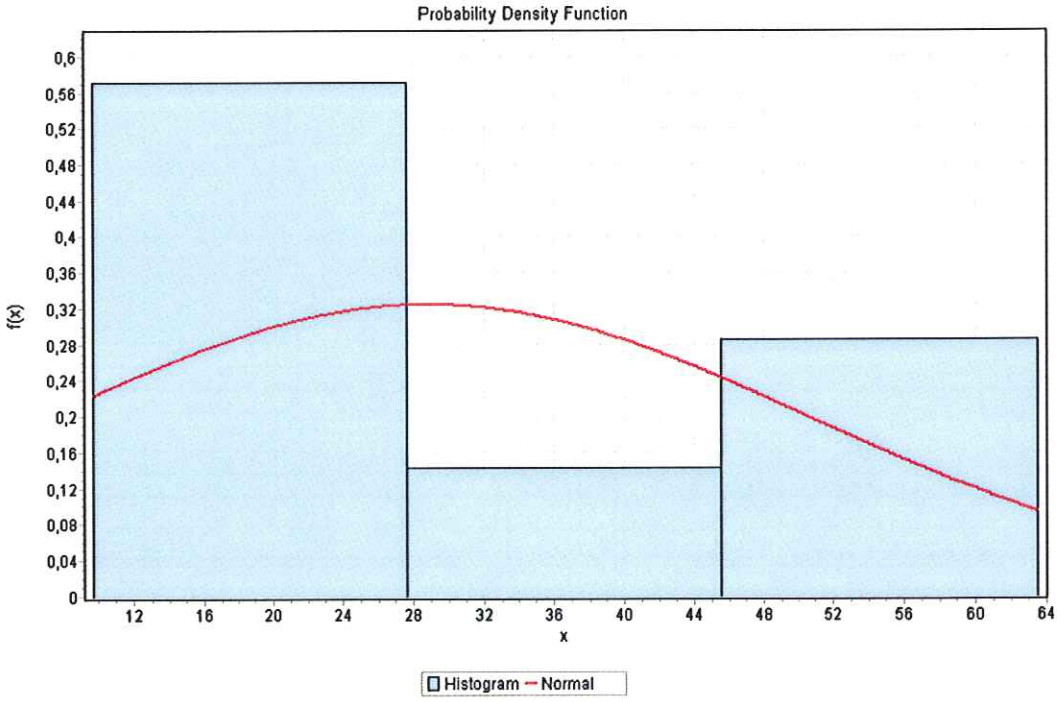

Figure C.2.15 PDF & Histogram Well#197 Facies B

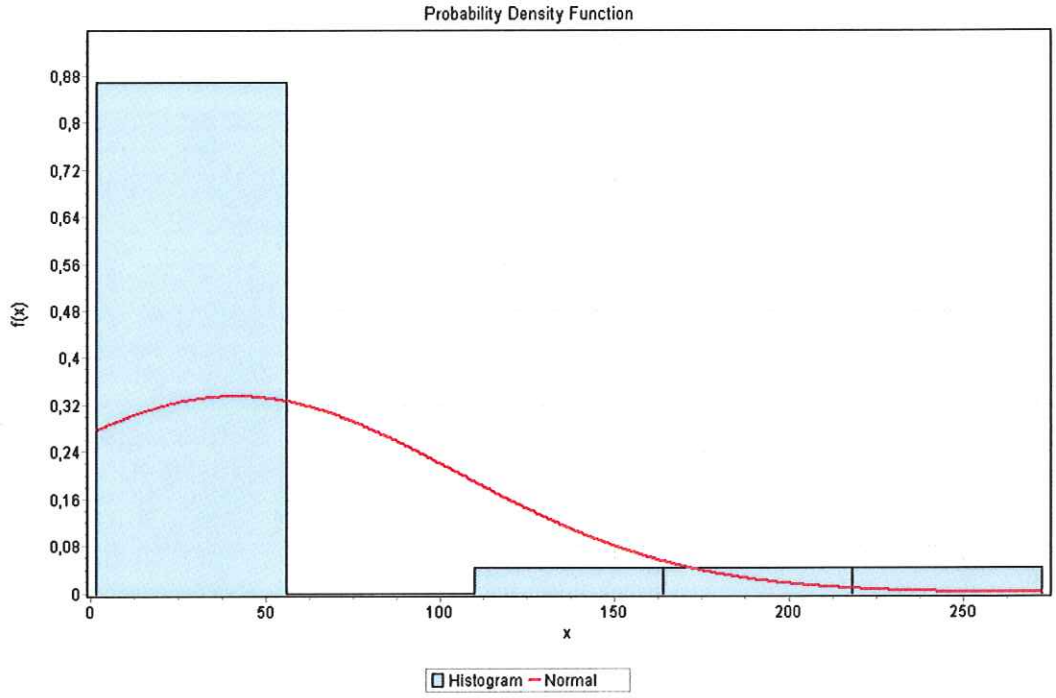

Figure C.2.16 PDF & Histogram Well#284 Facies B

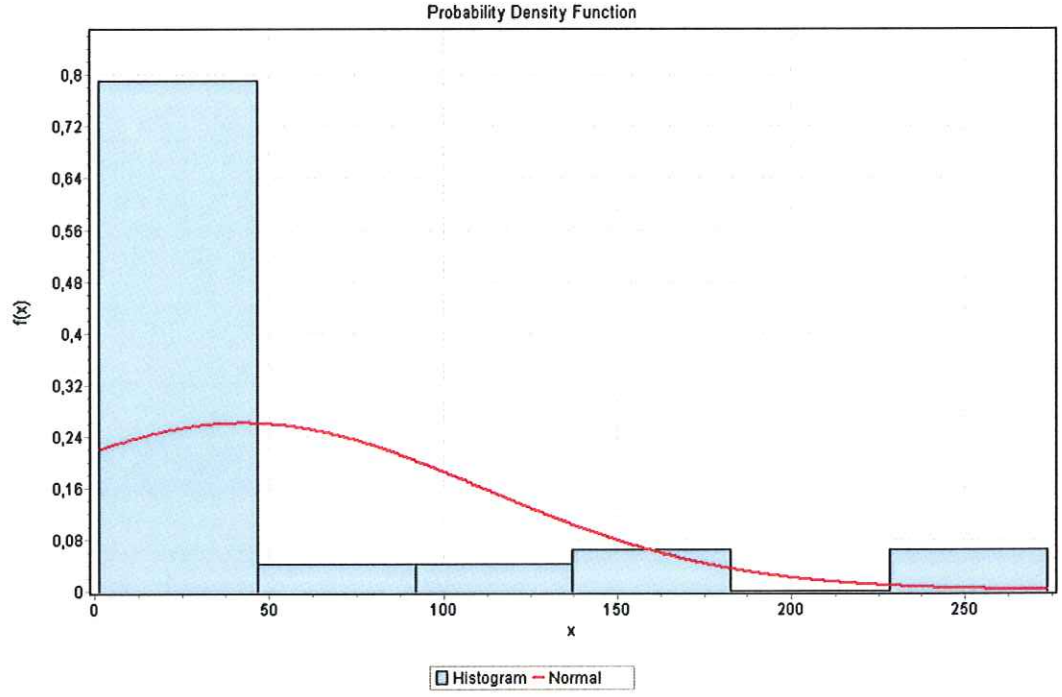

Figure C.2.17 PDF & Histogram Well#331 Facies B

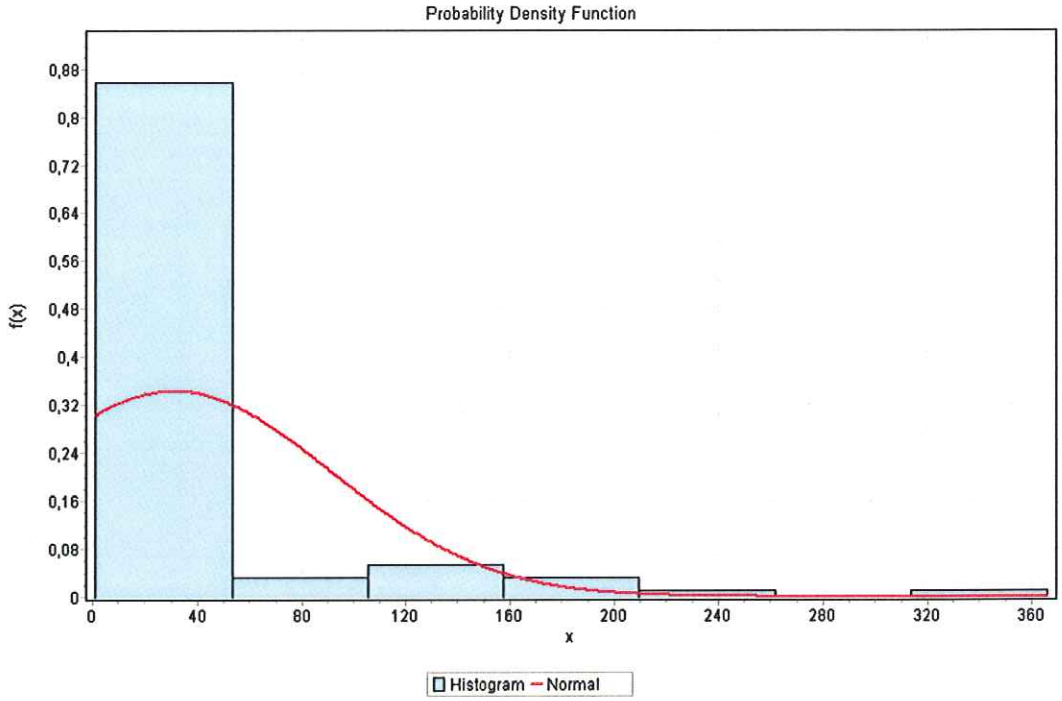

Figure C.2.18 PDF & Histogram Well#334 Facies B

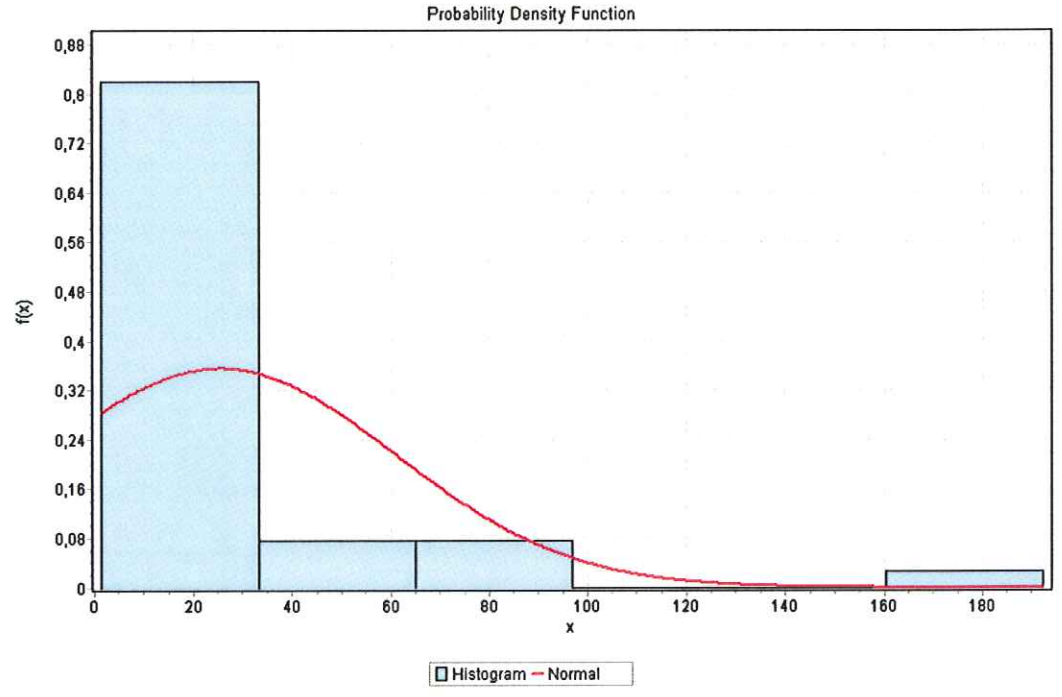

Figure C.2.19 PDF & Histogram Well#335 Facies B

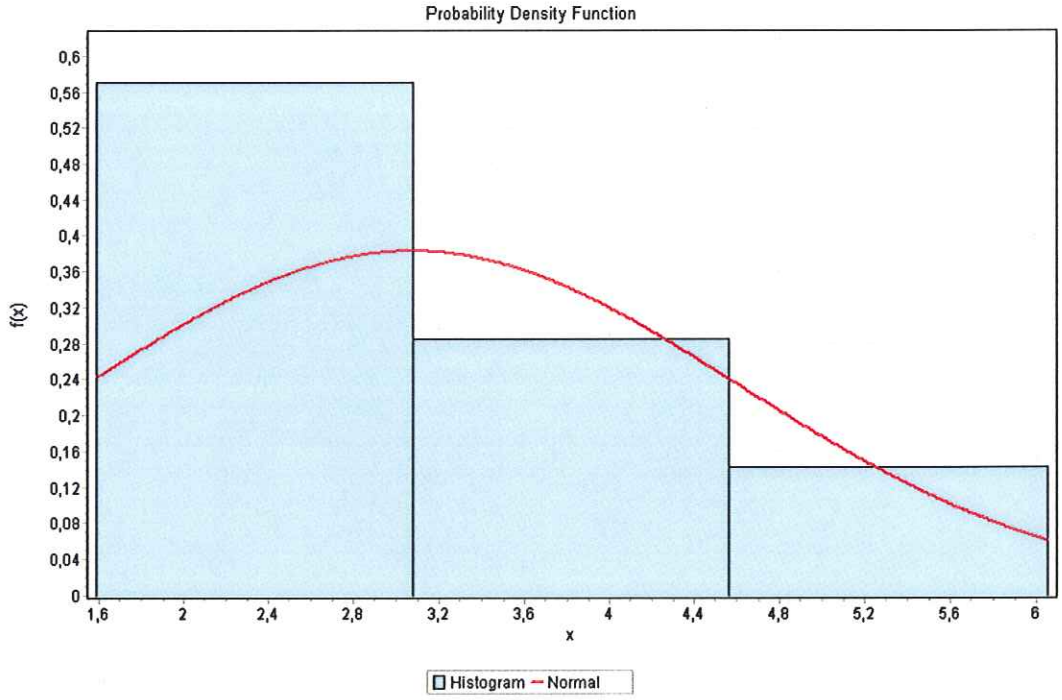

Figure C.2.20 PDF & Histogram Well#180 Facies D

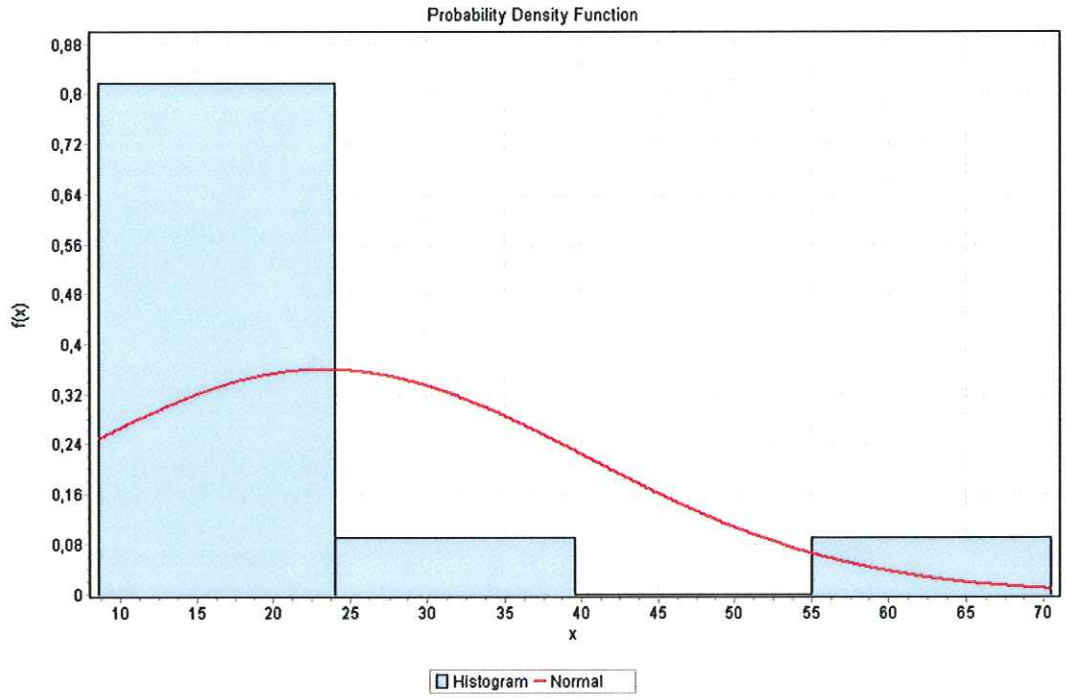

Figure C.2.21 PDF & Histogram Well#334 Facies G

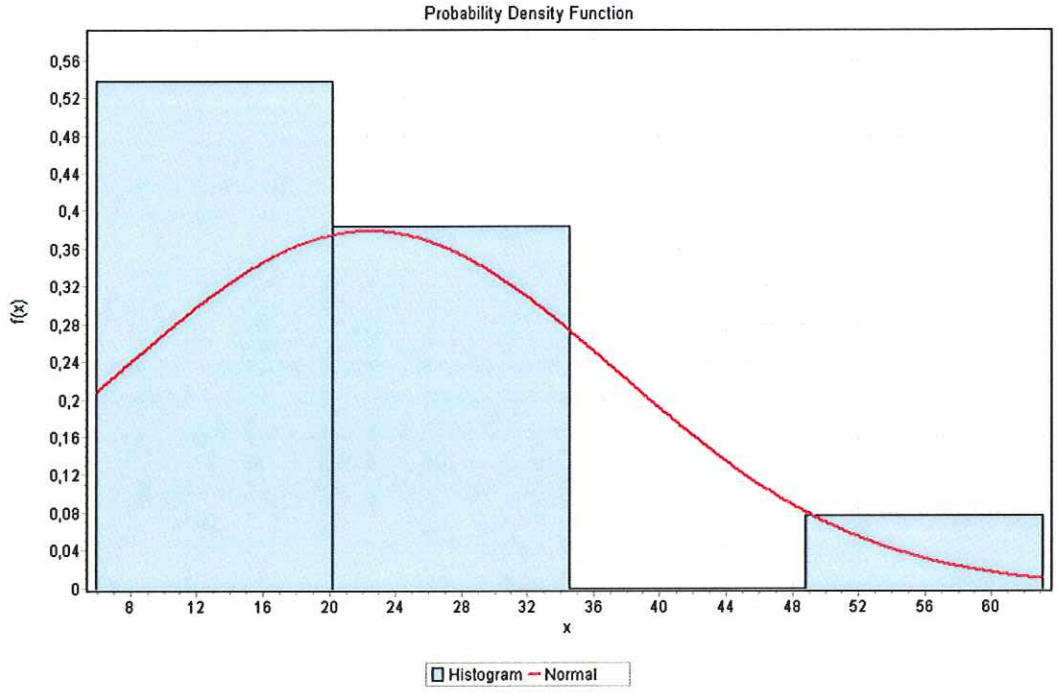

Figure C.2.22 PDF & Histogram Well#335 Facies G

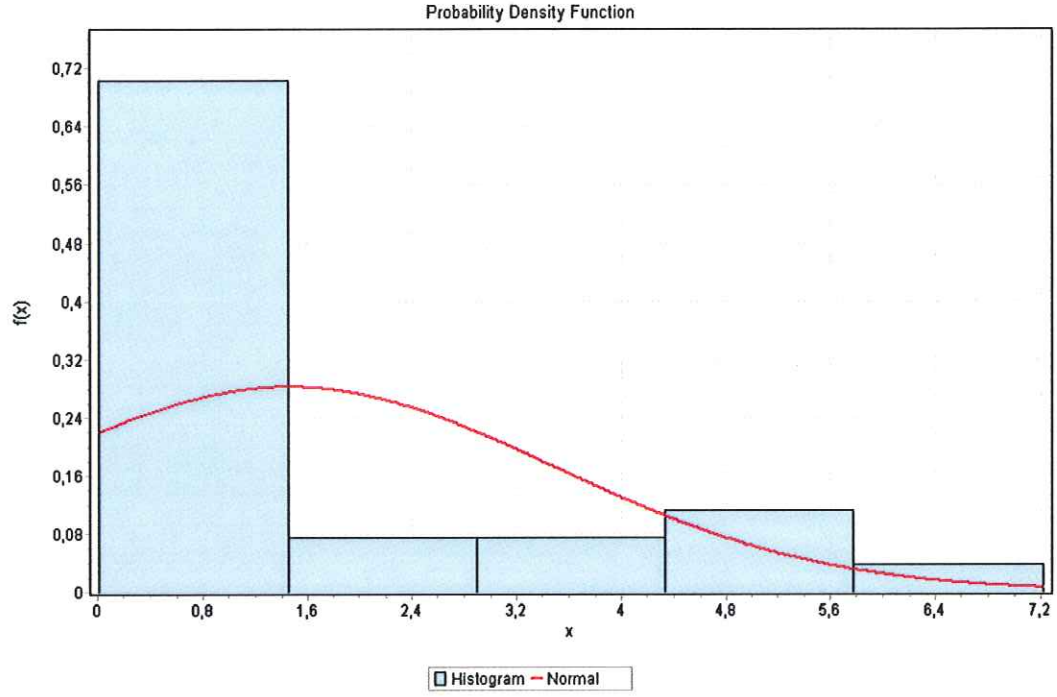

Figure C.2.23 PDF & Histogram Well#176 Facies H

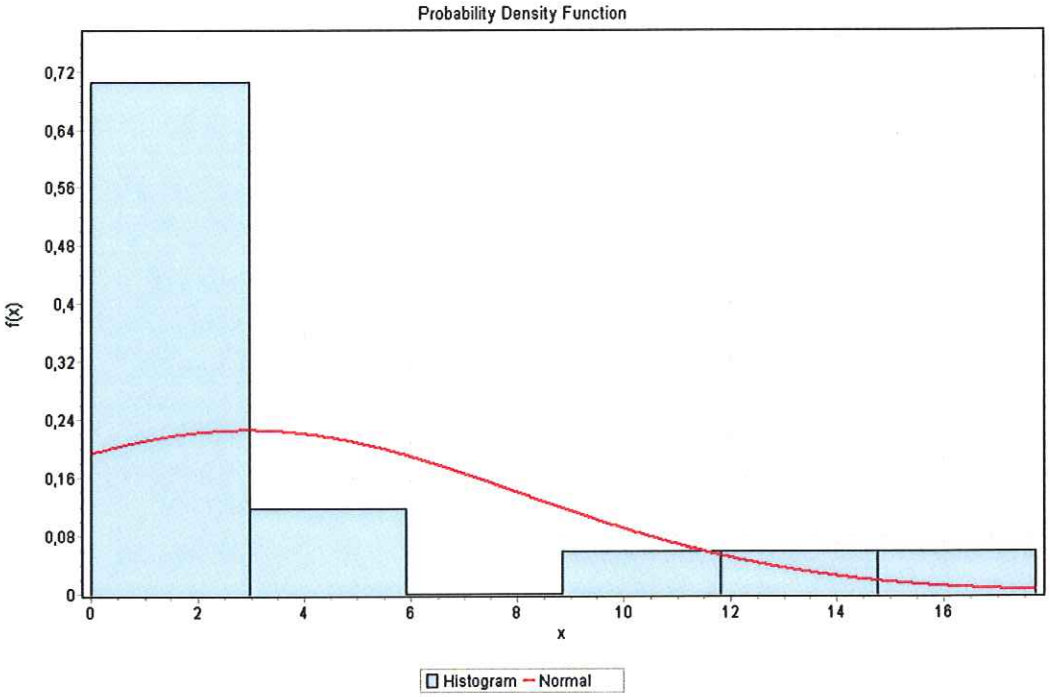

Figure C.2.24 PDF & Histogram Well#334 Facies H

APPENDIX D

BOX-COX POWER TRANSFORMATION & NORMALIZATION PLOTS

The Procedure for Well#182 Facies A

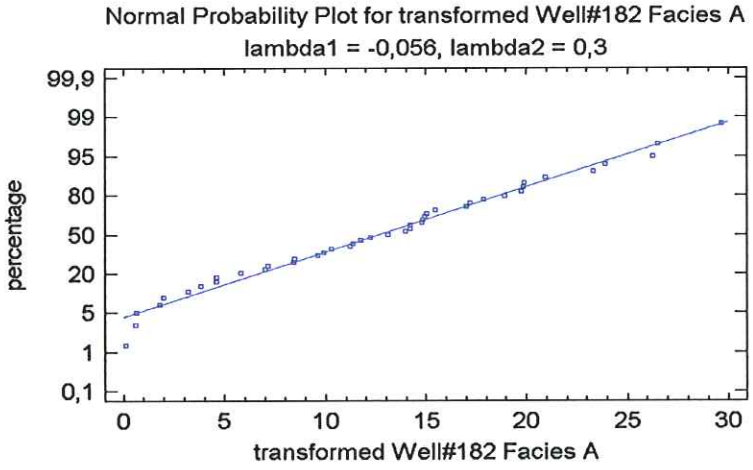

This procedure is designated to compare the effect of various power transformations on the normality of the distribution of Well#182 Facies A. The current transformation takes the form

1 + ((Well#182 Facies A+0,3)^-0,056-1)/(-0,056*6,21574^-1,056)

This is a Box-Cox transformation with power determined so as to minimize the mean squared error (MSE). The MSE Comparison table or plot to is exhibited to compare this result against the untransformed data.

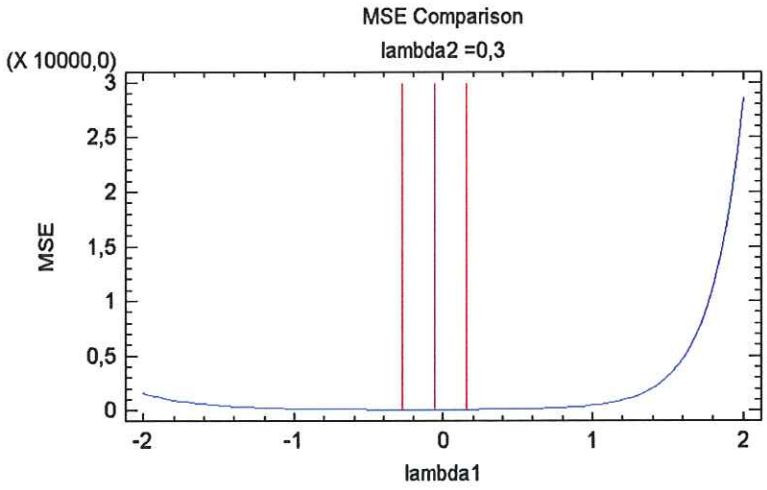

This plot shows the mean squared error (MSE) for various values of the power transformation parameter lambda1 between -2,0 and 2,0. The MSE is smallest at lambda1 = -0,0990099. This is 87,445% less than the MSE for the untransformed values of Well#182 Facies A.

The Procedure for Well#190 Facies A

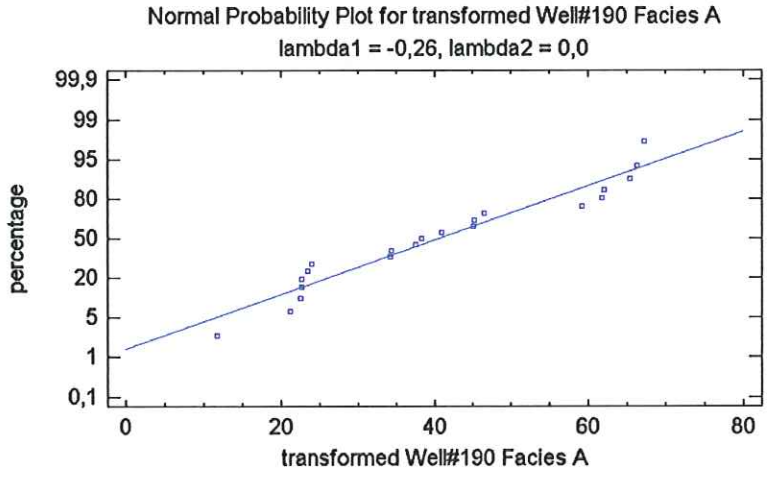

This procedure is designated to compare the effect of various power transformations on the normality of the distribution of Well#190 Facies A. The current transformation takes the form

1 + (Well#190 Facies A^-0,26-1)/(-0,26*12,1877^-1,26)

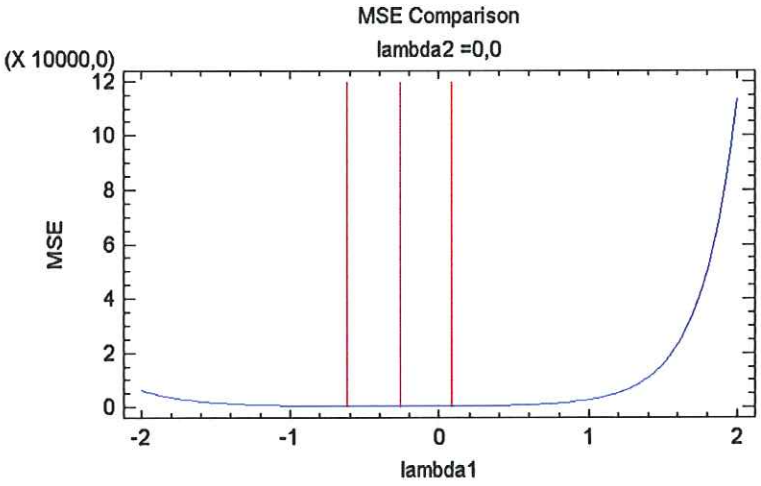

The MSE is smallest at lambda1 = -0,26. This is 89,3154% less than the MSE for the untransformed values of Well#190 Facies A.

The Procedure for Well#341 Facies A

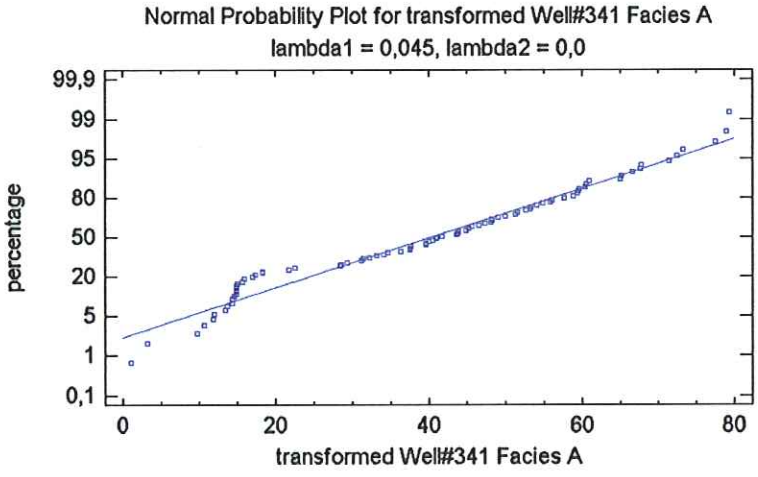

This procedure is designated to compare the effect of various power transformations on the normality of the distribution of Well#341 Facies A. The current transformation takes the form

1 + (Well#341 Facies A^0,045-1)/(0,045*15,0673^-0,955)

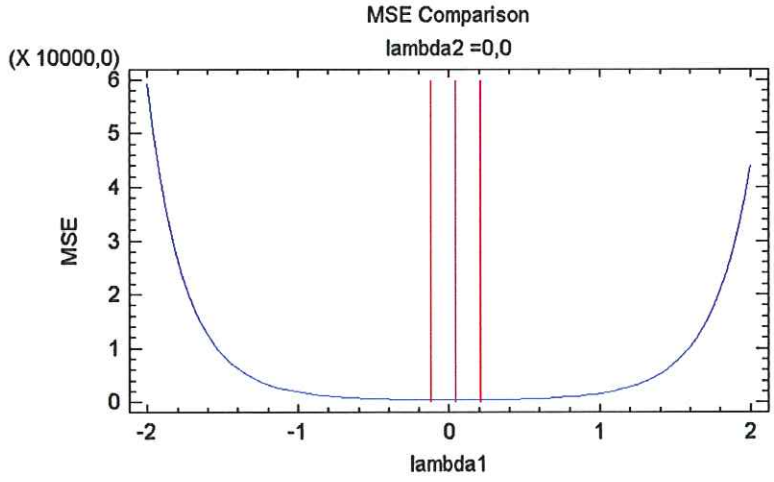

The MSE is smallest at lambda1 = 0,045. This is 75,0231% less than the MSE for the untransformed values of Well#341 Facies A.

The Procedure for Well#172 Facies B

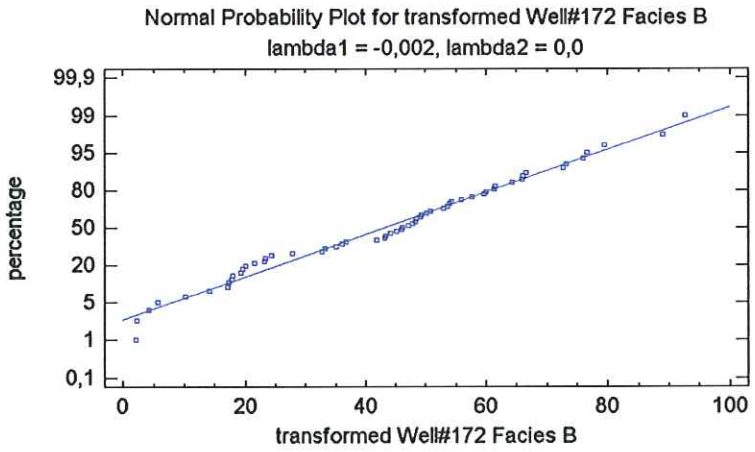

This procedure is designated to compare the effect of various power transformations on the normality of the distribution of Well#172 Facies B. The current transformation takes the form

1 + (Well#172 Facies B^-0,002-1)/(-0,002*15,4288^-1,002)

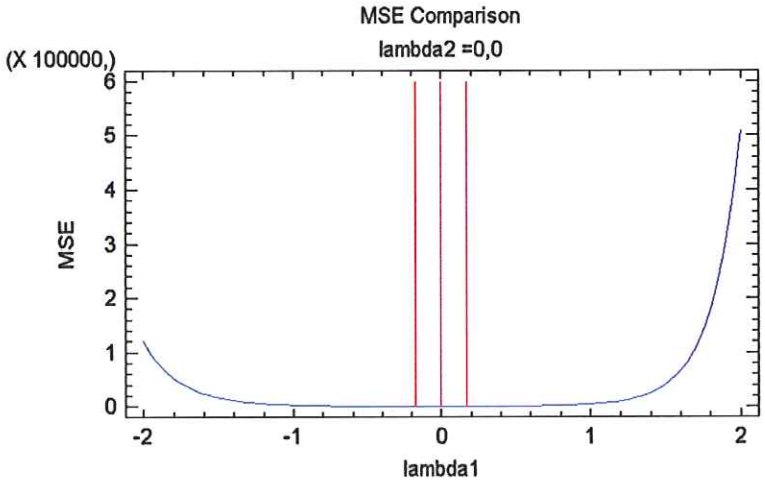

The MSE is smallest at lambda1 = -0,002. This is 89,0391% less than the MSE for the untransformed values of Well#172 Facies B.

The Procedure for Well#193 Facies B

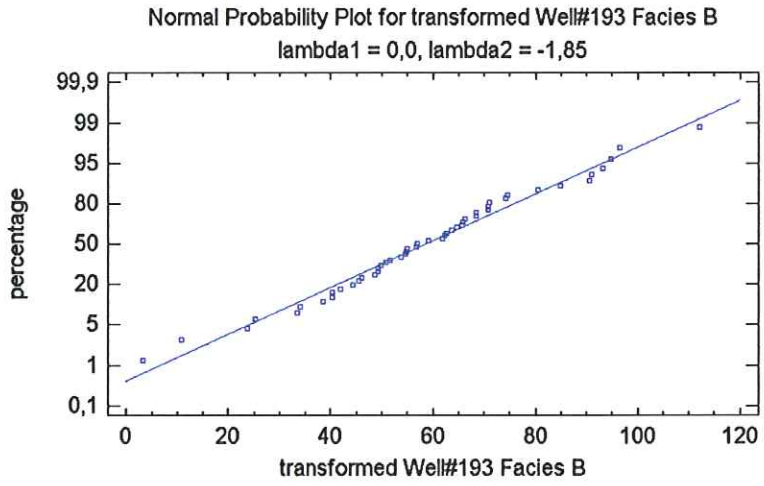

This procedure is designated to compare the effect of various power transformations on the normality of the distribution of Well#193 Facies B. The current transformation takes the form

1 + 19,4203*log(Well#193 Facies B-1,85)

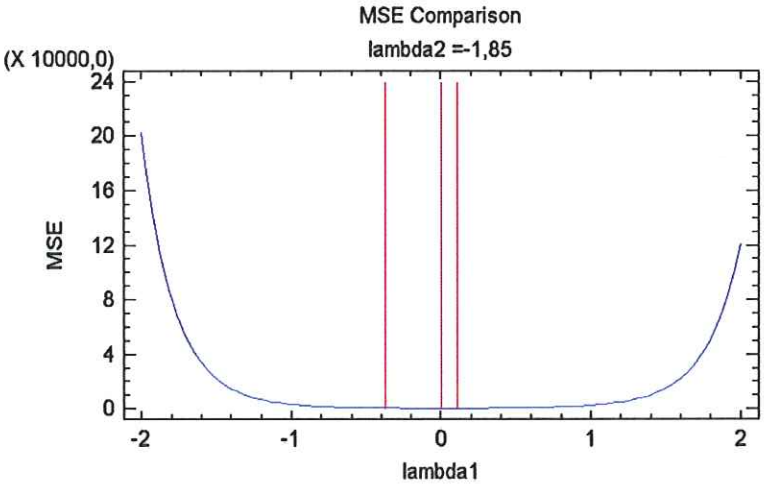

The MSE is smallest at lambda1 = 0,019802. This is 81,9289% less than the MSE for the untransformed values of Well#193 Facies B.

The Procedure for Well#284 Facies B

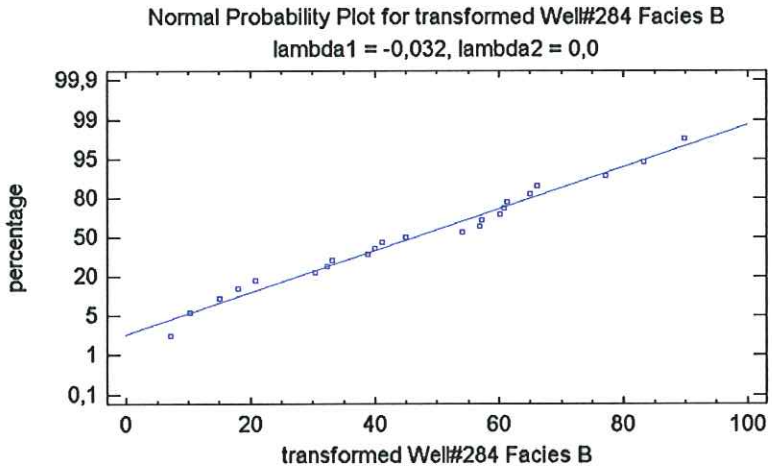

This procedure is designated to compare the effect of various power transformations on the normality of the distribution of Well#284 Facies B. The current transformation takes the form

1 + (Well#284 Facies B^-0,032-1)/(-0,032*15,8542^-1,032)

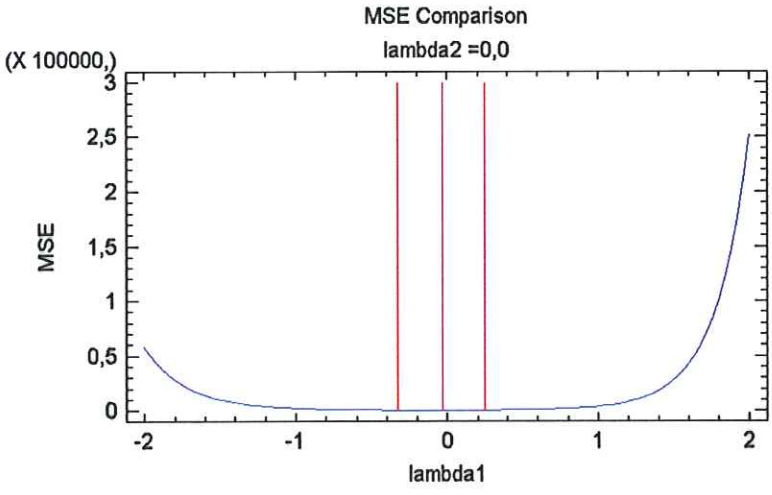

The MSE is smallest at lambda1 = -0,032. This is 87,0601% less than the MSE for the untransformed values of Well#284 Facies B.

The Procedure for Well#331 Facies B

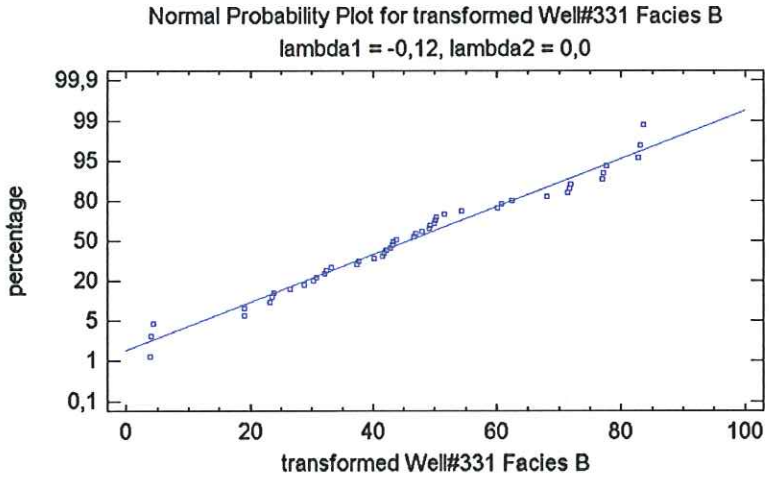

This procedure is designated to compare the effect of various power transformations on the normality of the distribution of Well#331 Facies B. The current transformation takes the form

1 + (Well#331 Facies B^-0,12-1)/(-0,12*14,663^-1,12)

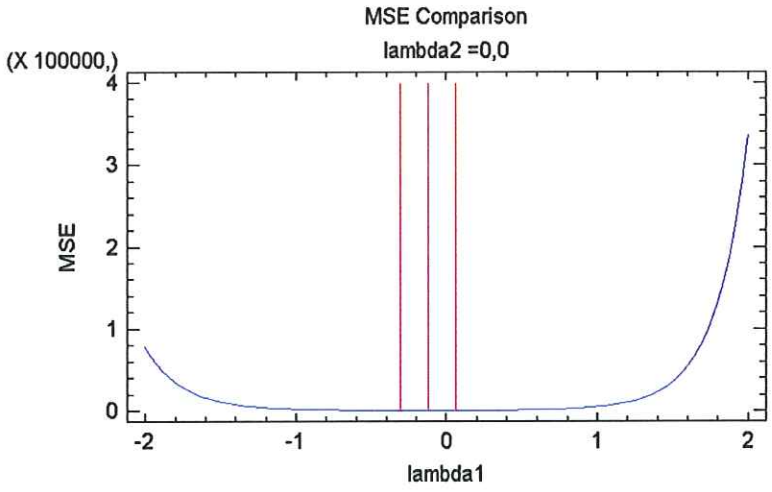

The MSE is smallest at lambda1 = -0,12. This is 90,9291% less than the MSE for the untransformed values of Well#331 Facies B.

The Procedure for Well#334 Facies B

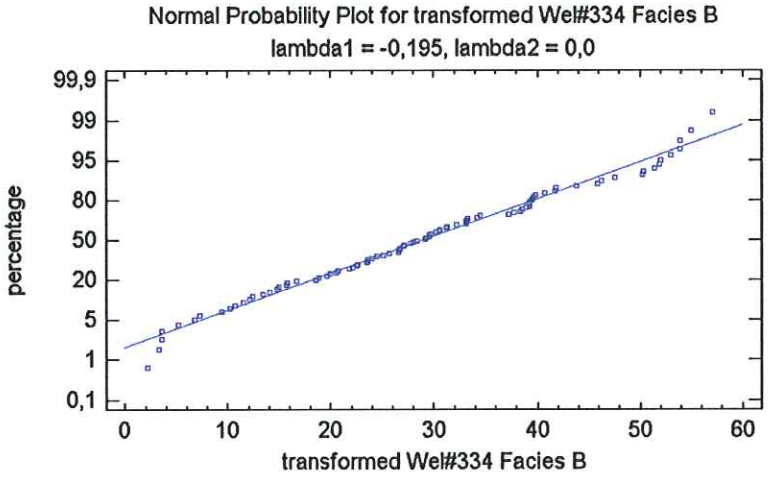

This procedure is designated to compare the effect of various power transformations on the normality of the distribution of Well#334 Facies B. The current transformation takes the form

1 + (Wel#334 Facies B^-0,195-1)/(-0,195*10,1704^-1,195)

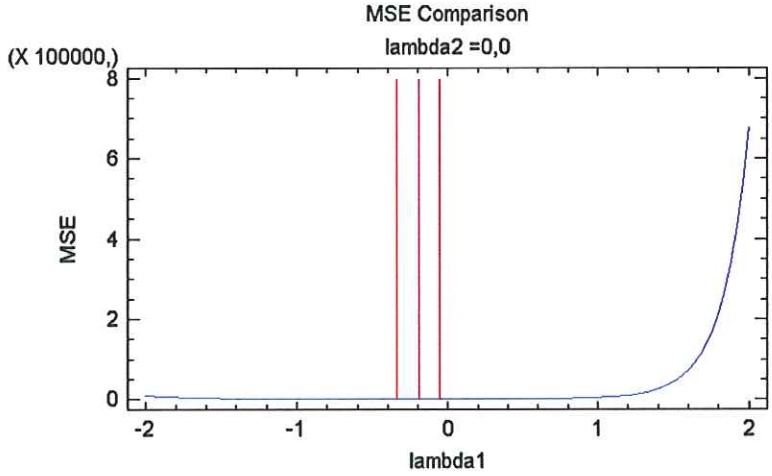

The MSE is smallest at lambda1 = -0,195. This is 94,8957% less than the MSE for the untransformed values of Wel#334 Facies B.

The Procedure for Well#335 Facies B

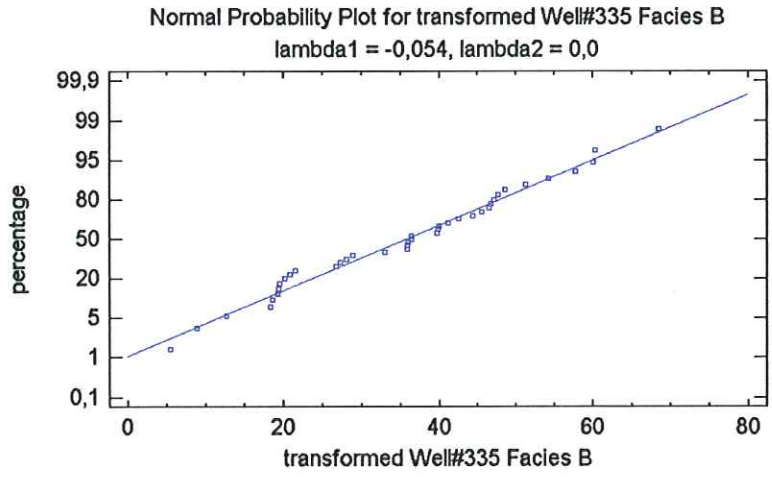

This procedure is designated to compare the effect of various power transformations on the normality of the distribution of Well#335 Facies B. The current transformation takes the form

1 + (Well#335 Facies B^-0,054-1)/(-0,054*12,8611^-1,054)

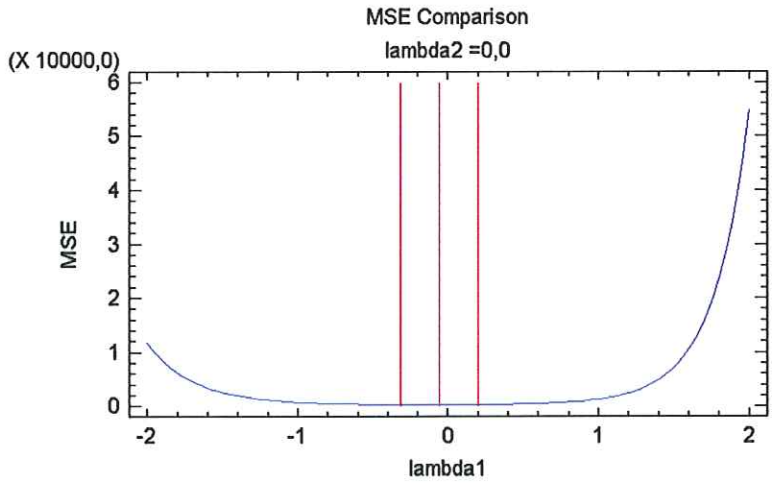

The MSE is smallest at lambda1 = -0,054. This is 81,8924% less than the MSE for the untransformed values of Well#335 Facies B.

<u>The Procedure for Well#176 Facies H</u>

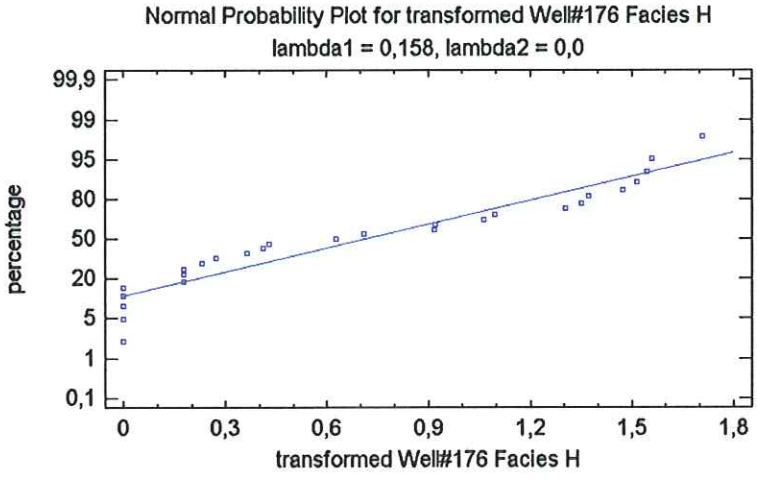

This procedure is designated to compare the effect of various power transformations on the normality of the distribution of Well#176 Facies H. The current transformation takes the form

1 + (Well#176 Facies H^0,158-1)/(0,158*0,244644^-0,842)

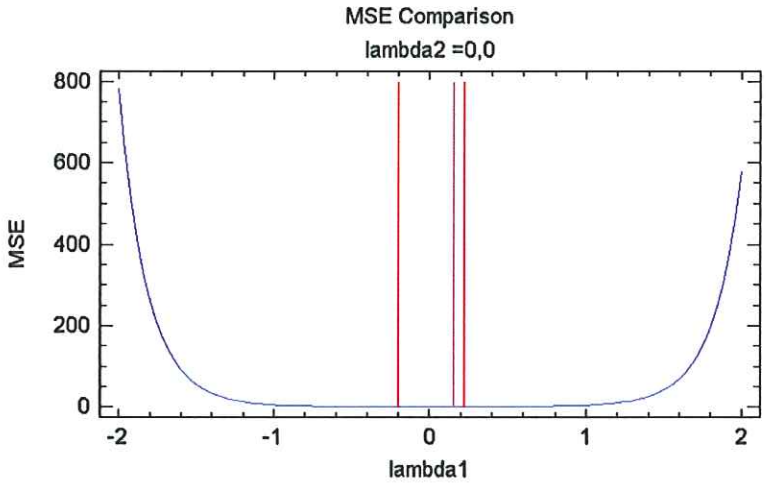

The MSE is smallest at lambda1 = 0,019802. This is 92,0112% less than the MSE for the untransformed values of Well#176 Facies H.

The Procedure for Well#334 Facies H

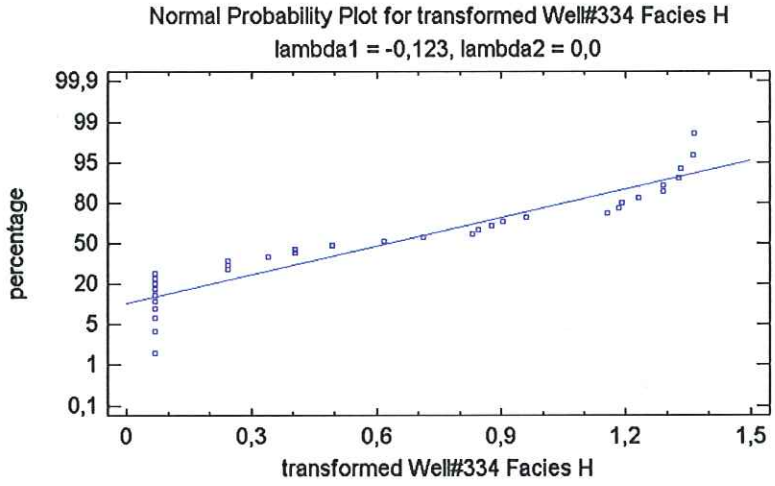

This procedure is designated to compare the effect of various power transformations on the normality of the distribution of Well#334 Facies H. The current transformation takes the form

1 + (Well#334 Facies H^-0,123-1)/(-0,123*0,185143^-1,123)

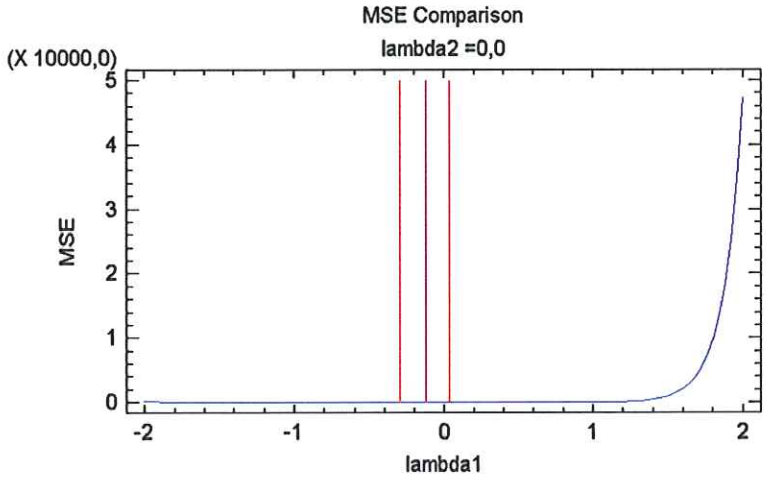

The MSE is smallest at lambda1 = -0,123. This is 99,0762% less than the MSE for the untransformed values of Well#334 Facies H.

APPENDIX E

THE DYSKTRA PARSON'S PLOTS

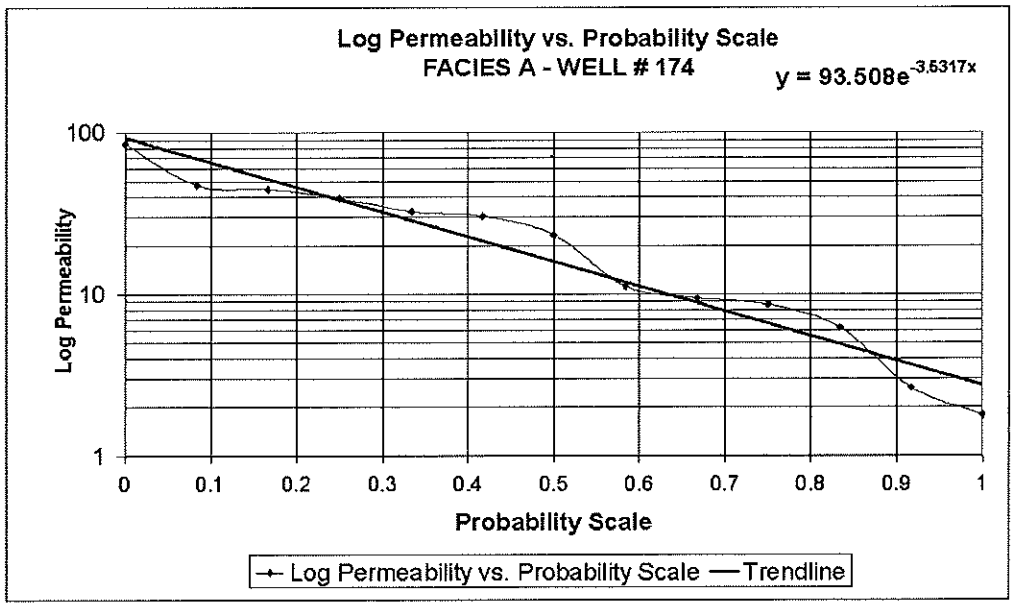

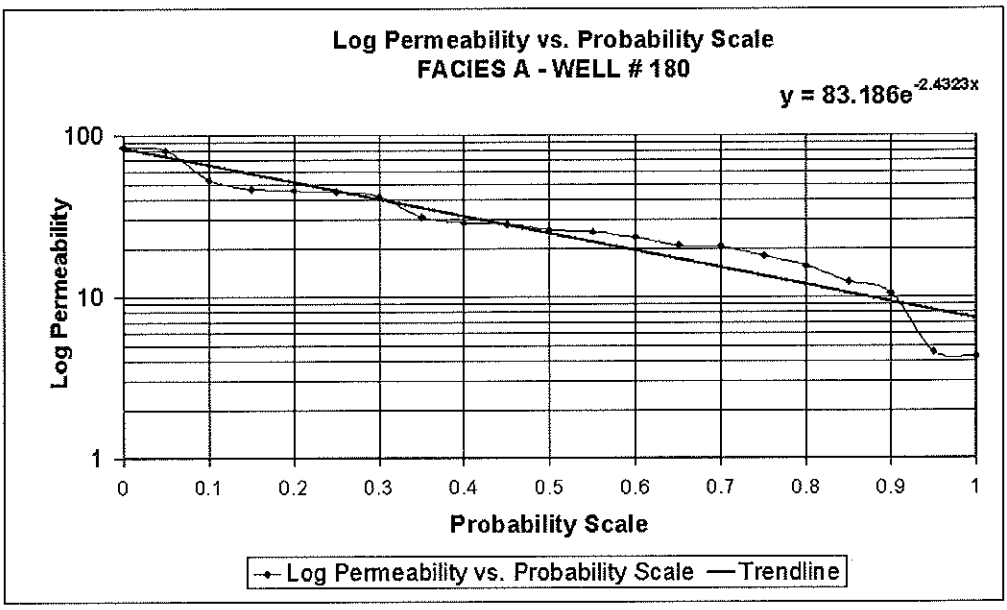
Log Permeability vs. Probability Scale
FACIES A - WELL # 180
y = 83.186e^-2.4323x
Log Permeability
100
10
1
0
0.1
0.2
0.3
0.4
0.5
0.6
0.7
0.8
0.9
1
Probability Scale
Log Permeability vs. Probability Scale
Trendline

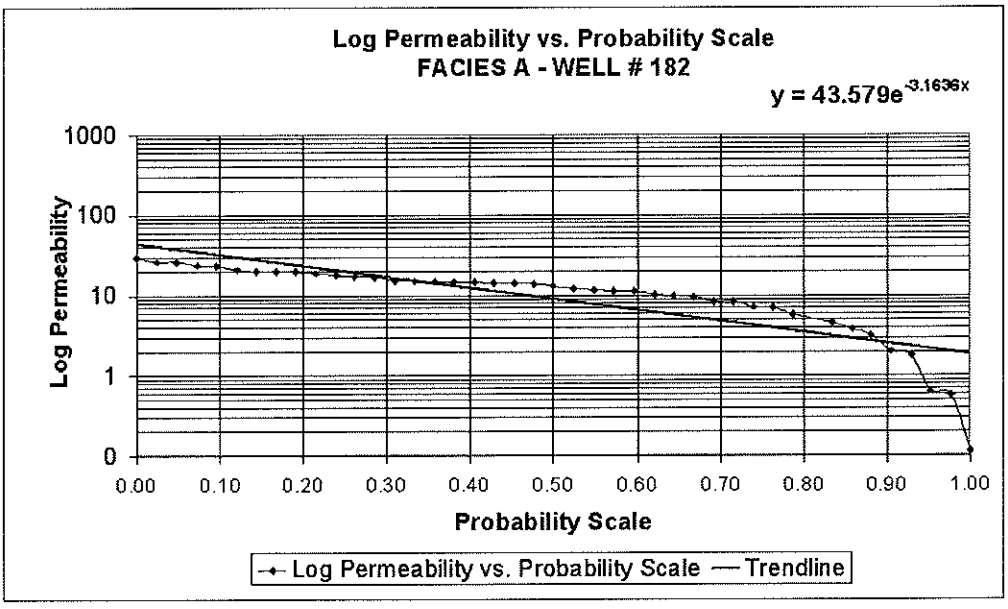
Log Permeability vs. Probability Scale
FACIES A - WELL # 182
y = 43.579e^-3.1636x
Log Permeability
1000
100
10
1
0
0.00
0.10
0.20
0.30
0.40
0.50
0.60
0.70
0.80
0.90
1.00
Probability Scale
Log Permeability vs. Probability Scale
Trendline

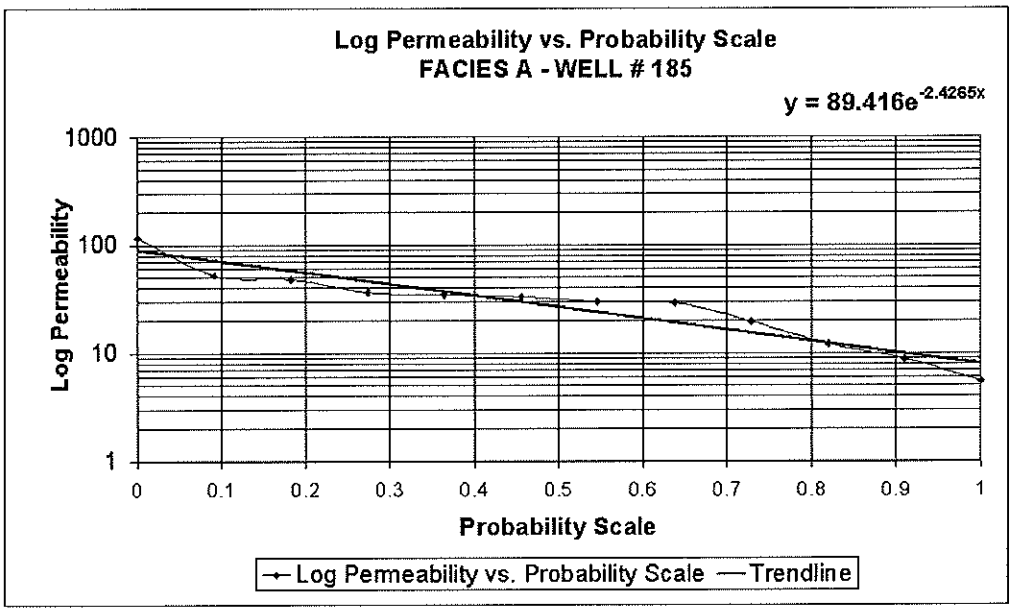
Log Permeability vs. Probability Scale
FACIES A - WELL # 185
y = 89.416e-2.4265x
1000
100
10
1
Log Permeability
0
0.1
0.2
0.3
0.4
0.5
0.6
0.7
0.8
0.9
1
Probability Scale
Log Permeability vs. Probability Scale
Trendline

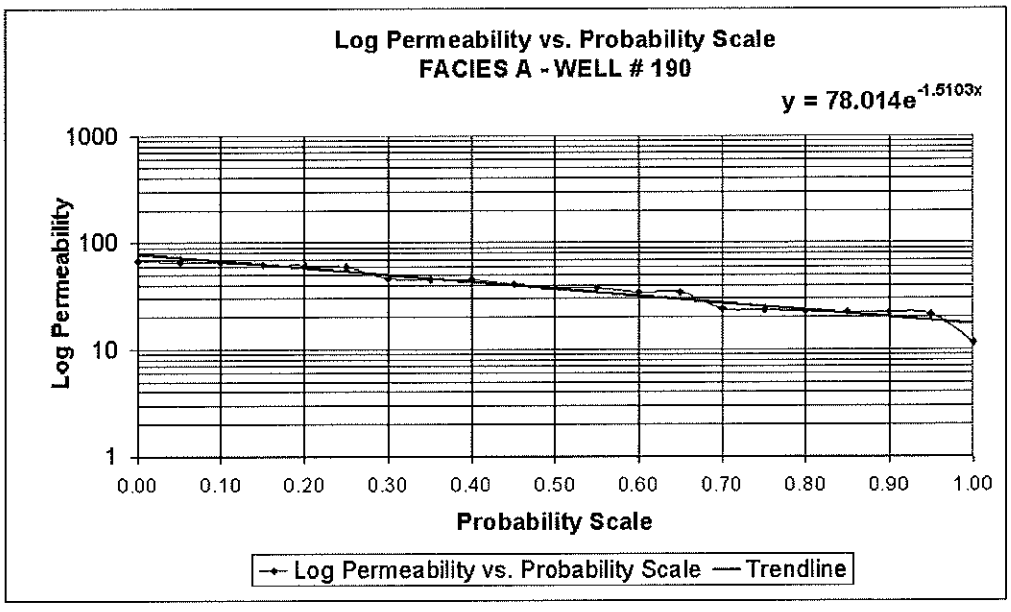
Log Permeability vs. Probability Scale
FACIES A - WELL # 190
y = 78.014e-1.5103x
1000
100
10
1
Log Permeability
0.00
0.10
0.20
0.30
0.40
0.50
0.60
0.70
0.80
0.90
1.00
Probability Scale
Log Permeability vs. Probability Scale
Trendline

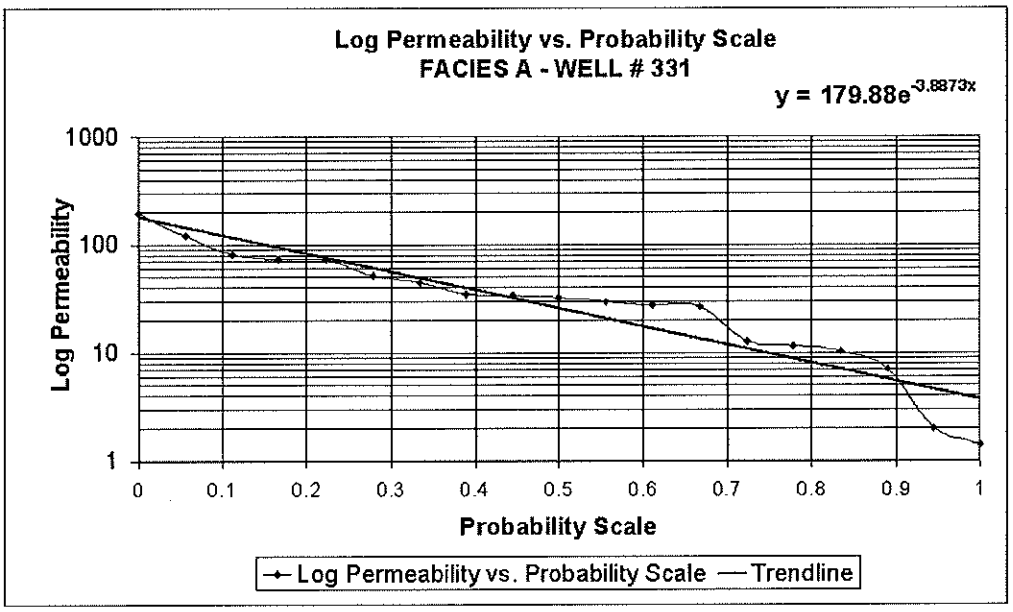
Log Permeability vs. Probability Scale
FACIES A - WELL # 331
y = 179.88e^-3.8873x
1000
100
10
1
Log Permeability
0
0.1
0.2
0.3
0.4
0.5
0.6
0.7
0.8
0.9
1
Probability Scale
Log Permeability vs. Probability Scale
Trendline

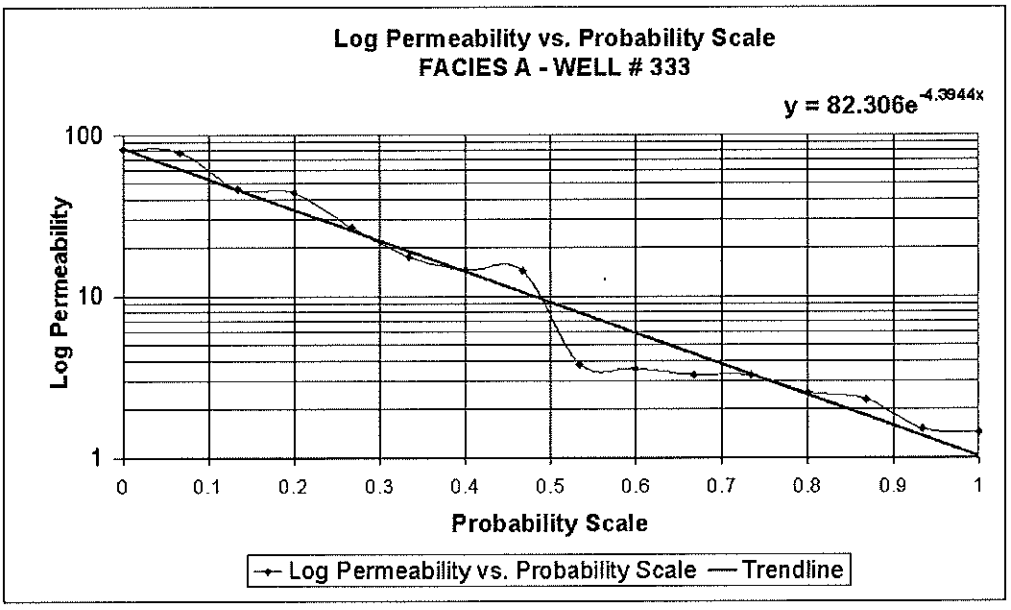
Log Permeability vs. Probability Scale
FACIES A - WELL # 333
y = 82.306e^-4.3944x
100
10
1
Log Permeability
0
0.1
0.2
0.3
0.4
0.5
0.6
0.7
0.8
0.9
1
Probability Scale
Log Permeability vs. Probability Scale
Trendline

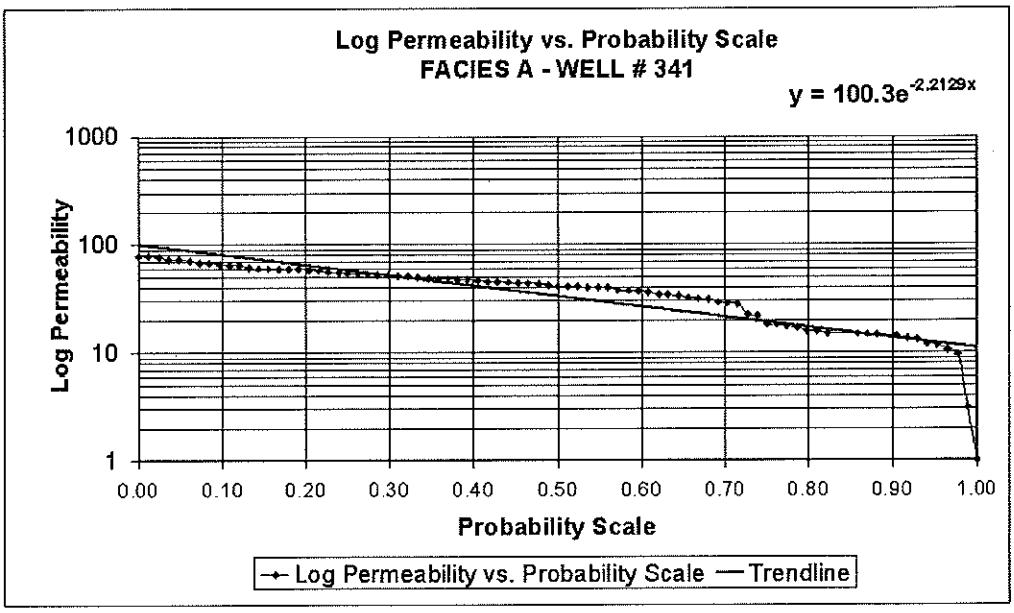
Log Permeability vs. Probability Scale
FACIES A - WELL # 341
y = 100.3e-2.2129x
1000
100
10
1
Log Permeability
0.00
0.10
0.20
0.30
0.40
0.50
0.60
0.70
0.80
0.90
1.00
Probability Scale
Log Permeability vs. Probability Scale
Trendline

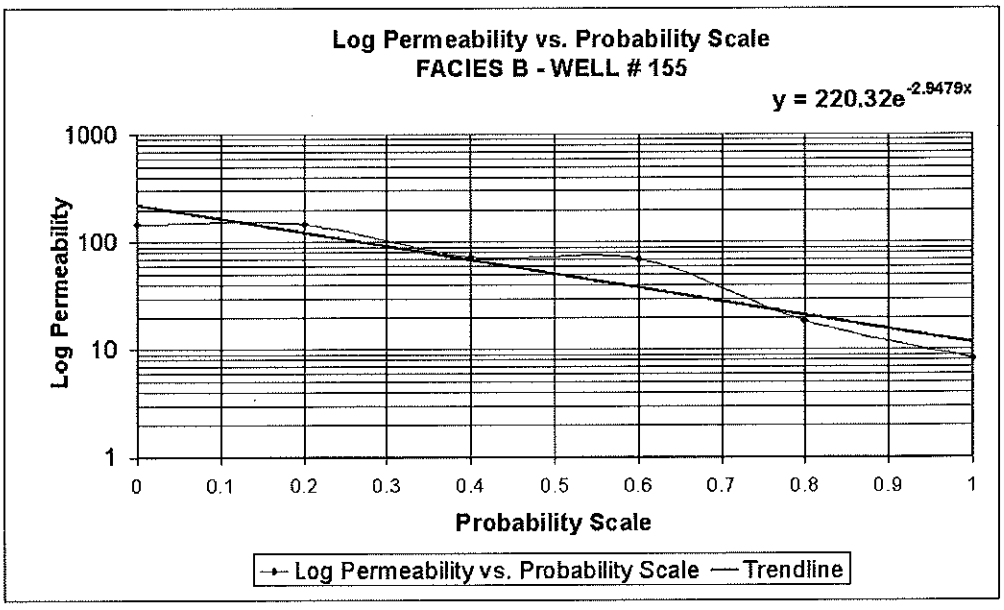
Log Permeability vs. Probability Scale
FACIES B - WELL # 155
y = 220.32e-2.9479x
1000
100
10
1
Log Permeability
0
0.1
0.2
0.3
0.4
0.5
0.6
0.7
0.8
0.9
1
Probability Scale
Log Permeability vs. Probability Scale
Trendline

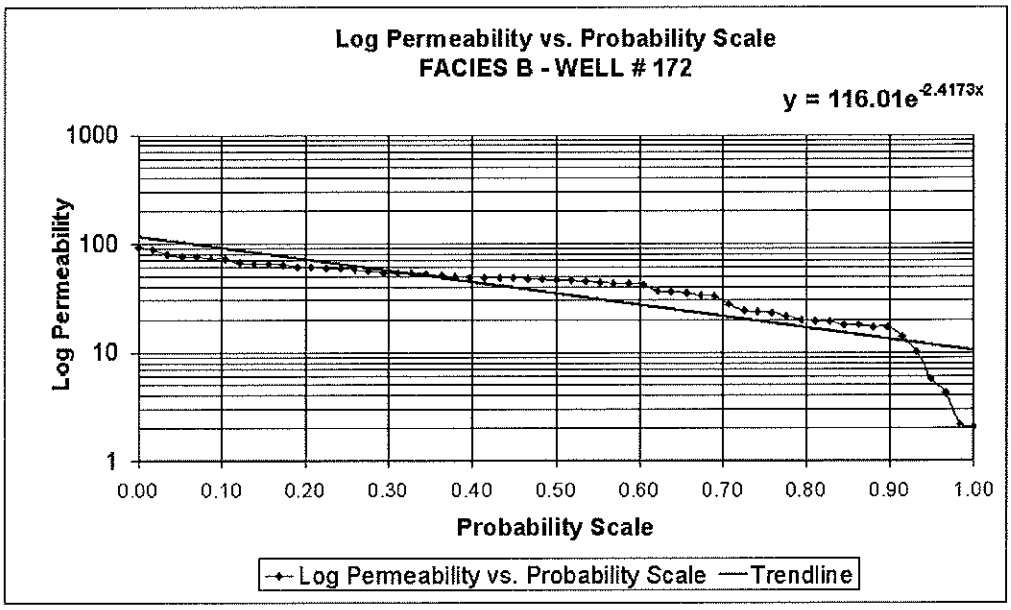
Log Permeability vs. Probability Scale
FACIES B - WELL # 172
y = 116.01e-2.4173x
1000
100
10
1
Log Permeability
0.00
0.10
0.20
0.30
0.40
0.50
0.60
0.70
0.80
0.90
1.00
Probability Scale
Log Permeability vs. Probability Scale
Trendline

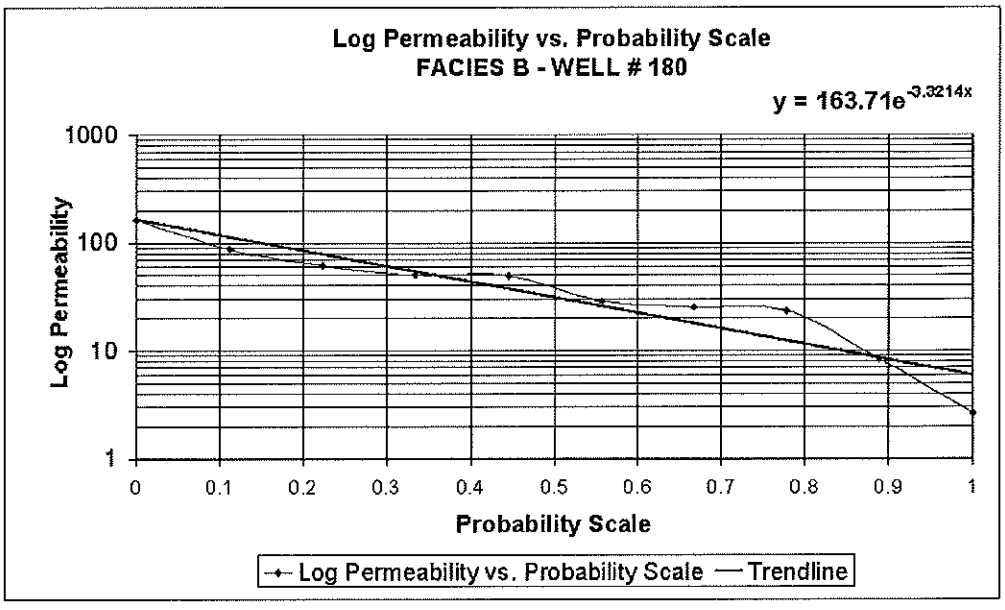
Log Permeability vs. Probability Scale
FACIES B - WELL # 180
y = 163.71e-3.3214x
1000
100
10
1
Log Permeability
0
0.1
0.2
0.3
0.4
0.5
0.6
0.7
0.8
0.9
1
Probability Scale
Log Permeability vs. Probability Scale
Trendline

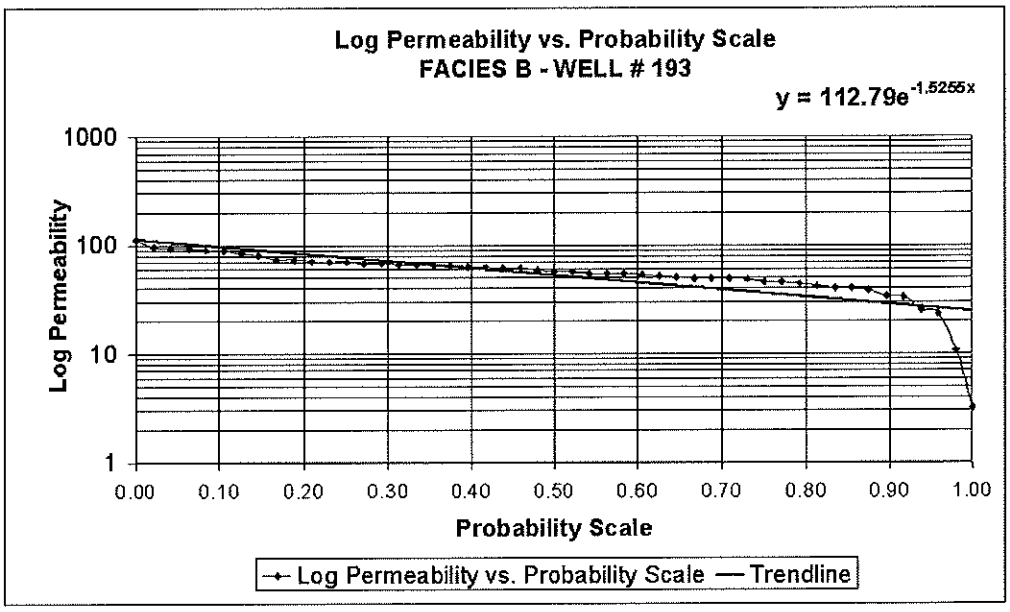
Log Permeability vs. Probability Scale
FACIES B - WELL # 193
y = 112.79e^-1.5255x
1000
100
10
1
Log Permeability
0.00
0.10
0.20
0.30
0.40
0.50
0.60
0.70
0.80
0.90
1.00
Probability Scale
Log Permeability vs. Probability Scale
Trendline

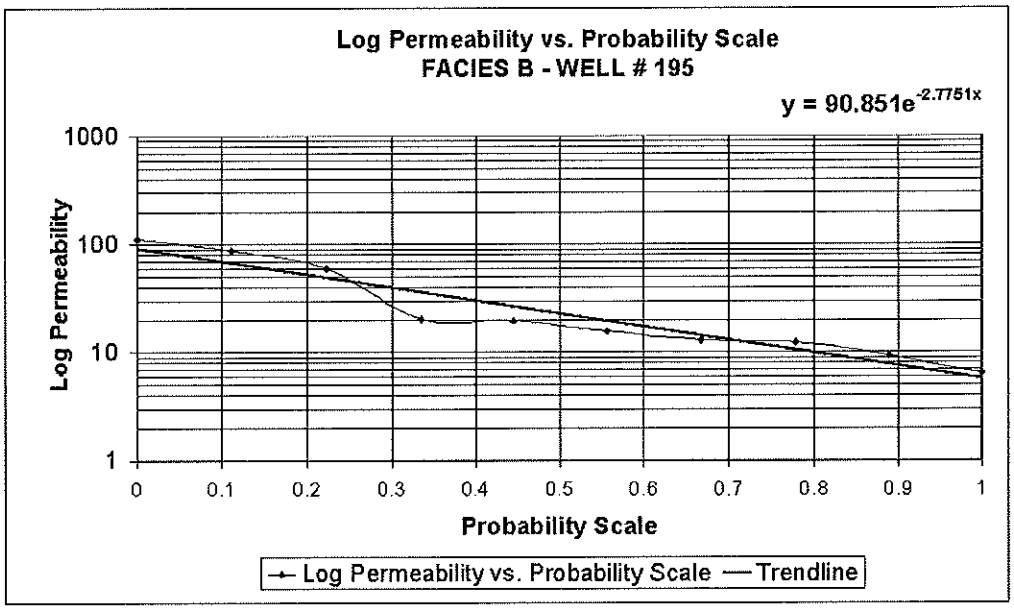
Log Permeability vs. Probability Scale
FACIES B - WELL # 195
y = 90.851e^-2.7751x
1000
100
10
1
Log Permeability
0
0.1
0.2
0.3
0.4
0.5
0.6
0.7
0.8
0.9
1
Probability Scale
Log Permeability vs. Probability Scale
Trendline

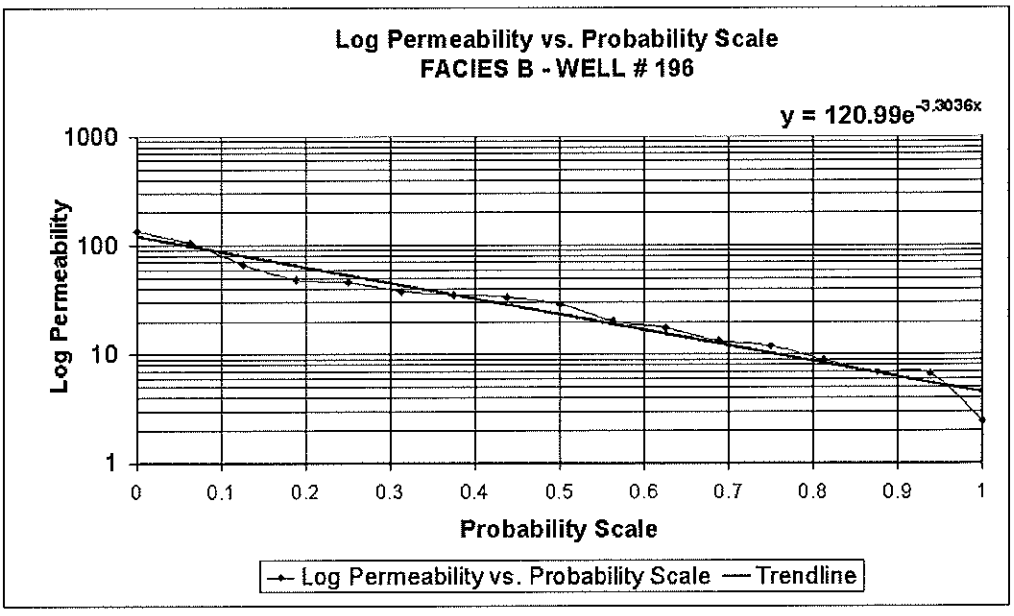
Log Permeability vs. Probability Scale
FACIES B - WELL # 196
y = 120.99e-3.3036x
1000
100
10
1
Log Permeability
0
0.1
0.2
0.3
0.4
0.5
0.6
0.7
0.8
0.9
1
Probability Scale
Log Permeability vs. Probability Scale
Trendline

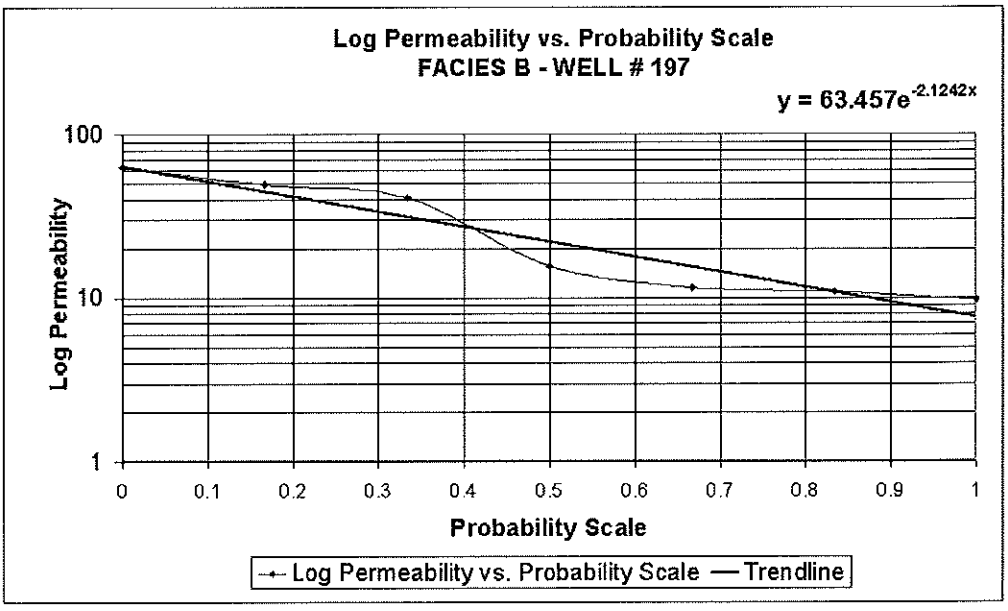
Log Permeability vs. Probability Scale
FACIES B - WELL # 197
y = 63.457e-2.1242x
100
10
1
Log Permeability
0
0.1
0.2
0.3
0.4
0.5
0.6
0.7
0.8
0.9
1
Probability Scale
Log Permeability vs. Probability Scale
Trendline

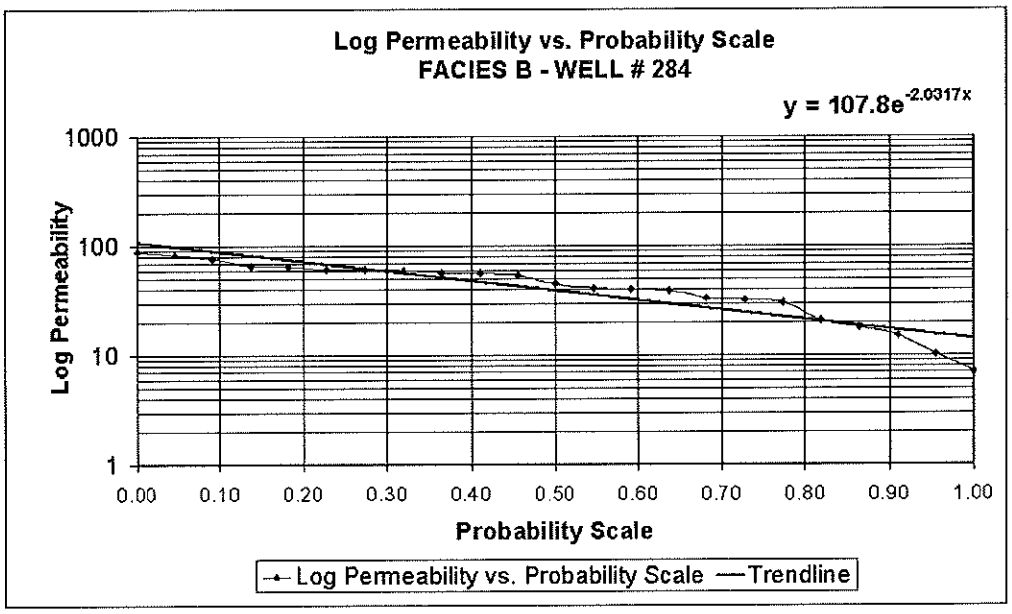
Log Permeability vs. Probability Scale
FACIES B - WELL # 284
y = 107.8e-2.0317x
1000
100
10
1
Log Permeability
0.00
0.10
0.20
0.30
0.40
0.50
0.60
0.70
0.80
0.90
1.00
Probability Scale
Log Permeability vs. Probability Scale
Trendline

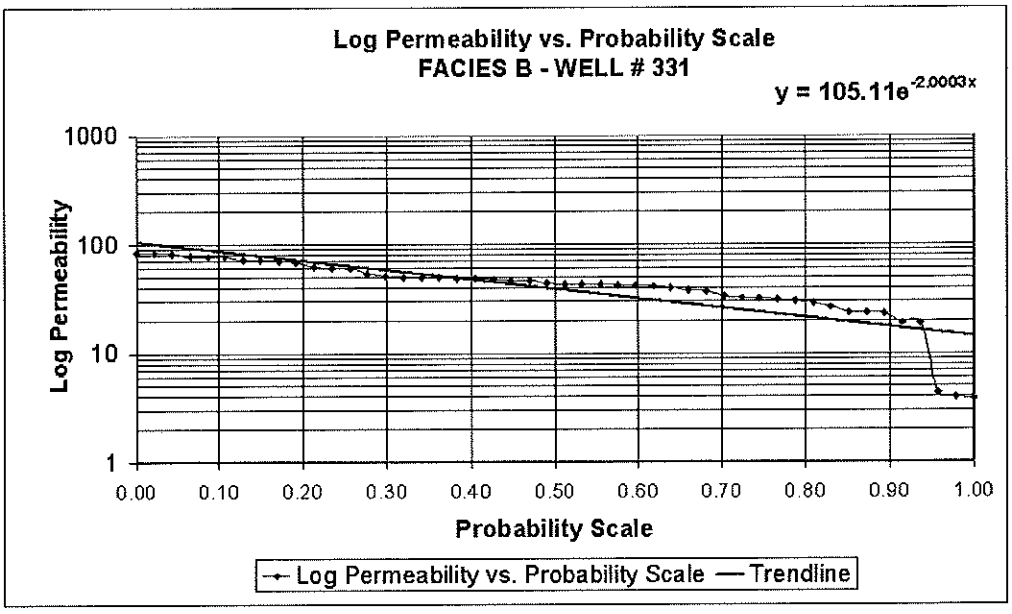
Log Permeability vs. Probability Scale
FACIES B - WELL # 331
y = 105.11e-2.0003x
1000
100
10
1
Log Permeability
0.00
0.10
0.20
0.30
0.40
0.50
0.60
0.70
0.80
0.90
1.00
Probability Scale
Log Permeability vs. Probability Scale
Trendline

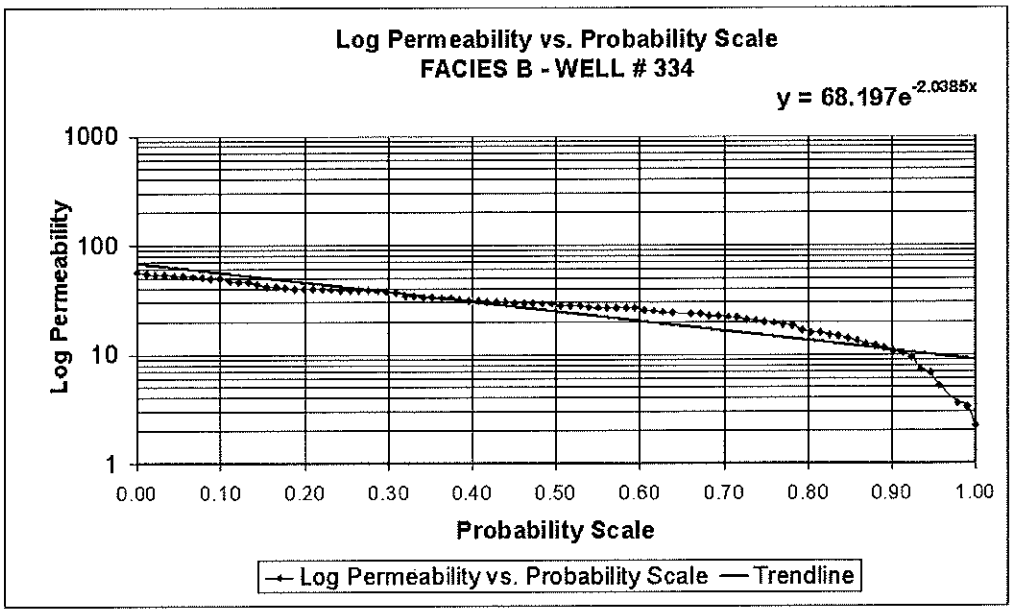
Log Permeability vs. Probability Scale
FACIES B - WELL # 334
y = 68.197e-2.0385x
1000
100
10
1
Log Permeability
0.00
0.10
0.20
0.30
0.40
0.50
0.60
0.70
0.80
0.90
1.00
Probability Scale
Log Permeability vs. Probability Scale
Trendline

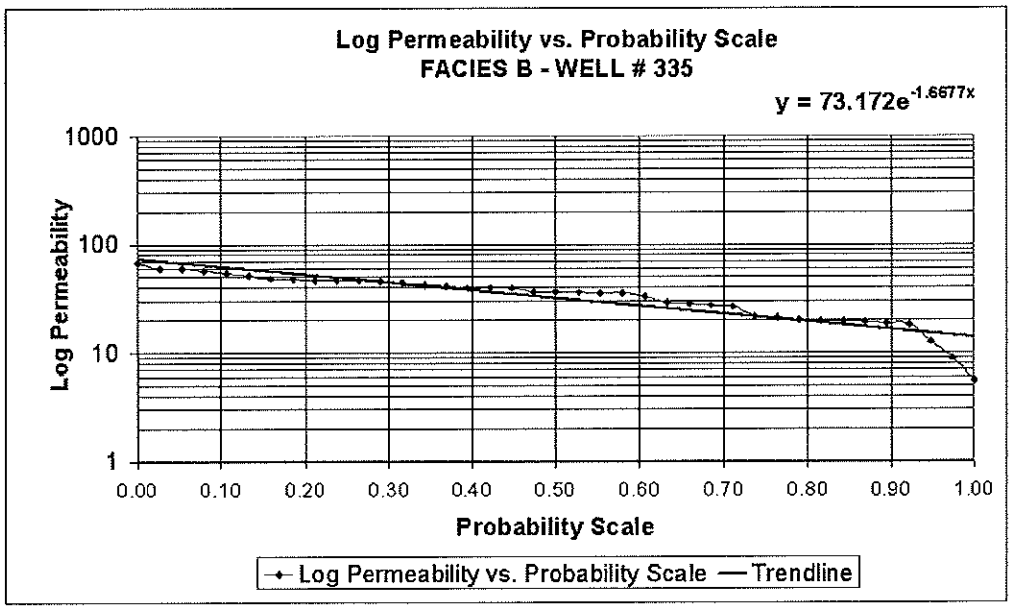
Log Permeability vs. Probability Scale
FACIES B - WELL # 335
y = 73.172e-1.6677x
1000
100
10
1
Log Permeability
0.00
0.10
0.20
0.30
0.40
0.50
0.60
0.70
0.80
0.90
1.00
Probability Scale
Log Permeability vs. Probability Scale
Trendline

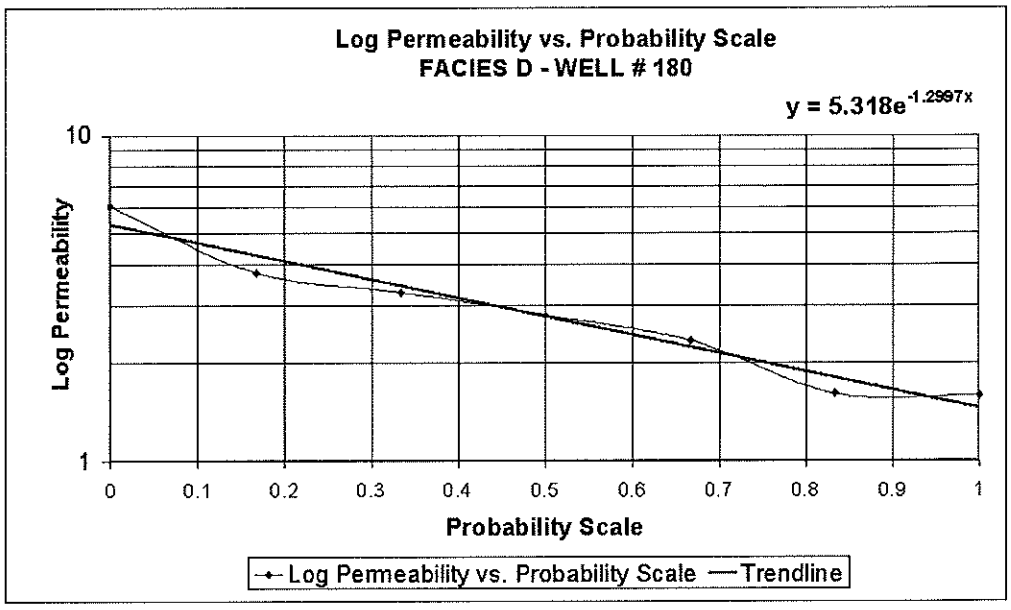
Log Permeability vs. Probability Scale
FACIES D - WELL # 180
y = 5.318e-1.2997x
10
1
Log Permeability
0
0.1
0.2
0.3
0.4
0.5
0.6
0.7
0.8
0.9
1
Probability Scale
Log Permeability vs. Probability Scale
Trendline

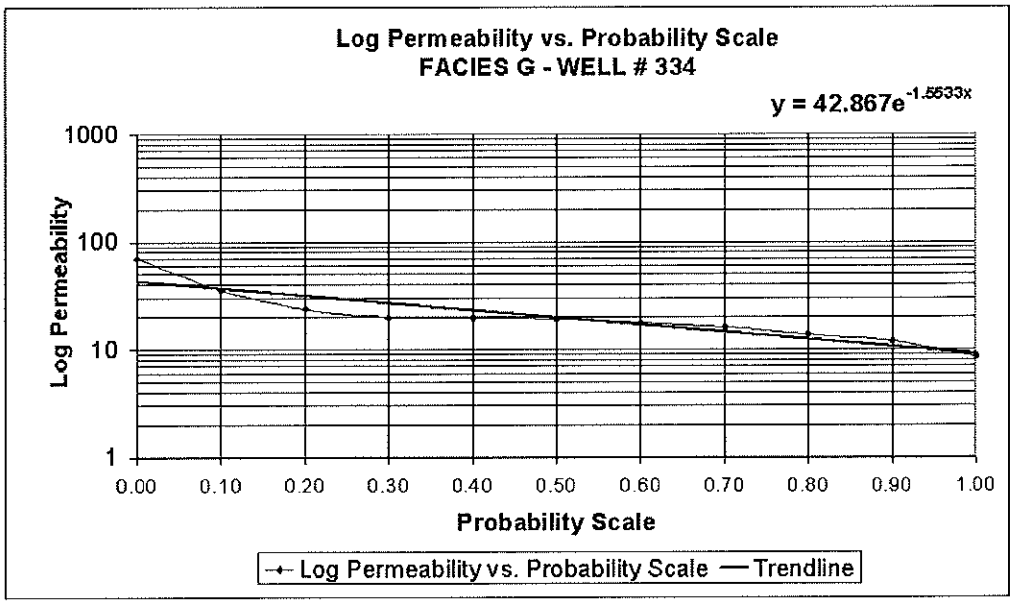
Log Permeability vs. Probability Scale
FACIES G - WELL # 334
y = 42.867e-1.5533x
1000
100
10
1
Log Permeability
0.00
0.10
0.20
0.30
0.40
0.50
0.60
0.70
0.80
0.90
1.00
Probability Scale
Log Permeability vs. Probability Scale
Trendline

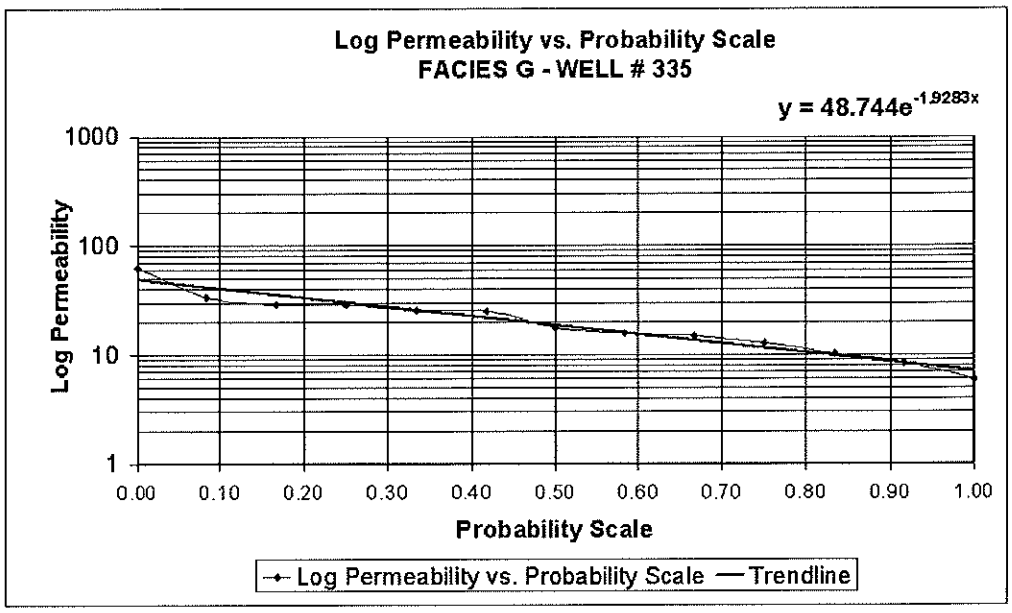
Log Permeability vs. Probability Scale
FACIES G - WELL # 335
y = 48.744e-1.9283x
1000
100
10
1
Log Permeability
0.00
0.10
0.20
0.30
0.40
0.50
0.60
0.70
0.80
0.90
1.00
Probability Scale
Log Permeability vs. Probability Scale
Trendline

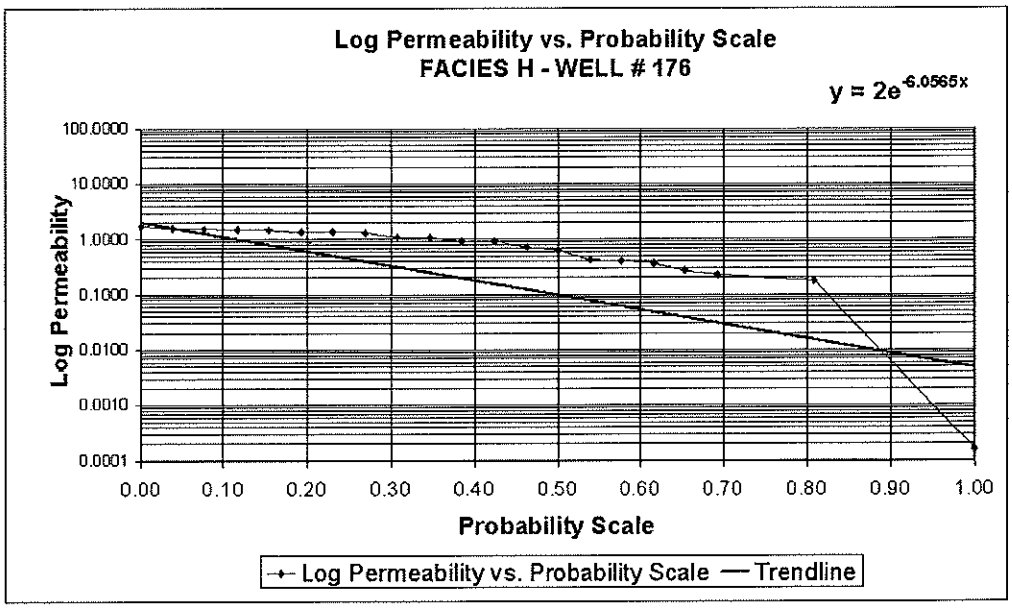
Log Permeability vs. Probability Scale
FACIES H - WELL # 176
y = 2e-6.0565x
100.0000
10.0000
1.0000
0.1000
0.0100
0.0010
0.0001
Log Permeability
0.00
0.10
0.20
0.30
0.40
0.50
0.60
0.70
0.80
0.90
1.00
Probability Scale
Log Permeability vs. Probability Scale
Trendline

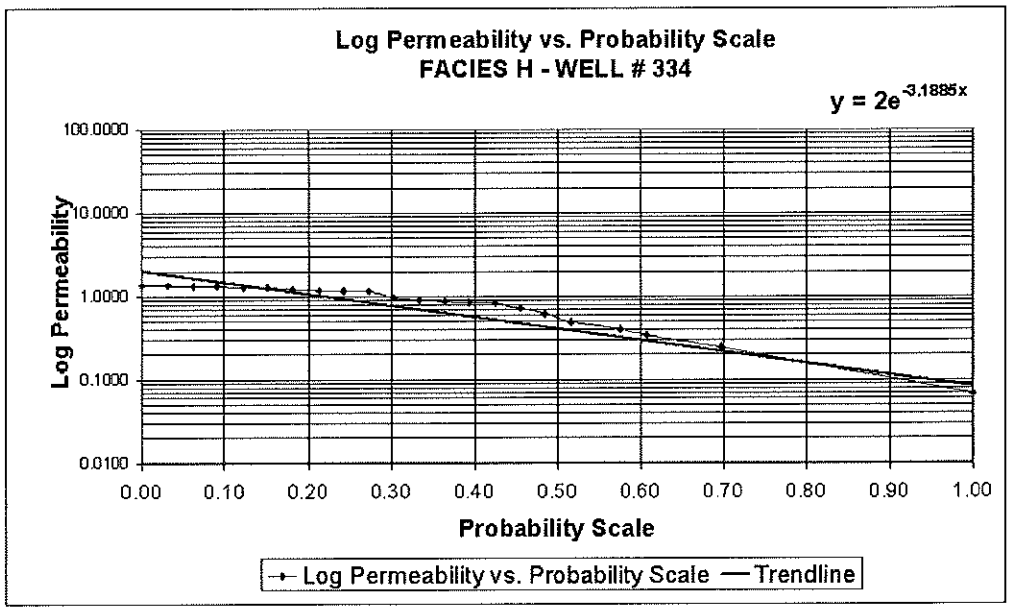
Log Permeability vs. Probability Scale
FACIES H - WELL # 334
y = 2e^-3.1885x
100.0000
10.0000
1.0000
0.1000
0.0100
Log Permeability
0.00
0.10
0.20
0.30
0.40
0.50
0.60
0.70
0.80
0.90
1.00
Probability Scale
Log Permeability vs. Probability Scale
Trendline

APPENDIX F

LORENZ PLOTS

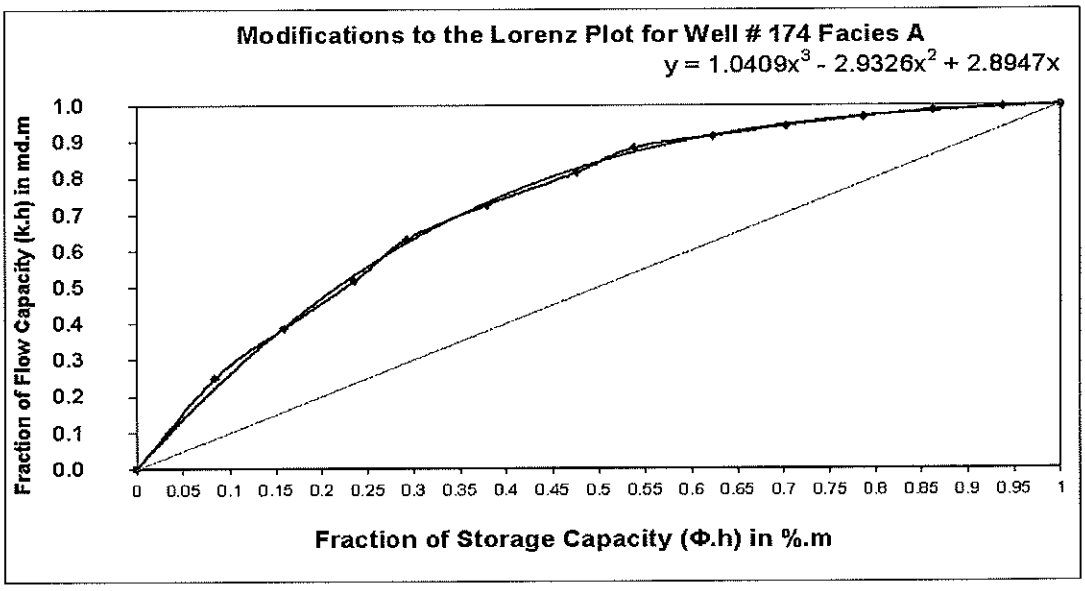

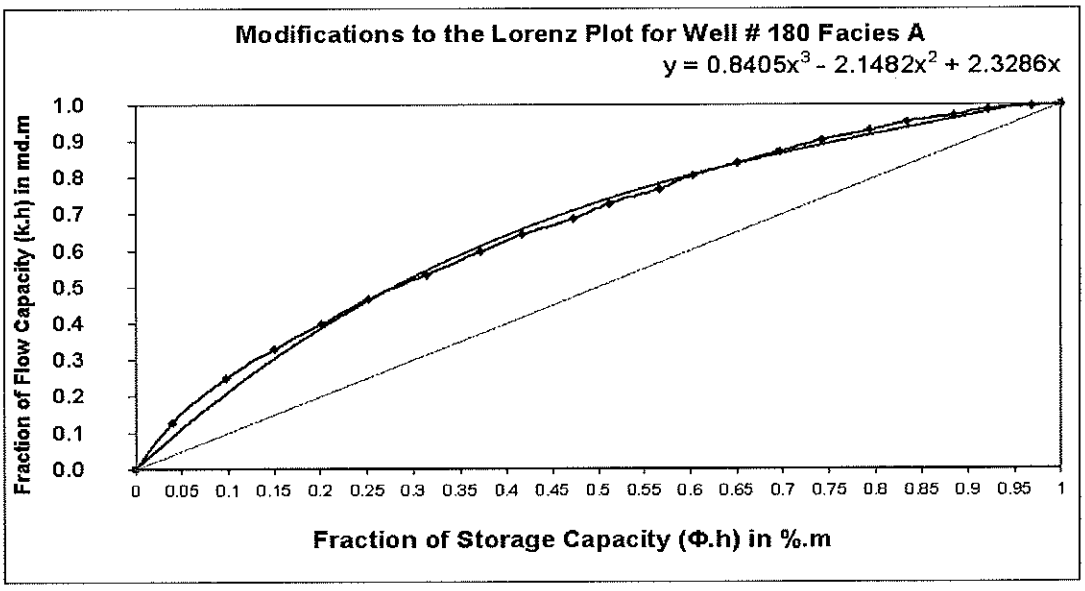
Modifications to the Lorenz Plot for Well # 180 Facies A
y = 0.8405x3 - 2.1482x2 + 2.3286x
Fraction of Flow Capacity (k.h) in md.m
1.0
0.9
0.8
0.7
0.6
0.5
0.4
0.3
0.2
0.1
0.0
0 0.05 0.1 0.15 0.2 0.25 0.3 0.35 0.4 0.45 0.5 0.55 0.6 0.65 0.7 0.75 0.8 0.85 0.9 0.95 1
Fraction of Storage Capacity (Φ.h) in %.m

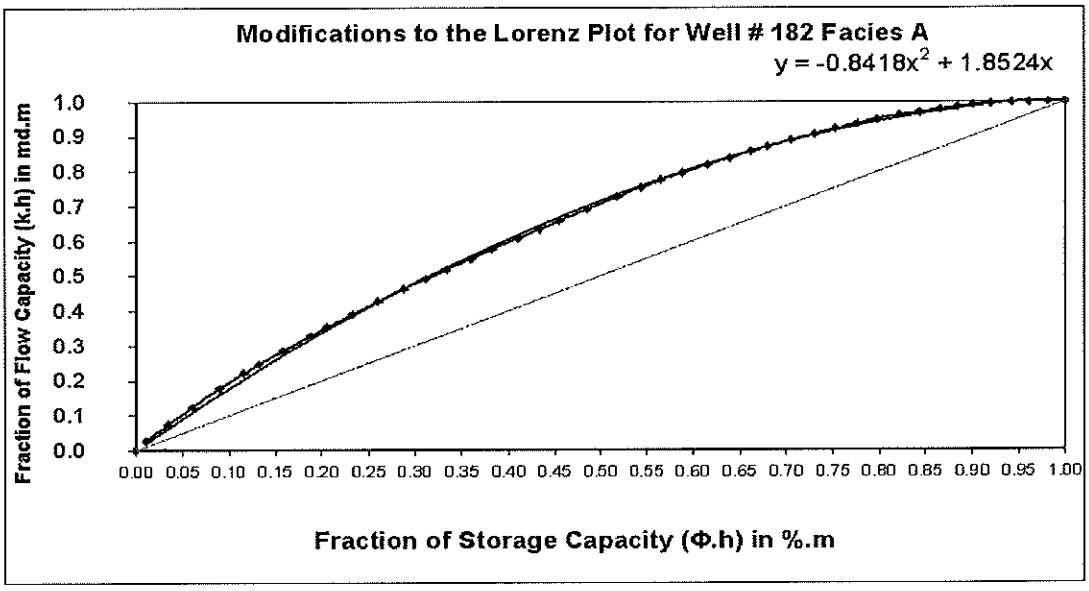
Modifications to the Lorenz Plot for Well # 182 Facies A
y = -0.8418x2 + 1.8524x
Fraction of Flow Capacity (k.h) in md.m
1.0
0.9
0.8
0.7
0.6
0.5
0.4
0.3
0.2
0.1
0.0
0.00 0.05 0.10 0.15 0.20 0.25 0.30 0.35 0.40 0.45 0.50 0.55 0.60 0.65 0.70 0.75 0.80 0.85 0.90 0.95 1.00
Fraction of Storage Capacity (Φ.h) in %.m

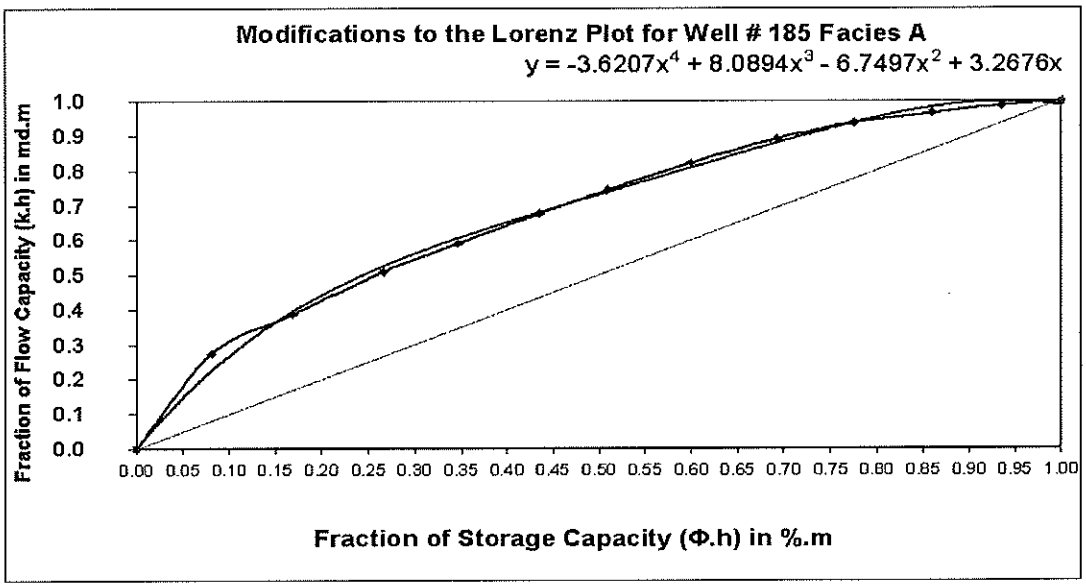
Modifications to the Lorenz Plot for Well # 185 Facies A
y = -3.6207x4 + 8.0894x3 - 6.7497x2 + 3.2676x
Fraction of Flow Capacity (k.h) in md.m
1.0
0.9
0.8
0.7
0.6
0.5
0.4
0.3
0.2
0.1
0.0
0.00 0.05 0.10 0.15 0.20 0.25 0.30 0.35 0.40 0.45 0.50 0.55 0.60 0.65 0.70 0.75 0.80 0.85 0.90 0.95 1.00
Fraction of Storage Capacity (Φ.h) in %.m

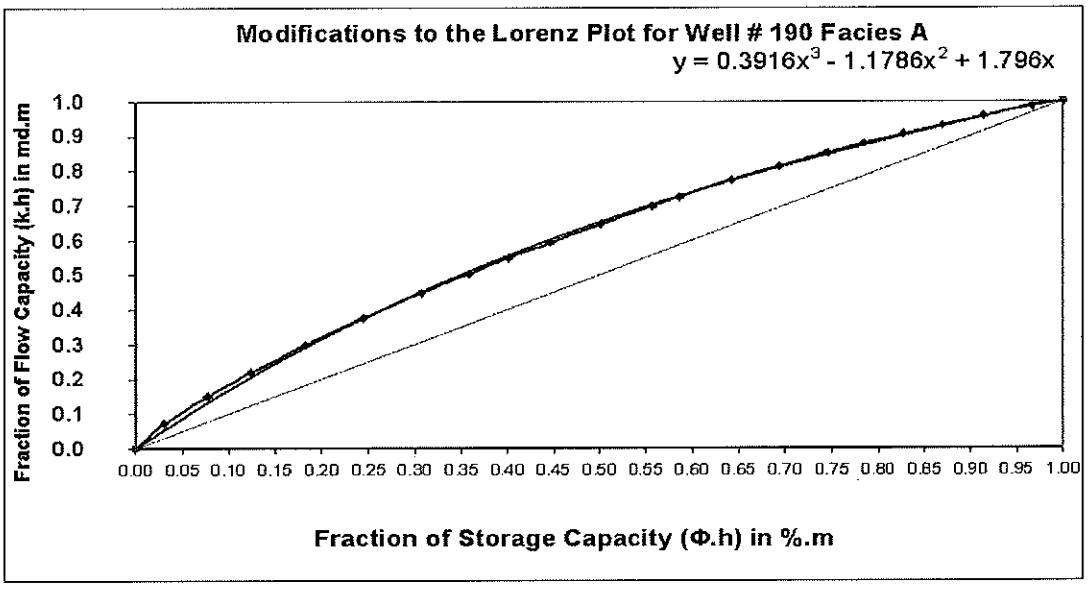
Modifications to the Lorenz Plot for Well # 190 Facies A
y = 0.3916x3 - 1.1786x2 + 1.796x
Fraction of Flow Capacity (k.h) in md.m
1.0
0.9
0.8
0.7
0.6
0.5
0.4
0.3
0.2
0.1
0.0
0.00 0.05 0.10 0.15 0.20 0.25 0.30 0.35 0.40 0.45 0.50 0.55 0.60 0.65 0.70 0.75 0.80 0.85 0.90 0.95 1.00
Fraction of Storage Capacity (Φ.h) in %.m

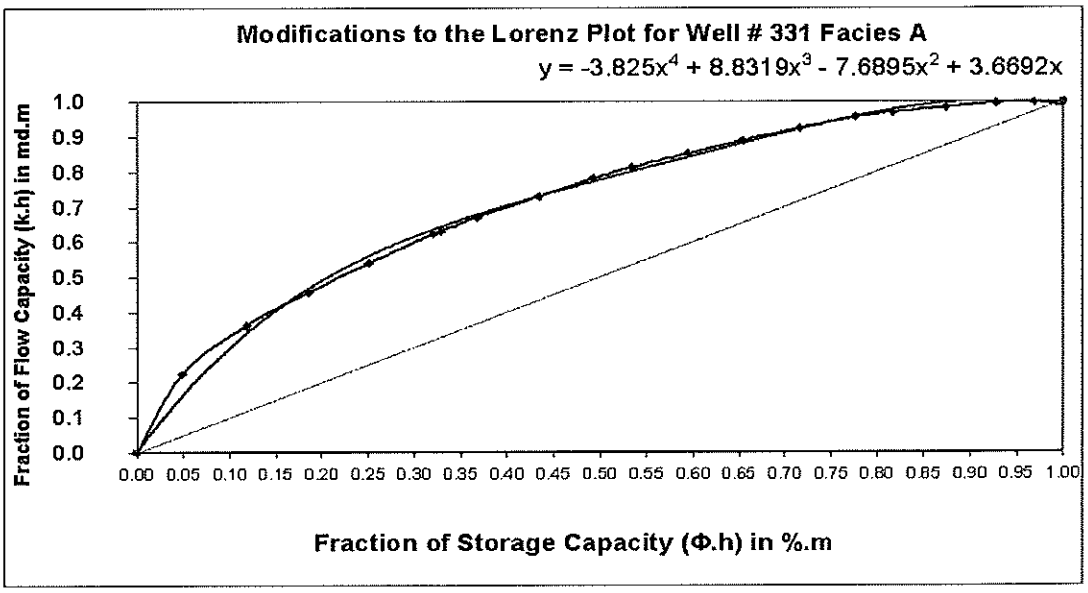
Modifications to the Lorenz Plot for Well # 331 Facies A
y = -3.825x4 + 8.8319x3 - 7.6895x2 + 3.6692x
Fraction of Flow Capacity (k.h) in md.m
1.0
0.9
0.8
0.7
0.6
0.5
0.4
0.3
0.2
0.1
0.0
0.00 0.05 0.10 0.15 0.20 0.25 0.30 0.35 0.40 0.45 0.50 0.55 0.60 0.65 0.70 0.75 0.80 0.85 0.90 0.95 1.00
Fraction of Storage Capacity (Φ.h) in %.m

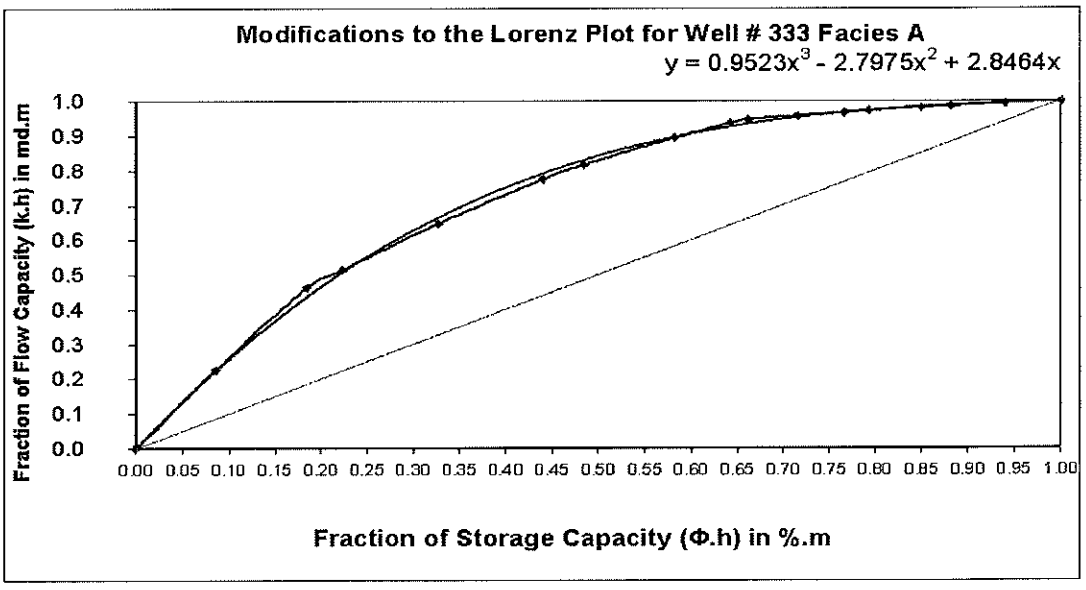
Modifications to the Lorenz Plot for Well # 333 Facies A
y = 0.9523x3 - 2.7975x2 + 2.8464x
Fraction of Flow Capacity (k.h) in md.m
1.0
0.9
0.8
0.7
0.6
0.5
0.4
0.3
0.2
0.1
0.0
0.00 0.05 0.10 0.15 0.20 0.25 0.30 0.35 0.40 0.45 0.50 0.55 0.60 0.65 0.70 0.75 0.80 0.85 0.90 0.95 1.00
Fraction of Storage Capacity (Φ.h) in %.m

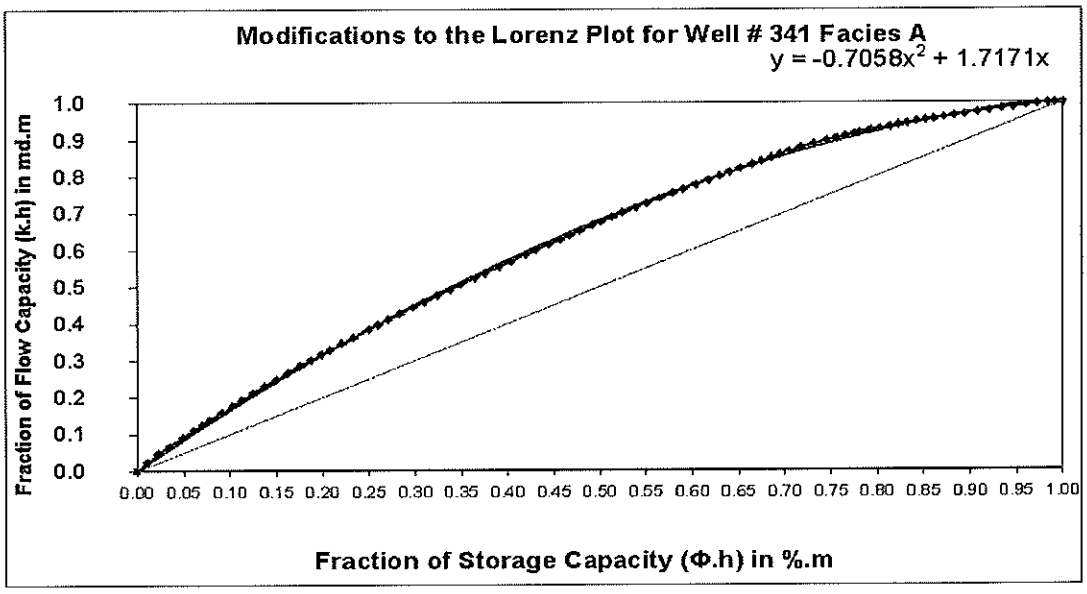
Modifications to the Lorenz Plot for Well # 341 Facies A
y = -0.7058x2 + 1.7171x
Fraction of Flow Capacity (k.h) in md.m
1.0
0.9
0.8
0.7
0.6
0.5
0.4
0.3
0.2
0.1
0.0
0.00 0.05 0.10 0.15 0.20 0.25 0.30 0.35 0.40 0.45 0.50 0.55 0.60 0.65 0.70 0.75 0.80 0.85 0.90 0.95 1.00
Fraction of Storage Capacity (Φ.h) in %.m

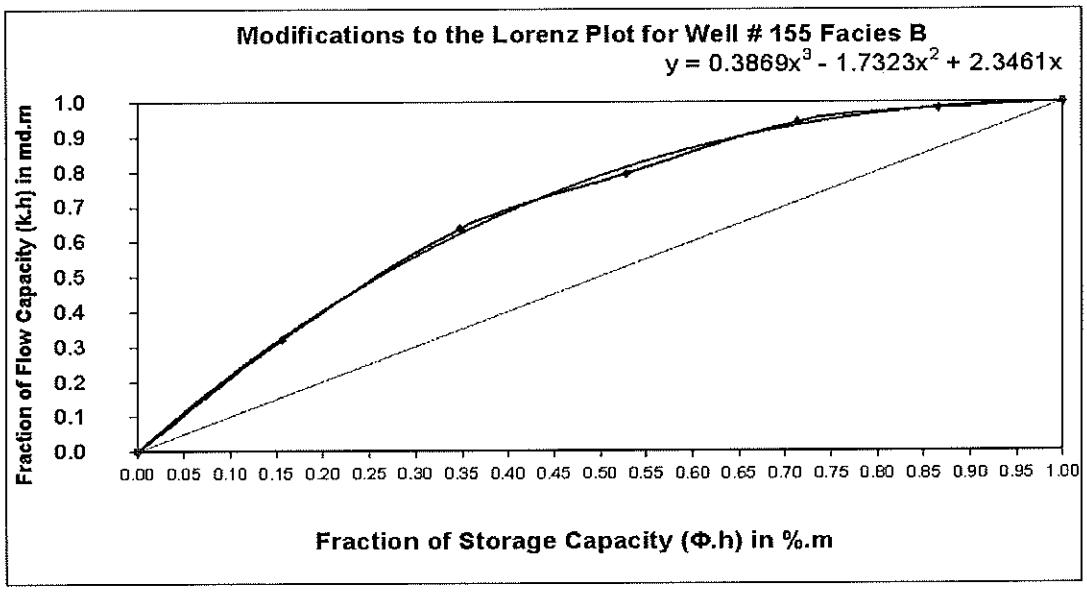
Modifications to the Lorenz Plot for Well # 155 Facies B
y = 0.3869x3 - 1.7323x2 + 2.3461x
Fraction of Flow Capacity (k.h) in md.m
1.0
0.9
0.8
0.7
0.6
0.5
0.4
0.3
0.2
0.1
0.0
0.00 0.05 0.10 0.15 0.20 0.25 0.30 0.35 0.40 0.45 0.50 0.55 0.60 0.65 0.70 0.75 0.80 0.85 0.90 0.95 1.00
Fraction of Storage Capacity (Φ.h) in %.m

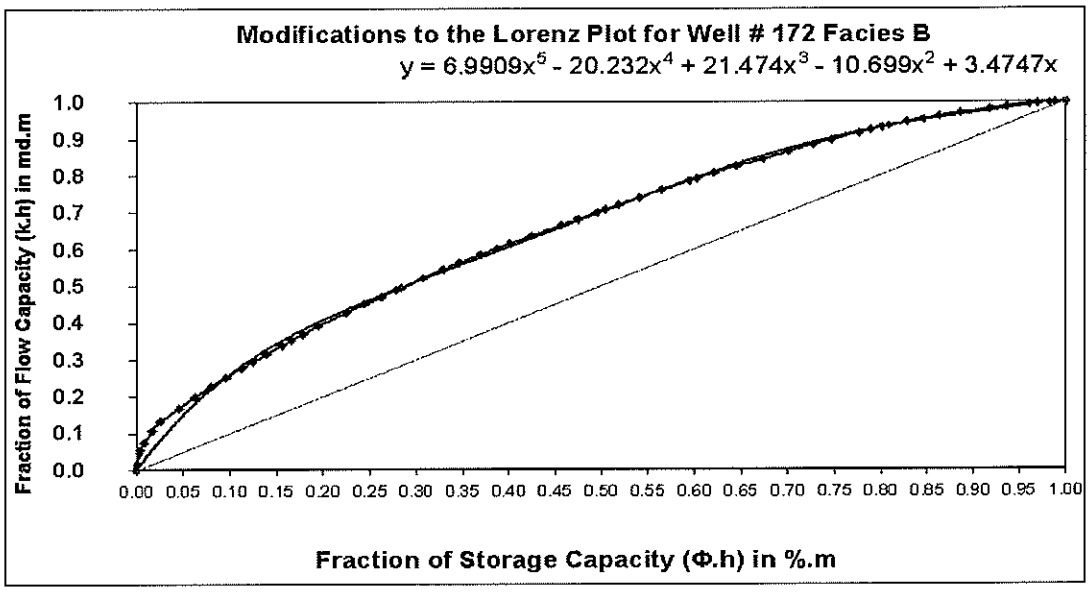
Modifications to the Lorenz Plot for Well # 172 Facies B
y = 6.9909x5 - 20.232x4 + 21.474x3 - 10.699x2 + 3.4747x
Fraction of Flow Capacity (k.h) in md.m
1.0
0.9
0.8
0.7
0.6
0.5
0.4
0.3
0.2
0.1
0.0
0.00 0.05 0.10 0.15 0.20 0.25 0.30 0.35 0.40 0.45 0.50 0.55 0.60 0.65 0.70 0.75 0.80 0.85 0.90 0.95 1.00
Fraction of Storage Capacity (Φ.h) in %.m

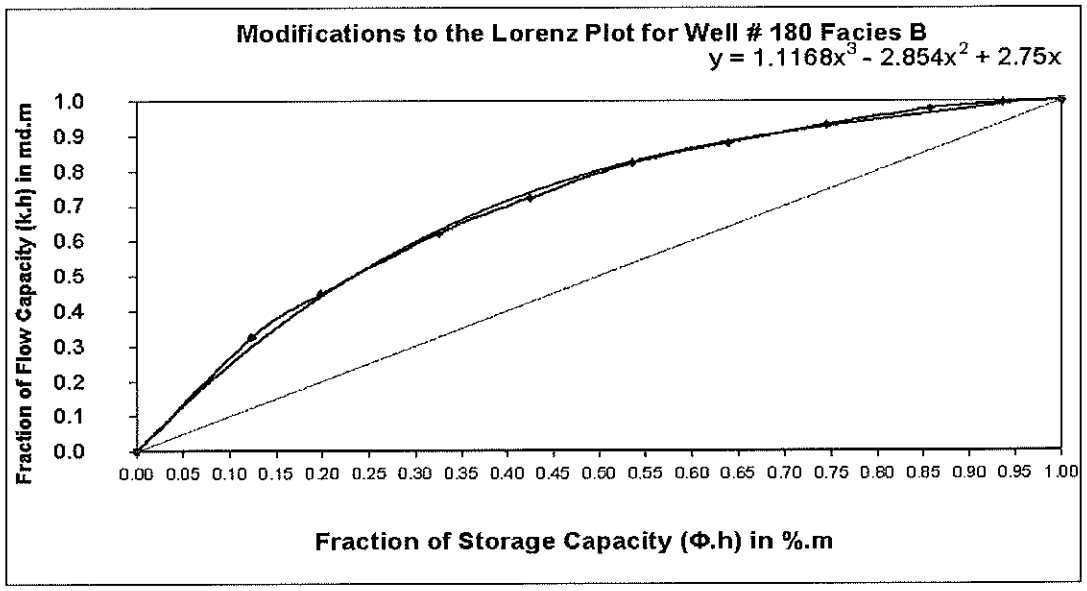
Modifications to the Lorenz Plot for Well # 180 Facies B
y = 1.1168x3 - 2.854x2 + 2.75x
Fraction of Flow Capacity (k.h) in md.m
1.0
0.9
0.8
0.7
0.6
0.5
0.4
0.3
0.2
0.1
0.0
0.00 0.05 0.10 0.15 0.20 0.25 0.30 0.35 0.40 0.45 0.50 0.55 0.60 0.65 0.70 0.75 0.80 0.85 0.90 0.95 1.00
Fraction of Storage Capacity (Φ.h) in %.m

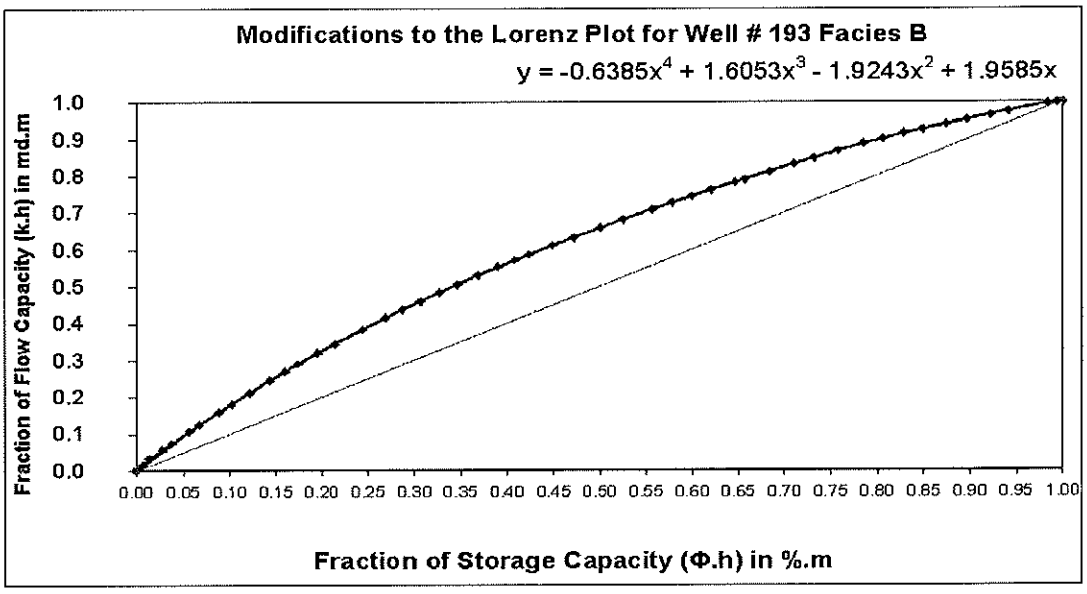
Modifications to the Lorenz Plot for Well # 193 Facies B
y = -0.6385x4 + 1.6053x3 - 1.9243x2 + 1.9585x
Fraction of Flow Capacity (k.h) in md.m
1.0
0.9
0.8
0.7
0.6
0.5
0.4
0.3
0.2
0.1
0.0
0.00 0.05 0.10 0.15 0.20 0.25 0.30 0.35 0.40 0.45 0.50 0.55 0.60 0.65 0.70 0.75 0.80 0.85 0.90 0.95 1.00
Fraction of Storage Capacity (Φ.h) in %.m

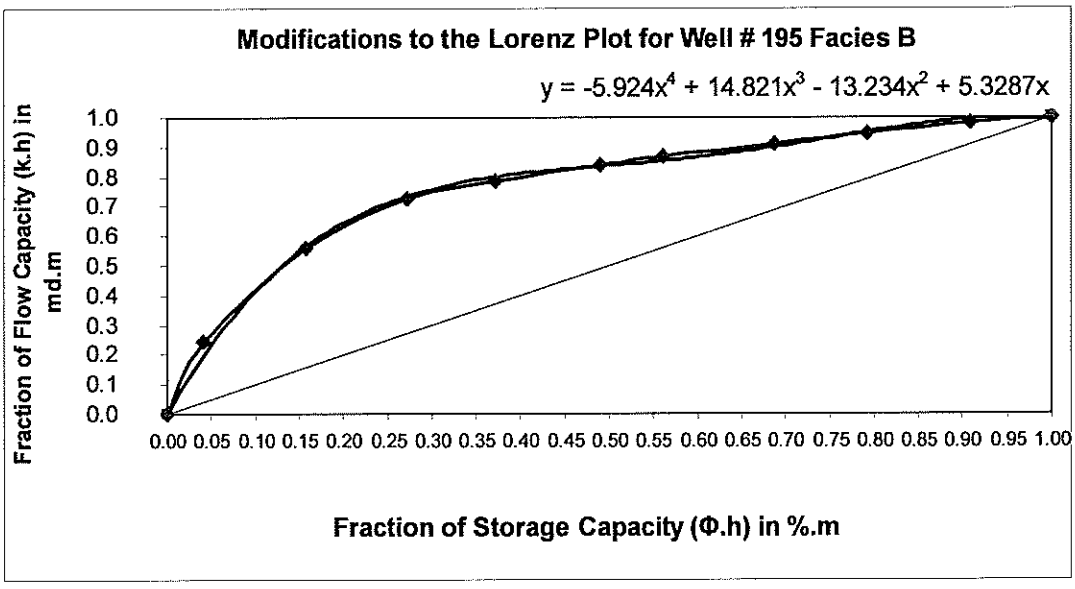
Modifications to the Lorenz Plot for Well # 195 Facies B
y = -5.924x4 + 14.821x3 - 13.234x2 + 5.3287x
Fraction of Flow Capacity (k.h) in md.m
1.0
0.9
0.8
0.7
0.6
0.5
0.4
0.3
0.2
0.1
0.0
0.00 0.05 0.10 0.15 0.20 0.25 0.30 0.35 0.40 0.45 0.50 0.55 0.60 0.65 0.70 0.75 0.80 0.85 0.90 0.95 1.00
Fraction of Storage Capacity (Φ.h) in %.m

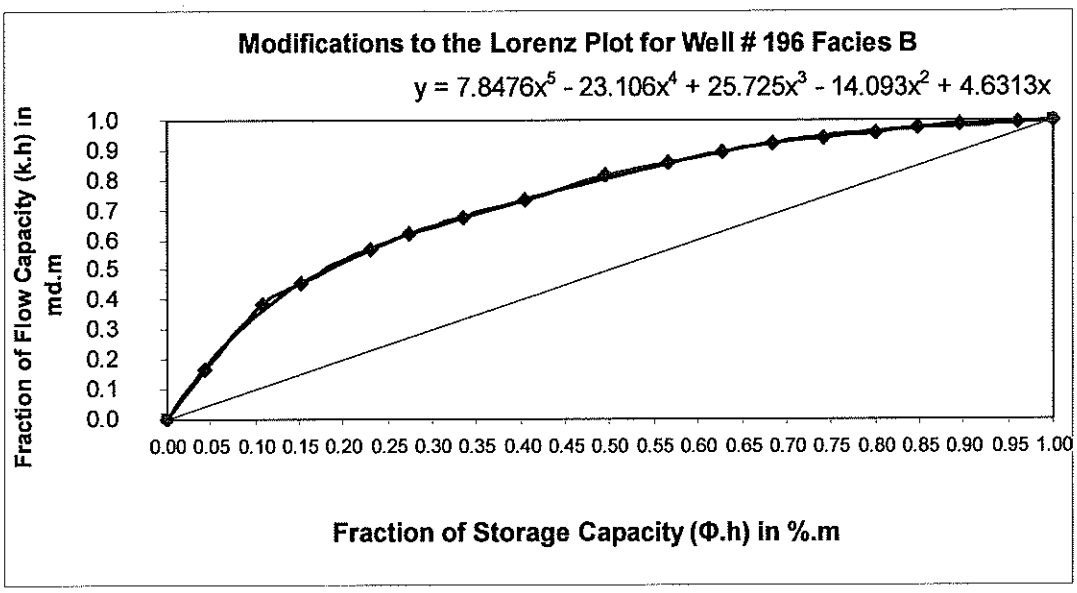
Modifications to the Lorenz Plot for Well # 196 Facies B
y = 7.8476x5 - 23.106x4 + 25.725x3 - 14.093x2 + 4.6313x
Fraction of Flow Capacity (k.h) in md.m
1.0
0.9
0.8
0.7
0.6
0.5
0.4
0.3
0.2
0.1
0.0
0.00 0.05 0.10 0.15 0.20 0.25 0.30 0.35 0.40 0.45 0.50 0.55 0.60 0.65 0.70 0.75 0.80 0.85 0.90 0.95 1.00
Fraction of Storage Capacity (Φ.h) in %.m

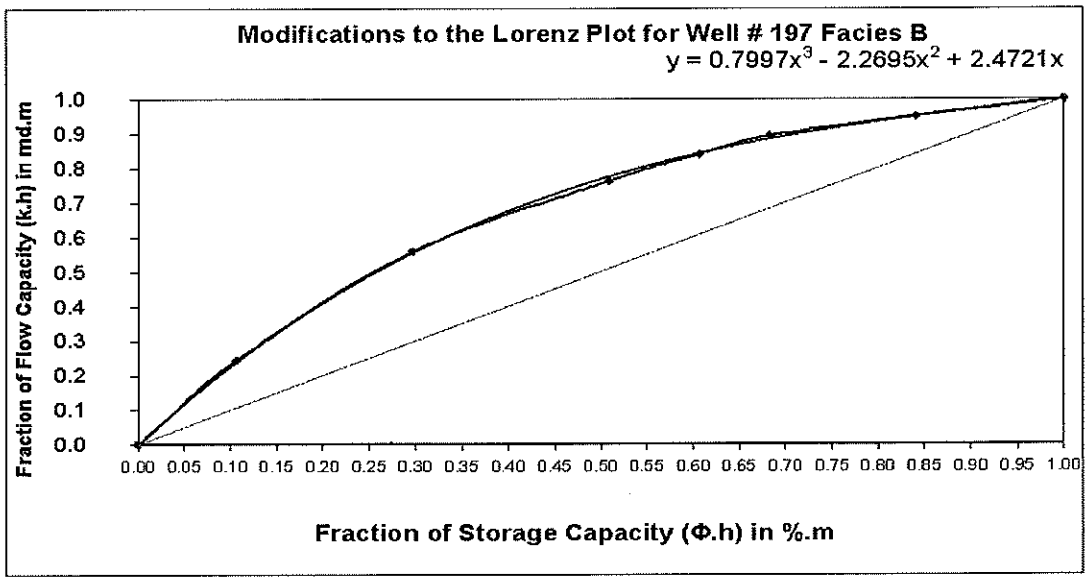
Modifications to the Lorenz Plot for Well # 197 Facies B
y = 0.7997x3 - 2.2695x2 + 2.4721x
Fraction of Flow Capacity (k.h) in md.m
1.0
0.9
0.8
0.7
0.6
0.5
0.4
0.3
0.2
0.1
0.0
0.00 0.05 0.10 0.15 0.20 0.25 0.30 0.35 0.40 0.45 0.50 0.55 0.60 0.65 0.70 0.75 0.80 0.85 0.90 0.95 1.00
Fraction of Storage Capacity (Φ.h) in %.m

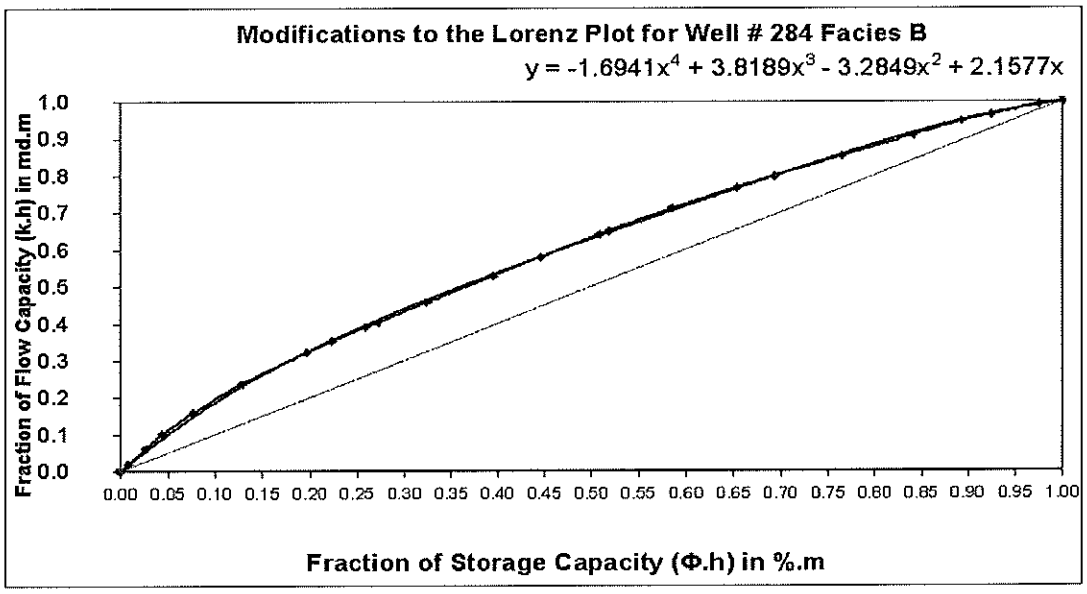
Modifications to the Lorenz Plot for Well # 284 Facies B
y = -1.6941x4 + 3.8189x3 - 3.2849x2 + 2.1577x
Fraction of Flow Capacity (k.h) in md.m
1.0
0.9
0.8
0.7
0.6
0.5
0.4
0.3
0.2
0.1
0.0
0.00 0.05 0.10 0.15 0.20 0.25 0.30 0.35 0.40 0.45 0.50 0.55 0.60 0.65 0.70 0.75 0.80 0.85 0.90 0.95 1.00
Fraction of Storage Capacity (Φ.h) in %.m

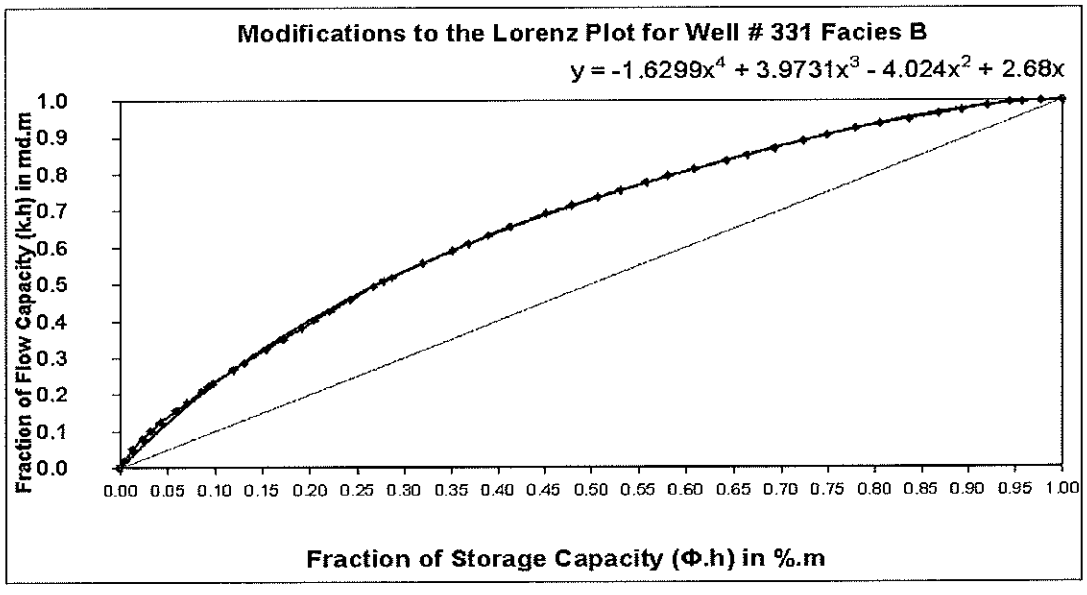
Modifications to the Lorenz Plot for Well # 331 Facies B
y = -1.6299x4 + 3.9731x3 - 4.024x2 + 2.68x
Fraction of Flow Capacity (k.h) in md.m
1.0
0.9
0.8
0.7
0.6
0.5
0.4
0.3
0.2
0.1
0.0
0.00 0.05 0.10 0.15 0.20 0.25 0.30 0.35 0.40 0.45 0.50 0.55 0.60 0.65 0.70 0.75 0.80 0.85 0.90 0.95 1.00
Fraction of Storage Capacity (Φ.h) in %.m

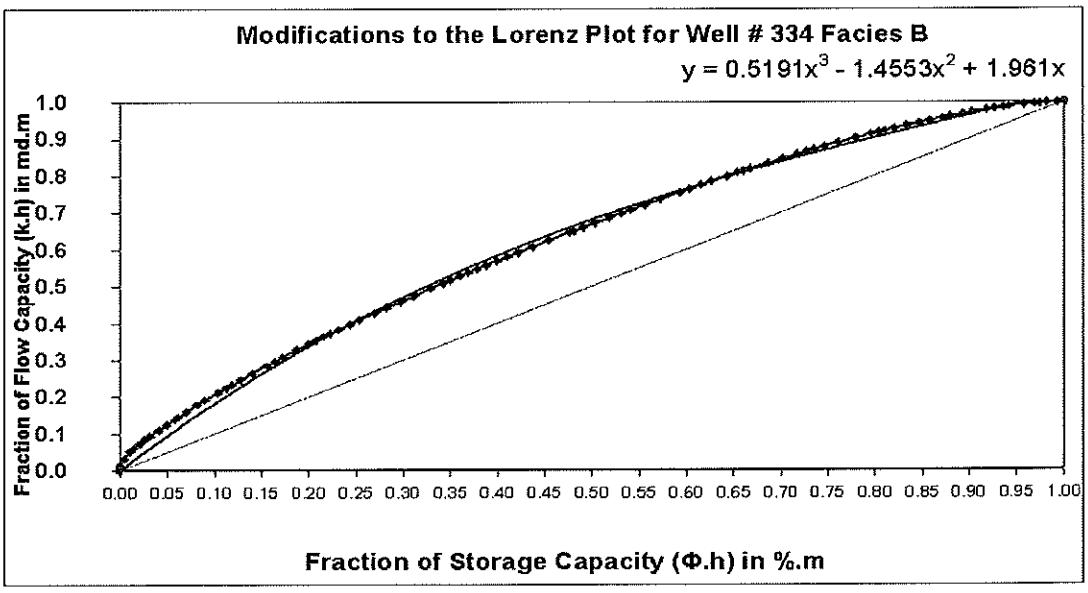
Modifications to the Lorenz Plot for Well # 334 Facies B
y = 0.5191x3 - 1.4553x2 + 1.961x
Fraction of Flow Capacity (k.h) in md.m
1.0
0.9
0.8
0.7
0.6
0.5
0.4
0.3
0.2
0.1
0.0
0.00 0.05 0.10 0.15 0.20 0.25 0.30 0.35 0.40 0.45 0.50 0.55 0.60 0.65 0.70 0.75 0.80 0.85 0.90 0.95 1.00
Fraction of Storage Capacity (Φ.h) in %.m

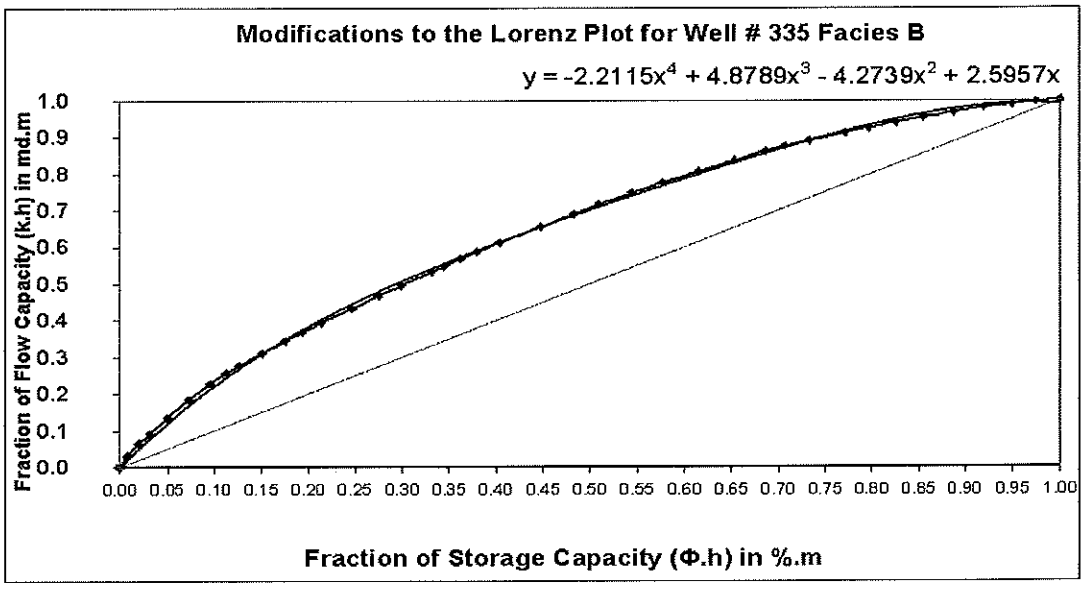
Modifications to the Lorenz Plot for Well # 335 Facies B
y = -2.2115x4 + 4.8789x3 - 4.2739x2 + 2.5957x
Fraction of Flow Capacity (k.h) in md.m
1.0
0.9
0.8
0.7
0.6
0.5
0.4
0.3
0.2
0.1
0.0
0.00 0.05 0.10 0.15 0.20 0.25 0.30 0.35 0.40 0.45 0.50 0.55 0.60 0.65 0.70 0.75 0.80 0.85 0.90 0.95 1.00
Fraction of Storage Capacity (Φ.h) in %.m

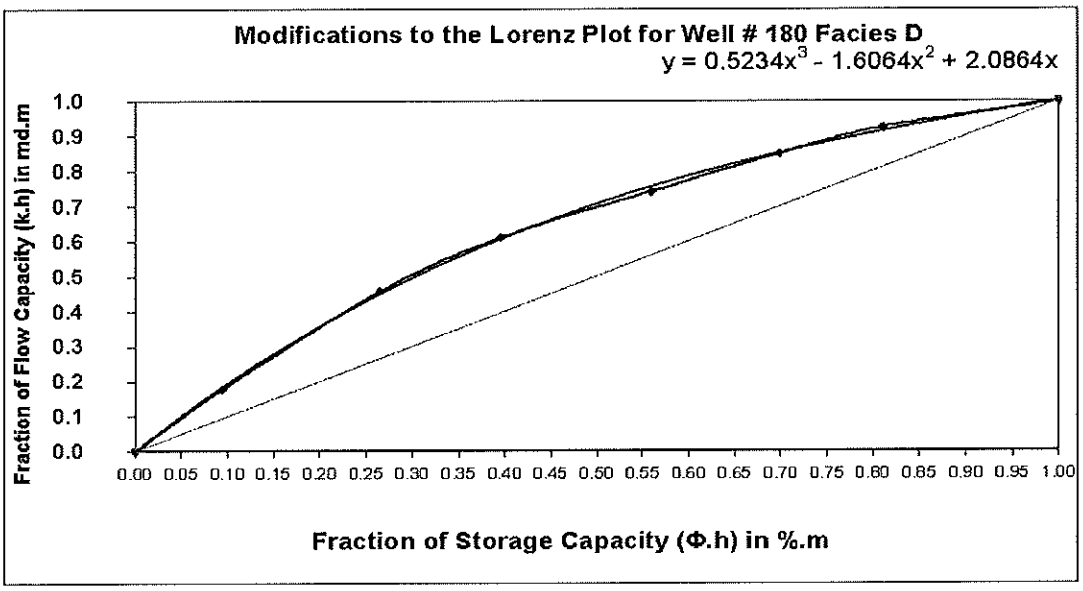
Modifications to the Lorenz Plot for Well # 180 Facies D
y = 0.5234x3 - 1.6064x2 + 2.0864x
Fraction of Flow Capacity (k.h) in md.m
1.0
0.9
0.8
0.7
0.6
0.5
0.4
0.3
0.2
0.1
0.0
0.00 0.05 0.10 0.15 0.20 0.25 0.30 0.35 0.40 0.45 0.50 0.55 0.60 0.65 0.70 0.75 0.80 0.85 0.90 0.95 1.00
Fraction of Storage Capacity (Φ.h) in %.m

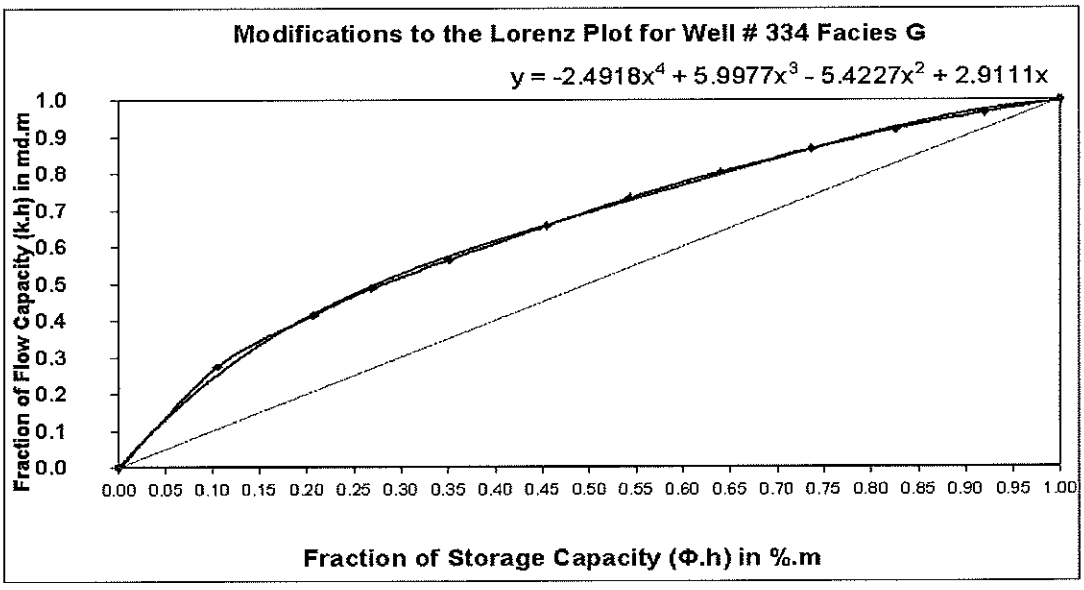
Modifications to the Lorenz Plot for Well # 334 Facies G
y = -2.4918x4 + 5.9977x3 - 5.4227x2 + 2.9111x
Fraction of Flow Capacity (k.h) in md.m
1.0
0.9
0.8
0.7
0.6
0.5
0.4
0.3
0.2
0.1
0.0
0.00 0.05 0.10 0.15 0.20 0.25 0.30 0.35 0.40 0.45 0.50 0.55 0.60 0.65 0.70 0.75 0.80 0.85 0.90 0.95 1.00
Fraction of Storage Capacity (Φ.h) in %.m

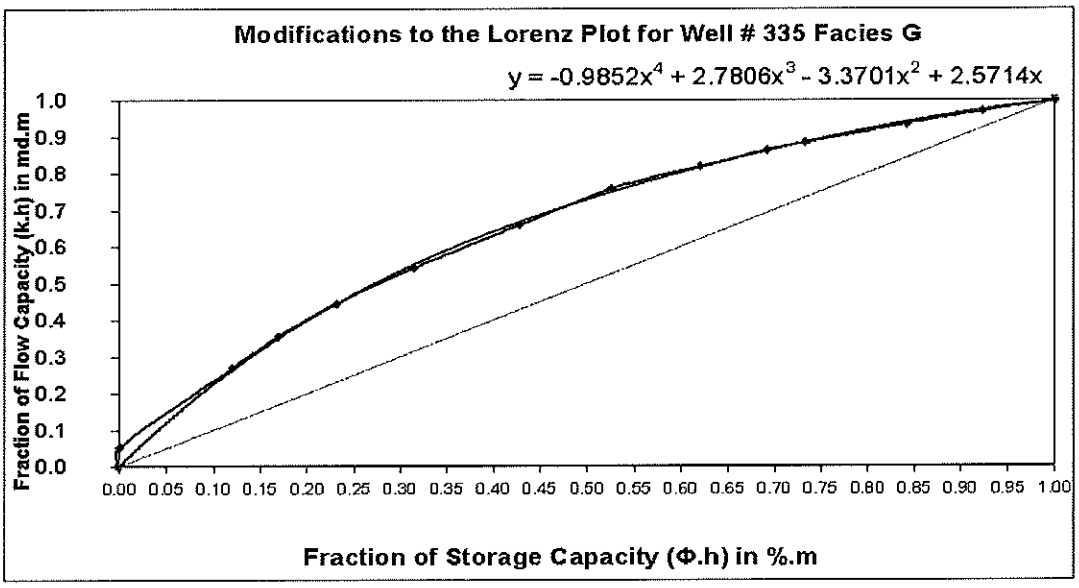
Modifications to the Lorenz Plot for Well # 335 Facies G
y = -0.9852x4 + 2.7806x3 - 3.3701x2 + 2.5714x
Fraction of Flow Capacity (k.h) in md.m
1.0
0.9
0.8
0.7
0.6
0.5
0.4
0.3
0.2
0.1
0.0
0.00 0.05 0.10 0.15 0.20 0.25 0.30 0.35 0.40 0.45 0.50 0.55 0.60 0.65 0.70 0.75 0.80 0.85 0.90 0.95 1.00
Fraction of Storage Capacity (Φ.h) in %.m

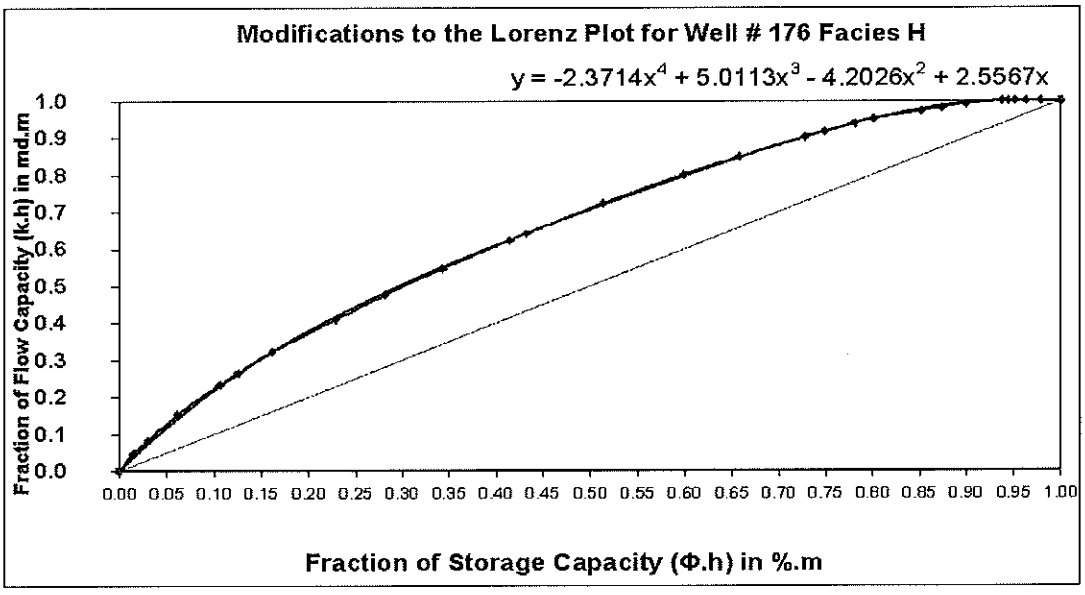
Modifications to the Lorenz Plot for Well # 176 Facies H
y = -2.3714x4 + 5.0113x3 - 4.2026x2 + 2.5567x
Fraction of Flow Capacity (k.h) in md.m
1.0
0.9
0.8
0.7
0.6
0.5
0.4
0.3
0.2
0.1
0.0
0.00 0.05 0.10 0.15 0.20 0.25 0.30 0.35 0.40 0.45 0.50 0.55 0.60 0.65 0.70 0.75 0.80 0.85 0.90 0.95 1.00
Fraction of Storage Capacity (Φ.h) in %.m

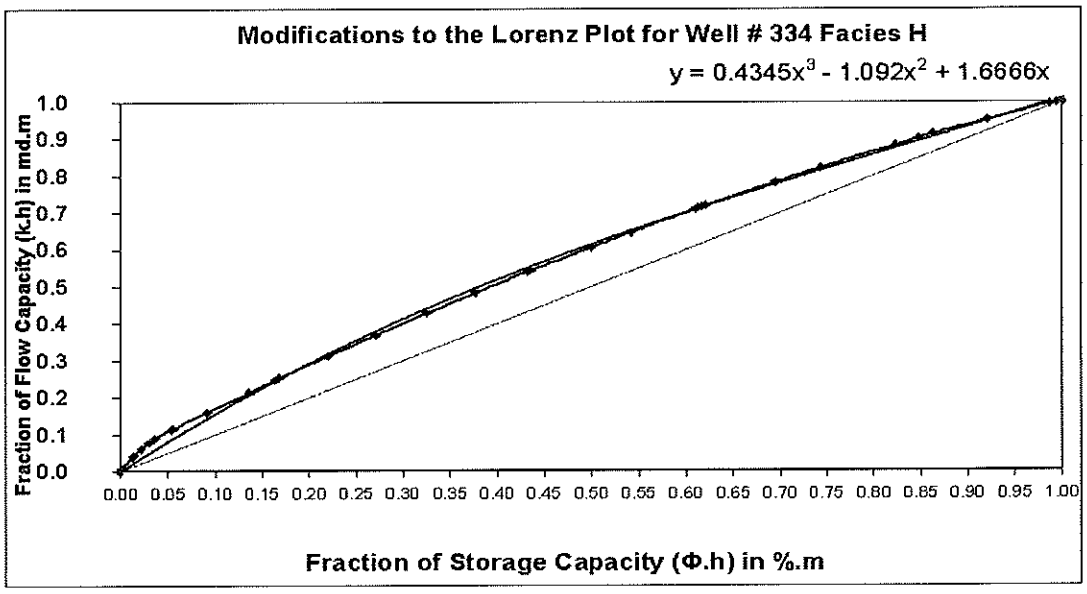
Modifications to the Lorenz Plot for Well # 334 Facies H
y = 0.4345x^3 - 1.092x^2 + 1.6666x
Fraction of Flow Capacity (k.h) in md.m
1.0
0.9
0.8
0.7
0.6
0.5
0.4
0.3
0.2
0.1
0.0
0.00 0.05 0.10 0.15 0.20 0.25 0.30 0.35 0.40 0.45 0.50 0.55 0.60 0.65 0.70 0.75 0.80 0.85 0.90 0.95 1.00
Fraction of Storage Capacity (Φ.h) in %.m

APPENDIX G

PRESSURE BUILD-UP LOG-LOG PLOTS

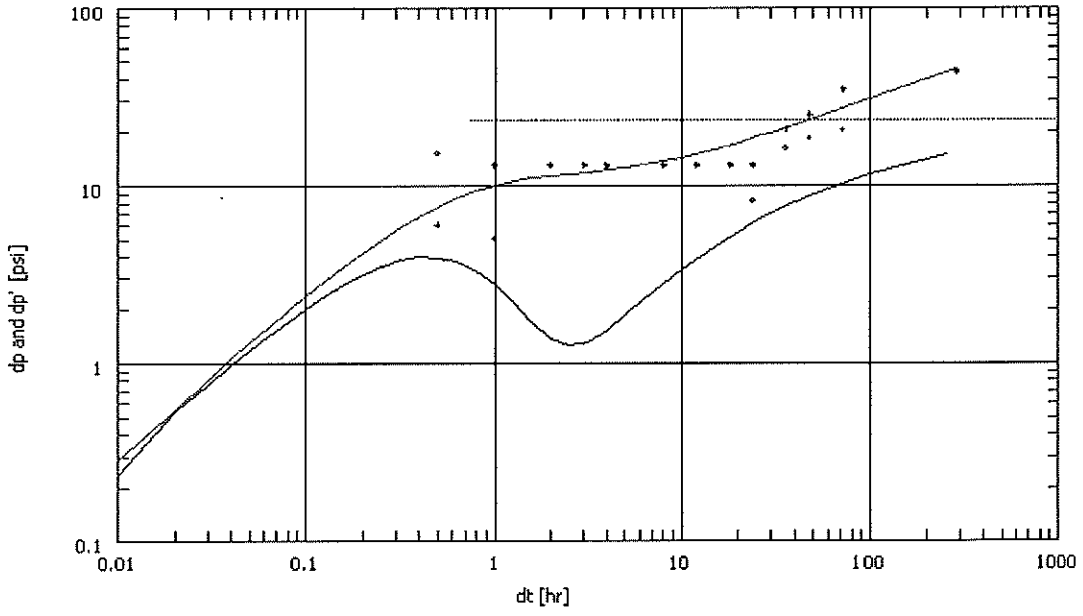

Figure G.1 Pressure Build-Up Log-Log Plot for Well#21

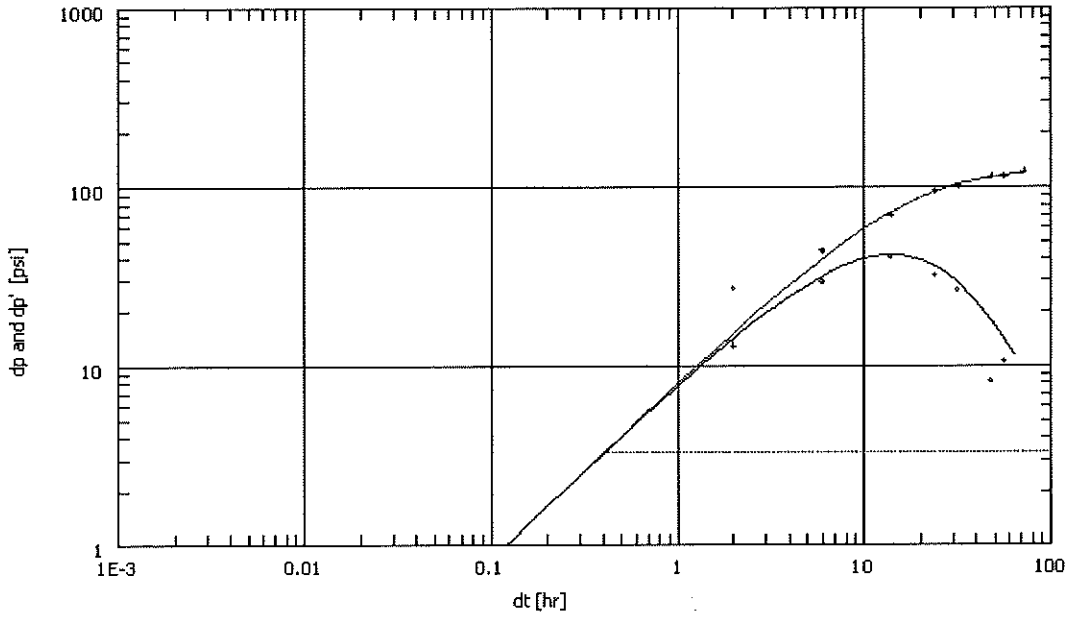

Figure G.2 Pressure Build-Up Log-Log Plot for Well#28

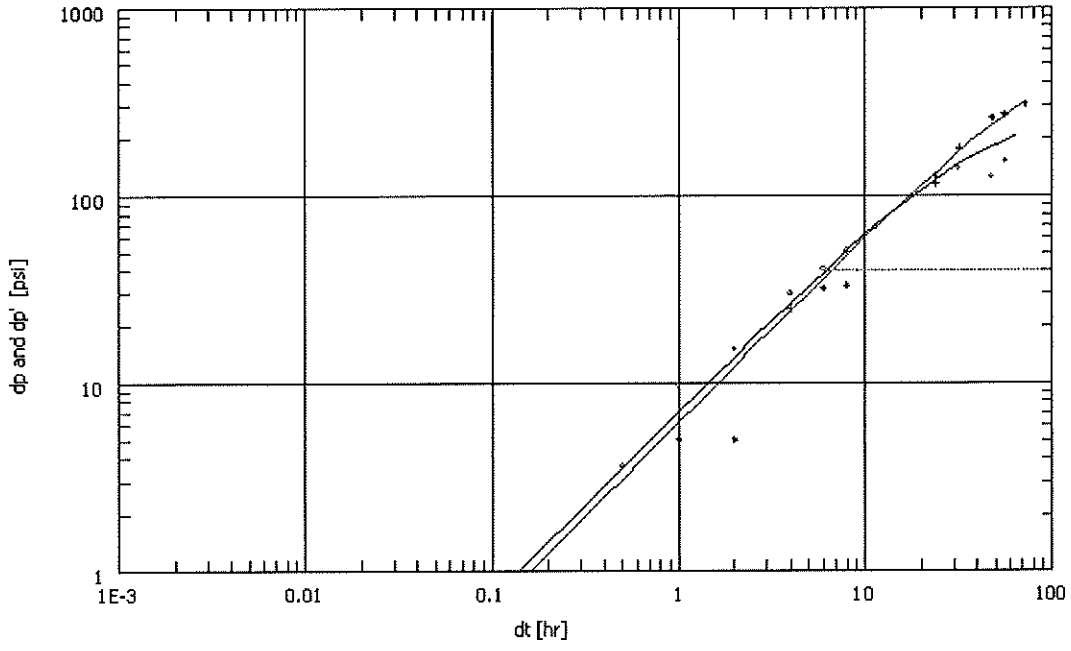

Figure G.3 Pressure Build-Up Log-Log Plot for Well#35

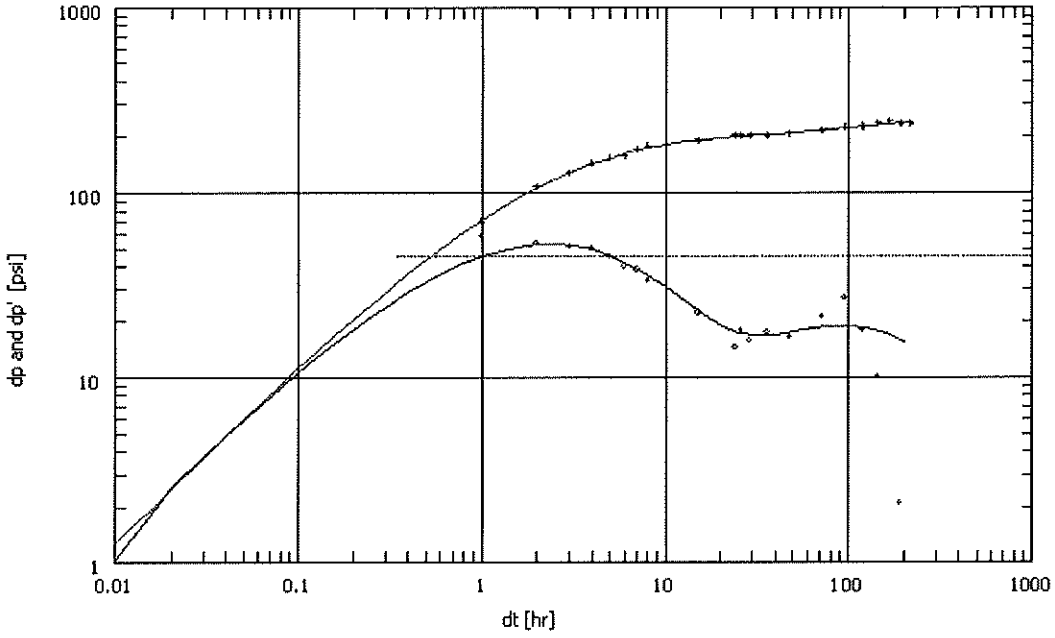

Figure G.4 Pressure Build-Up Log-Log Plot for Well#80

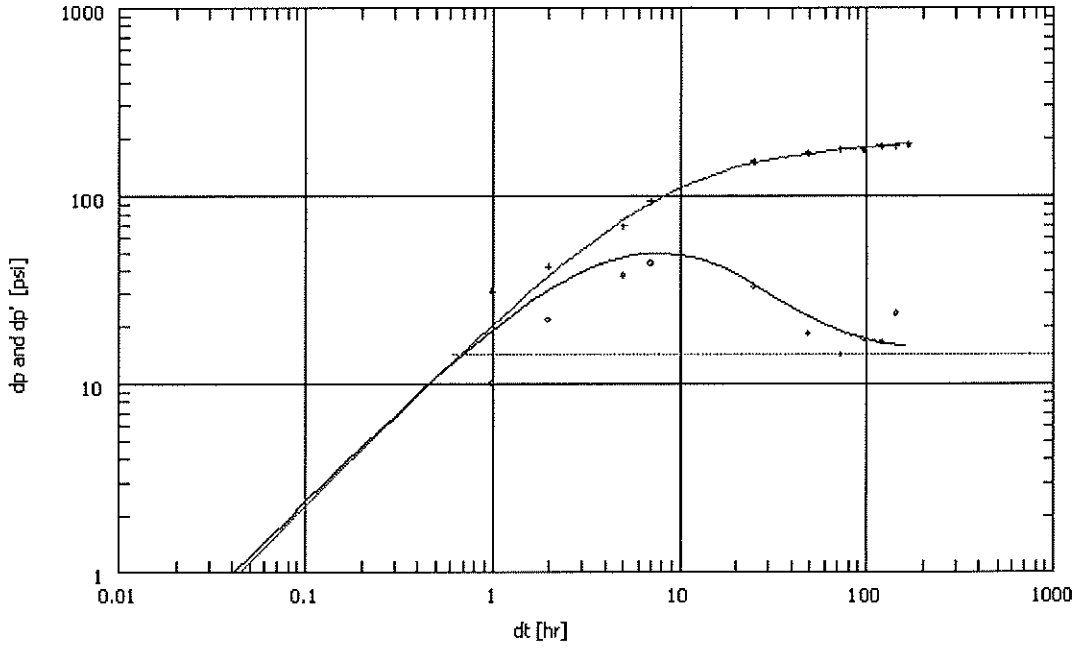

Figure G.5 Pressure Build-Up Log-Log Plot for Well#148

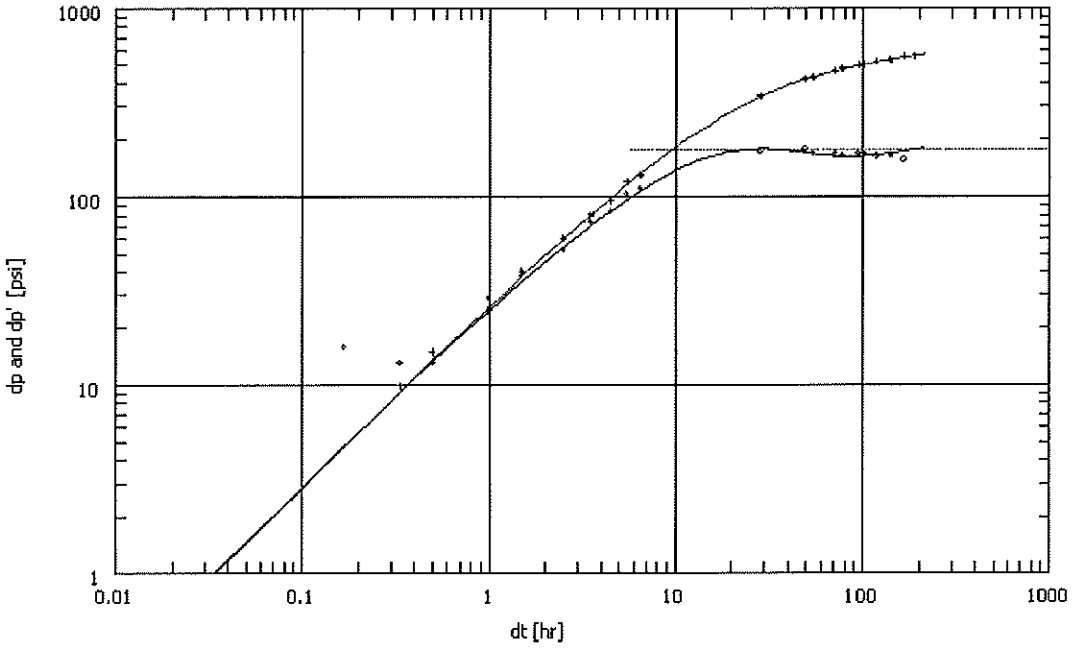

Figure G.6 Pressure Build-Up Log-Log Plot for Well#172